COAL SOLUBILIZATION BY NON-CATALYTIC TRANSFER HYDROGENATION WITH FORMATE

Soon Chuan Lim and Edwin N. Givens
University of Kentucky, Center for Applied Energy Research
3572 Iron Works Pike, Lexington, KY 40511-8433

Keywords: Liquefaction, hydrothermal treatment, carbon monoxide, formate, water

Abstract

Non-Catalytic transfer hydrogenation using formate as the hydrogenating agent significantly reduces the severity necessary for solubilizing coal. Moisture and mineral matter free solubilization of coal up to 94% in pyridine was observed for a Wyodak coal that was treated at 340 °C for 1 hr with CO and aqueous NaOH. Loss of oxygen from coal as CO_2 agrees with a forced balance based upon elemental and mass recoveries. A hydrogen consumption of 0.6 wt %, calculated from this balance, agrees with hydrogen consumptions independently determined based upon CO conversion. The hydrogen to carbon ratio in the total water-insoluble product increased to 0.88 versus a corresponding value of 0.80 in the starting coal. The pyridine soluble and insoluble fractions had H/C values of 0.97 and 0.59, respectively. Reaction in the absence of added salt produced a water-insoluble product that was 50% soluble in pyridine and had a H/C value of 0.79.

Introduction

CO-promoted hydrothermal treatment of low-rank coals has been found by several groups to be quite effective for converting these coals to soluble products.[1] A group at Exxon reported that hydrothermal treatment of a Wyoming subbituminous coal in the presence of CO at 345 °C for 6 hours produced a material that was largely soluble in THF and was more soluble than material produced by hydrothermal treatment in the absence of CO.[2] Treating the coal under the same conditions in decalin failed to increase the solubility relative to that of the raw coal. Hydrothermal treatment substantially depolymerized the coal making it more reactive for producing distillate product in a hydrogen donor solvent.[2,3] The hydrothermal product was enriched in hydrogen and had reduced oxygen content. The CO-aqueous system presumably promotes decarboxylation of oxygen-containing constituents and cleavage of ether and ester groups attached to aromatic ring systems. Under these reaction conditions, a Martin Lake, Texas lignite heated in $^{13}CO/D_2O$ was shown to produce formate ion with most of the deuterium in the reacted D_2O being transferred into the coal.[4] The recovered CO_2 contained 60% $^{12}CO_2$ from the coal, presumably formed via decarboxylation, and 40% $^{13}CO_2$ from ^{13}CO via the water-gas-shift reaction. Adding alkali metal salts to the CO/H_2O mixture presumably increases the concentration of formate ion further enhancing the solubility of the product.[5] In the work reported here, the reactivity of a Wyodak coal under hydrothermal conditions in the presence of CO and sodium hydroxide is discussed.

Experimental

Wyodak coal from the Black Thunder mine in Wright, Wyoming, was ground to -200 mesh, riffled and stored in tightly sealed containers. Ultimate analysis: carbon, 73.9%; hydrogen, 5.2%; nitrogen, 1.3%; sulfur, 0.6%; oxygen, 19.0% (by difference). Ash content (dry basis) was 6.12 wt%. All results are expressed as weight percent moisture and ash-free coal (maf).

In the experiments conducted in a 300 ml stirred autoclave, 50 g of as-received coal containing approximately 20% moisture were mixed with 4.2 g NaOH in 75 ml. of distilled and de-ionized water. The reactor was sealed, leak tested and pressurized with CO to 1000 psig. In experiments in the absence of base, only 40 ml of water was added. Heat-up time from ambient to reaction time at 340 °C was approximately 3.5 hr. The reaction was allowed to proceed at this temperature for an additional hour. The reactor was cooled to ambient temperature within 1.5 hr. A gas sample was collected and analyzed by gas chromatography and the solid products were removed from the reactor, washed with distilled and de-ionized water and dried at 40 °C under vacuum. Soluble humic acids were recovered from the aqueous phase by precipitating the colloidal material with HCl (pH 1-2) followed by centrifugation and drying. The acidified aqueous layer was further extracted with ether. Product distribution and recovery of water-insoluble product, humic acids and ether solubles, on a maf basis, are shown in Table 1. A 5 g sample of the water-insoluble product was extracted with THF in a Soxhlet thimble for 18 hours. The Soxhlet extraction technique was exceptionally slow since colored material continued to exude from the thimble after a week of continuous extraction. A smaller sample (0.5 g) of product was placed in 200 mL of pyridine or THF and extracted using a sonication/vacuum filtration

technique at ambient temperature. Samples ultrasonicated in either solvent for 10 min filtered rapidly within minutes under vacuum at ambient temperature. Material was collected after solvents were removed, dried overnight at 80 °C at 16 kPa and weighed to determine solubility in the solvent. A reliable pyridine solubility value could not be obtained for the water-insoluble product from treating coal in the absence of NaOH. Material that was ultrasonicated in pyridine clogged the filter paper within minutes. The same material also clogged the Soxhlet thimble filters which resulted in less material dissolving in pyridine than in THF (see Table 2). This underscores the different properties of the material generated when salt was present during the reaction.

Discussion

The water-gas-shift reaction in the presence of NaOH is quite sensitive to temperatures between 250 and 340 °C with CO conversion increasing from <10% up to approximately 90%, respectively. At 300 °C in the presence of ~0.3 M NaOH, the conditions under which many of the earlier runs were made, the shift reaction goes to the extent of about 20-25%. In the absence of NaOH, the CO conversion at 340 °C is only ~40%. At 300 °C, very little H_2 is actually recovered, most of it being incorporated into the water-insoluble product. At 340 °C, about half of the H_2 that is formed is recovered. In every case, the amount of hydrocarbon gases formed in the reaction was quite small.

The amount of humic acids and ether-extracted material (fulvic acids) in the aqueous phase was small, being 1.3% in the presence of NaOH. The highest yields of these products (~7%) were observed at 300 °C, either at low CO pressures or in the absence of CO. Solubility of the water-insoluble material indicates the degree to which reaction occurred. Previously, solubilities in THF and pyridine were determined using a Soxhlet apparatus. The materials generated at 340 °C could not be evaluated in this manner since the extraction thimbles readily blinded. It was found that solubilities of the NaOH treated materials in these two solvents could be determined at ambient temperature using a sonication technique in which the extracted THF and pyridine solutions filtered quite readily without blinding the filter paper. Higher pyridine and THF solubilities were obtained using the ultrasonication technique compared to Soxhlet extraction. For the reactions run with NaOH, pyridine and THF solubilities reached 94 and 78 wt % (maf product basis), respectively. The ultrasonication technique could not be used on the product produced in the absence of added NaOH since it readily blinded the filter paper when filtered.

Chemical compositions of water-insoluble product and the solvent-separated fractions from the NaOH treated coal are shown in Table 3. For the 82.3 wt % of water-insoluble product plus humic acids, the 8% ash content was too high relative to the 5.5% concentration in the starting coal. In the absence of NaOH the ash content was closer to the expected value. In both cases, there was a decrease in the oxygen content from 17.9% in the starting coal to 4.7% in the water-insoluble product for the NaOH-treated coal and 5.2% for the NaOH-free case. Approximately 75% of the oxygen was removed in both cases. The hydrogen-carbon ratio for the NaOH-treated coal increased to 0.88 versus a value of 0.80 for the starting coal. By contrast, the H/C ratio of the product generated in the absence of base is essentially the same as that of the starting coal, indicating a loss of hydrogen in the reaction. The hydrogen concentration in the pyridine soluble fraction (0.97 H/C) is higher than in the starting coal (0.80 H/C), whereas the concentration in the insoluble fraction is much less (0.59 H/C). Oxygen concentration is much higher in the insoluble fraction. Note that the oxygen values for the solvent separated fractions are higher than observed in the water-insoluble product. This suggests a possible reactivity upon exposure to air since no special precautions were followed in handling these samples. The concentrations of nitrogen and sulfur in the solvent separated products are similar to the total water-insoluble product suggesting enrichment of nitrogen in the pyridine insoluble product.

Mass and elemental balances were calculated for the 300 mL autoclave experiments. The balance for the experiment run in the presence of NaOH, as shown in Table 4, was calculated by correcting the ash concentration in the water-insoluble product, which includes the humic acids and ether-soluble product, to a level consistent with the ash in the starting coal and adjusting the remaining elements to account for this correction. Since the gas analysis showed that hydrocarbon gases were quite small (see Table 1) the other products are water, CO and CO_2. Because very large concentrations of CO are present as a reactant and much of the CO_2 is formed as a result of the water-gas-shift reaction, the amount of these carbon oxides that are formed from carbon in the coal cannot be measured directly. The ratio of the additional oxygen and carbon needed to force the balance of these two elements in the product is greater than the 2 to 1 ratio in CO_2. Therefore, in the product, of the 78% of the oxygen in the starting coal that was absent from the water-insoluble product, most was present as CO_2 (60% of the original oxygen) with the remaining 18% of the original oxygen being present as

water. Formation of CO_2 is consistent with the results of Horvath and Siskin.[4] The hydrogen necessary to form the water was 0.42 wt % of ash-free coal, while the total hydrogen consumed in the reaction was ~0.6 wt % of the coal. Using these assumptions, all of the starting material is accounted for in the products.

The elemental balance for the experiment made in the absence of NaOH (see Table 5) showed that more carbon and less hydrogen was recovered in the water-insoluble product than for the NaOH treated coal. In fact, the amount of hydrogen was less than in the starting coal. Forcing a carbon balance indicated that less oxygen could be removed as CO_2 and the amount of water necessary to balance the oxygen was much higher. Of the 75% of oxygen removed from the coal, 23% was removed as CO_2 and 52% as water. The net H_2 consumption of 1.0 wt % hydrogen, which would have been formed via the water-gas-shift reaction, accounted for 85% of the hydrogen incorporated into the water. The remaining hydrogen came from the coal accounting for the decrease in hydrogen in the water-insoluble product.

The heating value of the treated coals were calculated using the equation developed by Boie and used by Ringen and co-workers.[6]

$$H_g(\text{cal/g}) = 8400C + 27765H + 1500N - 2500S - 26500$$

where H_g is the gross heating value and C, H, N, S and O are the normalized weight fractions of these elements in the sample. Multiplication by the factor 1.8 converts the results to units of Btu/lb.

	with NaOH	without NaOH	Coal
Heating Value, Btu/lb maf	16,400	16,000	12,900

The heating values for both CO-treated coals were significantly higher than the starting coal.

Summary

Reacting Wyodak coal with CO and H_2O at 340 °C, both in the presence and absence of base, produced materials having reduced oxygen contents. Oxygen removals in excess of 75% were obtained regardless of whether base was present. Addition of base gave a material which was highly soluble in both pyridine (95%) and THF (78%), whereas the solubility of the material produced in the absence of base was less. Water-insoluble materials produced in both cases had significantly higher heating values than the starting coal. Forced elemental balances based upon the absence of any significant hydrocarbons in the gaseous product provides insight into the probable reaction pathways for removal of oxygen. In the presence of base, a large part of the oxygen leaves as CO_2 while in the absence of base the water pathway is far more dominant. In both cases, the significant removal of oxygen can have a large economic impact on processing costs for low rank coals.

References

1. Lim, S. C.; Rathbone, R. F.; Rubel, A. M.; Givens, E. N.; Derbyshire. F. J. Energy and Fuels, 1994, 8, 294
2. Stuntz, G. F.; Culross, C. C.; Reynolds, S. D. United States Patent No. 5,026,475, June 25; 1991.
3. Vaughn, S. N.; Siskin, M.; Katritzky, A.; Brons, G.; Reynolds, N.; Culross, C. C.; Neskora, D. R. United States Patent No. 5,151,173; Sept. 29, 1992.
4. Horvath, I. T.; Siskin, M. Energy Fuels 1991, 5, 933-934.
5. Ng, F. T. T.; Tsakiri, S. K. Fuel 1993, 72, 211.
6. S. Ringen, J. Lanum and F.P. Miknis Fuel, 1979, 58, 69

Table 1. Product distribution from aqueous CO treatment of Wyodak coal

	with NaOH[a]	without NaOH[b]
Gaseous Product		
Hydrogen, mol %	32	8
CO, mol %	7	52
CO_2, mol %	61	34
Hydrocarbon gases, mol %	<0.5	<0.5
Water-Insoluble Prod, wt% maf	81	85
Humic acids + ether solubles, wt% maf	1.3	n.d.

a. Wyodak coal, 1000 psig CO cold, 4.2 g NaOH, 75 mL H_2O, 340 °C, 300 mL reactor.
b. Wyodak coal, 1000 psig CO cold, 40 mL H_2O, 340 °C, 300 mL reactor.

Table 2. Solubility of water-insoluble product from CO-treated coal (maf basis)

Treatment	Ultrasonic/Filtration		Soxhlet Extraction	
	THF	Pyridine (RT)	THF	Pyridine
with NaOH	78	94	55	88
without NaOH	N.A.	N.A.	54	50

Table 3. Elemental analysis of CO-treated coals

	Starting coal	CO-treated coal			
		with NaOH			without NaOH
Element		Water-Insoluble	Pyridine Soluble	Pyridine Insoluble	Water-Insoluble
Carbon	70.3	79.5	85.2	40.5	81.0
Hydrogen	4.7	5.8	6.9	2.0	5.3
Nitrogen	1.0	1.7	1.5	1.5	1.7
Sulfur	0.5	0.4	0.3	0.3	0.4
Oxygen	17.9	4.7	6.1	16.9	5.2
Ash, SO_3-free	5.5	8.0	-	38.9	6.3
H/C atomic ratio	0.80	0.88	0.97	0.59	0.79

Table 4. Elemental balance for NaOH-treated coal

	Coal	Water Insoluble Product[a]	CO_2	H_2O	Total
Carbon	70.32	66.3	4.0		70.3
Hydrogen	4.68	4.83		0.42	5.25
Nitrogen	1.04	1.42			1.42
Oxygen	17.92	3.92	10.67	3.33	17.92
Sulfur	0.5	0.33			0.33
Ash	5.54	5.54			5.54
Total	100.00	82.3	14.67	3.75	100.72

a. Ash concentration corrected to starting coal.

Table 5. Elemental Balance for 300 mL Reactor Run without NaOH

	Coal	Water-Insol Product	CO_2	H_2O	Total
Carbon	70.32	68.76	1.56		70.32
Hydrogen	4.68	4.50		1.17	5.67
Nitrogen	1.04	1.44			1.44
Oxygen	17.92	4.41	4.16	9.35	17.92
Sulfur	0.5	0.34			0.34
Ash	5.54	5.54			5.54
Total	100.00	85.00	5.72	10.52	101.23

STEAM PRETREATMENT FOR COAL LIQUEFACTION

O. Ivanenko, R.A. Graff, V. Balogh-Nair, C. Brathwaite
Departments of Chemical Engineering and Chemistry
The City College of New York, New York, NY, 10031

Keywords: Coal, Liquefaction, Pretreatment

INTRODUCTION

Development of commercially viable and environmentally sound processes for coal liquefaction remains a formidable challenge. Although advances in coal liquefaction technology in recent years have led to the production of liquids of improved quality, this improvement has been achieved mainly by increased consumption of expensive catalyst. Catalyst and capital equipment costs are major factors in the high price of the coal-derived liquids.

One way to improve the economics of direct liquefaction is to modify the coal feed before solubilization. A variety of physical and chemical methods of coal treatment prior to low severity liquefaction have been found to significantly improve yield and quality of the product, making it superior to those obtained at high severity conditions. Many studies have shown that treatments such as alkylation, acylation, partial oxidation and alkali hydrolysis weaken and rupture the cross-linked bonds and result in a partially depolymerized coal. Although all of these methods of enhancing coal reactivity somewhat improve liquefaction yield, none has yet been employed as a process step in liquefaction. Chemical treatment methods remain in the laboratory mainly because they employ expensive and sometimes hazardous reagents.

The work described here is based on the use of steam as a pretreatment agent in noncatalytic coal-donor solvent liquefaction. Advantages of this approach are that steam is among the cheapest of reagents and does not incorporate undesired chemical residues into the coal structure.

Studies have already demonstrated the effectiveness of exposing Illinois No.6 coal to subcritical steam in the temperature range 320-360°C at 50 atm as a pretreatment for room temperature pyridine extraction and for flash pyrolysis (Graff and Brandes, 1987). It was observed that the pyridine extraction yield from steam treated coal gradually increases and reaches a maximum at a pretreatment temperature of 340-350°C. At temperatures above 370°C the effect is extinguished. Yield of liquids in coal pyrolysis was more than doubled and the total volatiles yield was increased by about 20%. When steam treated coal was exposed to ambient air, both pyrolysis and extraction yields were reduced to the level of raw coal. Analysis of pyrolysis liquids from pretreated Illinois No.6 coal showed a decrease in molecular weight with a simultaneous increase in oxygen content compared to raw coal (Graff *et al.*, 1988). Based on the results of analyses performed on raw and steam pretreated coal (Brandes *et al.*, 1989) it was concluded that during steam pretreatment new hydroxyl groups are introduced. As a result, the covalent cross-links in coal are greatly reduced yielding a partially depolymerized coal, potentially, an improved feedstock for liquefaction processes.

With this success of steam pretreatment in pyrolysis, it was logical to test its application to direct liquefaction. Previous attempts by others to obtain an improvement in liquefaction yield by this method had, however, failed. As noted above, pyrolysis studies showed that heating coal above 360°C could destroy the effect of pretreatment. It was, therefore, reasoned that the heating of pretreated coal to liquefaction temperatures must be done rapidly to minimize deleterious retrogressive reactions. A tubing bomb or stirred autoclave (employed in the conventional way) would not be adequate to carry out liquefaction under rapid heating conditions. One way to achieve high heating rates is to use a method in which a slurry of pretreated coal is injected into a hot liquefaction reaction vessel (Whitehurst *et al.* 1976). A system of this type, with some modifications, was designed, assembled, tested and used for the liquefaction tests. Furthermore, as it is known that the benefits of pretreatment are observed only if exposure of steam treated coal to air is rigorously avoided, it is necessary to conduct all operations with pretreated coal under an inert atmosphere. To satisfy this requirement, a nitrogen filled glove bag is used for sample workup and the oxygen concentration of the bag monitored by mass-spectrometer. To verify successful pretreatment, the pyridine extraction yield is determined for each steam treated coal sample.

In this work liquefaction tests of raw and steam pretreated Illinois No. 6 coal were made to determine the pretreatment effect on yield of liquids and on quality of product. These tests were conducted using the slurry injection autoclave described above pressurized with hydrogen and using tetralin as the donor solvent. The effect of exposure of treated coal to air and the role

of coal slurry heating rate were examined at three different conditions of liquefaction severity.

EXPERIMENTAL METHODS

Coal Sample. Pretreatment and liquefaction experiments were conducted with Illinois No.6 coal from the Pennsylvania State University Sample Bank (DECS-2) ground under nitrogen to pass 200 mesh using a gas impact pulverizer (Trost). Ground coal was riffled, placed in a glass jars, flushed with inert gas, sealed, and stored under refrigeration.

Steam Pretreatment. Steam pretreatment was conducted in a continuous flow of steam using the procedure described by Graff and Brandes (1987) and Graff *et al.* (1988, pp 3-5). The coal was reacted with 50 atm steam at 340°C for 15 minutes (optimum pretreatment conditions for Illinois No.6 coal).

Liquefaction. Liquefaction experiments were conducted with raw coal, steam treated coal and steam treated coal exposed to air under conditions of both rapid and slow heating, using tetralin as a hydrogen donor solvent. The liquefaction apparatus (Figure 1) consists of a 300 ml stirred autoclave (Autoclave Engineers EZE-Seal, model #P-419) and coal slurry injection system (loading reservoir and 1000 psia rupture disc assembly which separates the reservoir from the autoclave). Nitrogen and hydrogen are supplied from high pressure cylinders.

Rapid heating liquefaction is conducted as follows:

Sixty grams of deoxygenated tetralin are placed into the reaction vessel and the autoclave is sealed. After the system is leak tested with nitrogen at 2000 psia with the bypass line valve open, the reactor is flushed with hydrogen at atmospheric pressure and then heated using an electric furnace and keeping the bypass line valve closed. While the reactor is heated, slurry is prepared in a nitrogen filled glove bag from the pretreated coal and the solvent. The slurry is made of 1/3 part of coal and 2/3 parts of solvent using about 20 grams of coal. When the autoclave has been preheated to operating temperature, two syringes are filled, one with about 40 ml of slurry and one with 20 ml of solvent. The syringes are attached to the loading line, the loading valve is opened, and the slurry reservoir is sequentially filled with 10 ml of solvent, coal slurry (full contents of the syringe), and, finally, 10 ml of solvent. The loading valve is then sealed and hydrogen at the desired pressure is applied. This causes the rupture disc to burst, injecting slurry into the reactor and pressurizing the system. The valve above the reservoir is then closed. The reaction temperature is maintained with ± 5°C accuracy. The run duration is measured from coal injection. Then the heater is turned off, removed from the autoclave and the run is terminated.

In slow heating liquefaction tests the same procedure is employed except that slurry is injected when the autoclave is at room temperature. The reaction mixture is then heated to operating temperature. The reaction time count starts when the desired operating temperature is reached.

After the liquefaction run is completed and the reactor cooled down, coal conversion is determined using Soxhlet extraction as described by Joseph (1991). The liquid product is classified as hexane solubles (oils + gases), toluene solubles (asphaltenes), and THF solubles (preasphaltenes). In later runs, after cool down, vent gas from the autoclave is analyzed continuously sampling the gas vented from the autoclave directly into a mass spectrometer (Extranuclear Laboratories, Inc.; Model C50). The total gas yield, including volatiles loss during pretreatment (8 wt% at the conditions used), is determined and then subtracted from the value of hexane solubles (oil + gas) to obtain the yield of oils alone.

RESULTS AND DISCUSSION

Liquefaction runs were conducted with Illinois No. 6 coal at three sets of conditions:

High severity: 400°C, 1500 psia, 30 minutes,
Low severity a: 350°C, 1500 psia, 30 minutes, and
Low severity b: 385°C, 1500 psia, 15 minutes.

The results are shown in Tables 1, 2, and 3, classified according to the liquefaction conditions employed. All yields are based on the moisture and ash free (maf) raw coal charge.

High Severity Liquefaction. First, raw coal was examined under slow (run C2) and rapid (runs 2 and 8) heating liquefaction conditions. Then, a series of tests with steam treated coal were conducted: runs 6 and 12 were carried out under rapid heating conditions. The importance of preventing the exposure of pretreated coal to oxygen (run 11) and the importance of rapid heating (run 10) for the liquefaction were also demonstrated. Results are shown in Table 1.

The total yield of liquid product from raw coal obtained at rapid heating conditions appears to be slightly lower than at slow heating due to the longer overall reaction time in a slow heating run. The yield of oils, however, is increased and preasphaltene yield is decreased. No improvement in the yields was observed when steam pretreated coal was subjected to the liquefaction under slow heating. Compared to raw coal, a lower total yield as well as a lower yield of each fraction were obtained. In rapid heating liquefaction, however, the yield of hexane solubles are substantially increased while asphaltenes are reduced. When steam treated coal is deliberately exposed to ambient air for one hour before slurrying with deoxygenated tetralin, the pretreatment effect deteriorated. The oil yield decreased even below the value for raw coal with rapid heating. Total yield also decreased. Asphaltene yield is higher and preasphaltenes yield is lower when an exposure to air is prevented.

Low Severity Liquefaction a. Raw and steam pretreated coal were tested under rapid heating conditions at reduced severity (low severity liquefaction a). In addition to liquid product characterization, the amount of gas formed in the process was also determined. Liquefaction yields are shown in Table 2.

The results obtained under these reduced severity conditions show no improvement in the liquefaction yields between raw and steam pretreated coal. (That the pretreatments were successful was confirmed by the increased pyridine extraction yields.) Steam pretreatment did, however, increase gas yield at the expense of oils.

A possible explanation for the lack of improvement in yields after steam pretreatment may be found in the temperature history in the autoclave. The coal slurry (made of raw or steam treated coal) was injected into the autoclave preheated to 350°C. In all cases the injection caused the temperature to drop below 300°C. This was followed by a recovery to 350°C in about 1.5 minutes. Consequently, the sample had passed through a region below 360°C where retrogressive reactions occur, resulting in low yield of the liquid product and in a higher yield of gas. Perhaps, the chosen reaction temperature itself, 350°C, is where retrogressive reactions occur.

Low Severity Liquefaction b. To keep the reaction temperature higher after slurry injection and during the reaction, the low severity liquefaction temperature was increased to 385°C (which is above the upper limit of pretreatment), the reaction time reduced to 15 minutes, and the pressure was left unchanged at 1500 psia. The procedure was also slightly modified: the autoclave was initially preheated to 400°C. After the temperature drop caused by the slurry injection, the temperature was raised to 385°C. The results are shown in Table 3. In all rapid heating liquefaction experiments the reaction temperature never dropped below 320°C.

Low severity liquefaction b tests show a strong improvement in the quality of product resulting from steam pretreatment under rapid heating conditions (runs no. 31 and 34 compared to runs no. 32 and 33). The yields of hexane solubles were increased with a slight reduction in the total gas make. Remarkably, the oil yields are doubled while preasphaltenes are reduced. This improvement in the liquid quality occurred together with an increase in the total yield of liquids.

Exposure of steam treated coal to air (runs no. 35 and 36) resulted in a drop in the yield of hexane solubles and oils almost to the level of raw coal. The total yield of liquids also decreased. In slow heating liquefaction (runs no. 37 and 38), the total yield of liquids has dropped compared to rapid heating, but is still higher than raw coal under rapid heating. Of the three liquid fractions, only hexane solubles are distinctly affected by heating rate. Under slow heating conditions the highest total gas make was observed, the total yield of hexane solubles and oils alone have intermediate value between raw and steam treated coal under rapid heating. The higher total yield under slow heating liquefaction may result from a longer reaction time (it takes up to 30 minutes to preheat autoclave to 385°C), since the liquefaction process starts before the reactor temperature reaches 385°C, even under low pressure.

Summarizing these results, the behavior of Illinois No.6 coal in low severity b liquefaction follows the same trends as high severity. The best results, highest total yield and yield of hexane solubles, are obtained from steam pretreated coal under rapid heating conditions. Moreover, the improvement in the hexane solubles is achieved as a result of an increase in the yield of oils and a decrease in gas yield (at least at low severity). The liquefaction yields (total yield and hexane solubles) obtained from steam treated coal under slow heating conditions have intermediate values between raw and steam treated coal under rapid heating. When steam treated coal is deliberately exposed to air, the total yield drops to the level of raw coal (rapid heating), the yield of hexane solubles is slightly higher than from raw coal under rapid heating

but does not exceed the value obtained under slow heating.

CONCLUSIONS

The following conclusions are drawn from this work:

1. Steam pretreatment substantially improves the quality of the liquid product in coal slurry liquefaction. Under low severity conditions, the oil yield is more than doubled, going from 12.5 to 29 wt %.

2. The benefits of steam pretreatment can be realized only if the pretreated coal is rapidly heated to liquefaction temperature. This is necessary in order that the pretreated coal pass quickly through the region of retrogressive reactions. This region, in which retrogressive reactions can mitigate or even destroy the effects of pretreatment, extends downward from 360°C to perhaps as low as 320°C. The upper limit on heating time can not yet be specified, but appears to be about one minute (which was the recovery time for the low severity b series of tests).

3. Pretreated coal must be protected from oxygen to preserve the benefits of pretreatment.

ACKNOWLEDGMENT

This work was supported by the US Department of Energy under contract number DE-AC22-90PC90052.

REFERENCES

Brandes, S.D., Graff, R.A., Gorbaty, M.L., and Siskin, M., 1989, Energy & Fuels, 3, 494

Graff, R.A. and Brandes, S.D., 1987, Energy & Fuels, 1, 84

Graff, R.A. Zhou, P. and Brandes, S.D., 1988, *"Steam Conditioning of Coal for Synfuels Production"*, Final Report, DOE Contract No. DE-AC21-87MC23288.

Witehurst, D.D., Farcasiu, M., Mitchel, T.O., 1976, "The Nature *and Origin of Asphaltenes in Processed Coals"*, Annual Report, EPRI AF-252.

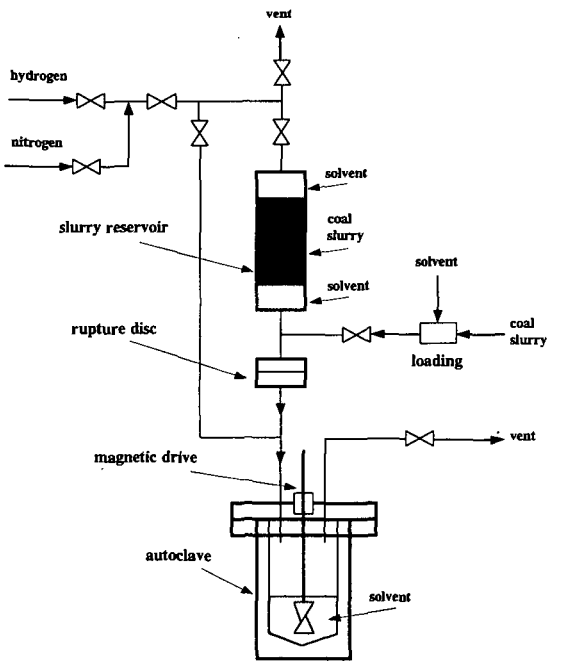

Figure 1. Stirred Autoclave with Coal Slurry Injection (Shown Prior to Coal Slurry Injection)

Table 1.
High Severity Liquefaction of Illinois No.6 coal.
(400°C, 1500 psia, 30 minutes)

		Conversion (%wt)			
Run No.	Conditions	Total (liquid + gas)	Hexane Solubles Oils+Gas	Toluene Solubles Asphaltenes	THF Solubles Preasphaltenes
C2	raw coal slow heating	81.6	37.0	16.9	27.7
2	raw coal	73.8	42.2	10.0	21.6
8	rapid heating	80.0	48.7	16.7	14.6
10	steam treated coal slow heating	73.8	35.2	14.4	24.2
6	steam treated coal	85.7	60.1	17.2	8.4
12	rapid heating	79.3	55.8	14.7	8.8
11	steam treated coal, exposure to air, rapid heating	66.3	38.6	19.8	7.9

Table 2.
Low Severity a Rapid Heating Liquefaction of Illinois No.6 Coal.
(350°C, 1500 psia, 30 min)

		Conversion (wt %)					
			Hexane Solubles			Toluene Solubles	THF Solubles
Run No.	Conditions	Total (liquid + gas)	Total	Gas	Oils	Asphaltenes	Preasphaltenes
28	raw coal	73.9	47.4	5.52	41.88	10.9	15.6
29	steam treated	71.3	47.1	13.52	33.58	9.5	14.7
30	coal	70.9	42.6	12.02	30.58	11.0	17.0

Table 3.
Low Severity b Liquefaction of Illinois No.6 Coal.
(385°C, 1500 psia, 15 min)

		Conversion (% wt)					
			Hexane Solubles			Toluene Solubles	THF Solubles
Run No.	Conditions	Total (liquid + gas)	Total	Gas	Oils	Asphaltenes	Preasphaltenes
32	raw coal	71.6	27.7	13.7	14.0	17.9	26.0
33	rapid heating	71.3	26.5	15.5	11.0	20.2	24.6
31	steam treated coal	71.3	41.8	11.9	29.9	16.4	19.3
34	rapid heating	70.9	38.9	10.3	28.6	15.8	21.5
35	steam treated coal,	71.3	30.5	14.9	15.6	18.9	23.3
36	exposure to air	70.9	31.2	13.8	17.4	17.1	23.1
37	steam treated coal	71.3	35.2	16.4	18.8	20.0	19.7
38	slow heating	70.9	34.1	19.2	14.9	18.6	27.2

EFFECT OF HYDROTREATING CONDITIONS ON HYDROCRACKING OF A COAL DERIVED LIQUID

X. Zhan, H.S. Joo, and J. A. Guin
Department of Chemical Engineering
Auburn University, AL 36849-5127

Keywords: Coal Liquid, Hydrotreating, Hydrocracking

ABSTRACT

Several coal derived liquids produced using different hydrotreating severities were hydrocracked to naphtha over a presulfided commercial hydrocracking catalyst. The feeds had similar boiling range and molecular type distribution but different nitrogen content. Feed nitrogen content had a significant effect on the hydrocracking activity, activity maintenance, and selectivity. Rapid deactivation was observed for feeds with nitrogen content higher than 50 ppm. For the feed with 50 ppm N, the gas oil (+205°C) conversion to naphtha decreased observably in the initial 4 hours. An initial catalytic activity study indicated that first order kinetics can be used to describe the gas oil conversion to naphtha. The initial hydrocracking rate of gas oil was approximately inversely proportional to the feed nitrogen content. Related model compound studies showed that the hydrocracking of cumene and hexadecane was very dependent on feed N content.

INTRODUCTION

Since it has been expected that total petroleum products demand will rise greatly before the end of this century, refiners are increasing the proportion of heavier, poorer quality crude or syncrude in their feedstocks. These feeds include less valuable petroleum stocks such as residua, and fuels derived from coal, shale, and tar sands. However, liquids derived from direct coal liquefaction still have low hydrogen to carbon ratio, high polyaromatic concentrations, and high sulfur and nitrogen concentrations. Upgrading of these liquids is required before they can be blended into refinery feeds. The primary upgrading process usually involves the hydrotreating of either the entire coal liquid or individual fractions obtained by distillation.

Although hydrogen content can be increased and heteroatoms reduced significantly in the hydrotreating process, the hydrotreated coal liquid still has a high boiling point because only minimal hydrocracking occurs in the hydrotreater. Further downstream treatment in the form of hydrocracking is necessary before fuels of high quality can be obtained. The hydrocracking process is required because coal liquids generally have a high content of polycyclic aromatic compounds, which are relatively unreactive in catalytic cracking.

Hydrocracking is a flexible refining process that allows conversion of feedstocks ranging from naphtha to residua into more valuable, lower boiling products. Hydrocracking catalysts are dual functional, consisting of hydrogenation metals on an acidic cracking base. There have been commercial hydrocracking processes using zeolite-based catalysts for converting petroleum distillates and residues.[1] The research on hydrocracking coal liquids is still very limited. In this work, we studied the activity and activity maintenance of a commercial hydrocracking catalyst using coal liquids with different hydrotreating conditions. The objective was to examine how hydrotreating conditions affect hydrocracking reactions. We also performed some model compound hydrocracking experiments to study the effect of N on hydrocracking rates.

EXPERIMENTAL

Model Compound Experiments. Reactions were performed in tubing bomb microreactors (TBMRs) charged with 1000 psig ambient hydrogen pressure. Two solutions were used : (1) 5g of hexane solution containing 2 wt% cumene, (2) 6g of pure hexadecane. Different nitrogen contents were obtained using pyridine. Experiments were performed at 350°C for cumene reactions and at 400°C for hexadecane reactions ; both for 20 min using 0.1g of a commercial NiMo/zeolite catalyst (Akzo KC2600, MoO_3 < 25%, NiO 1-10%, Al_2O_3 30-70%, SiO_2 20-50%).

Coal Liquid Experiments. The coal liquid hydrocracking experiments were carried out in both an upflow continuous reactor and TBMRs to study the deactivation behavior and

initial activity of the catalyst. The feed reactants were hydrotreated coal liquids prepared with different hydrotreating severities in a continuous reactor[2]. Four hydrotreated liquids with similar boiling range distribution and molecular type distribution but with different nitrogen contents, as summarized in Table 1, were prepared as hydrocracking feeds to investigate the effect of hydrotreating conditions on the hydrocracking reaction.

In the continuous reactor, liquid feed and hydrogen were mixed to produce a dispersive stream entering the bottom of the externally heated reactor tube. The catalyst (5 g) was crushed to 16-25 mesh, diluted with 1.0 mm glass beads (20 g), and then placed in the center of the reactor. The reactor was operated at 400°C and 9.7 MPa with a pressure drop across the reactor bed of about 0.1 MPa. Prior to the start of a run the catalyst was presulfided using 5 wt% CS_2 in cyclohexane at a liquid flow rate of 0.05 ccm and hydrogen at 100 sccm.

The TBMR runs were performed at 400°C and 6.9 MPa cold H_2 pressure. For the deactivation runs in TBMR, 4 g of liquid reactant was used with 1 g catalyst for 2 hours. The catalyst was recovered, washed in THF, and dried in air over night. This catalyst was then used for the next run with fresh feed and the same procedure was repeated for five times, so that the total time the catalyst exposed to the reaction environment was 10 hours. Prior to the first reaction, the catalyst was presulfided in the same type of TBMR using 0.5 g CS_2 for two hours at 400°C and 6.9 MPa cold H_2 pressure. For the kinetic experiments, approximately 4 g of liquid reactant was charged to the TBMR with different loadings of catalyst ranging from 0.1 g to 1 g. The reaction time was from 20 to 120 min. The liquid product was collected and analyzed using GC simulated distillation according to ASTM test method D2887. While the detailed GC boiling curve was obtained, for simplicity of discussion, the product boiling range distribution in this study was grouped into three cuts only: gas, naphtha (-205 °C), and gas oil (+205 °C). The gas make was obtained by difference using the weights of feed and liquid products. The percentage of gas make was defined as

$$\text{Gas Make} = \frac{\text{wt. of gases after RXN} - \text{wt. of Initial } H_2}{\text{wt. of liquid feed}} \qquad (1)$$

RESULTS AND DISCUSSION

Model Compounds Experiments. The effect of feed nitrogen content on cumene and hexadecane conversion is shown in Figure 1. Cumene conversion without nitrogen was 96%. It is relatively easy to crack cumene into benzene and propylene due to the tertiary carbon of cumene which can form very stable tertiary carbonium ions on acid sites. The reactions of hexadecane, a straight-chain paraffin, showed about 51% conversion in the absence of nitrogen. In this reaction (0 ppm N), 5% gas, 41% naphtha, and 54% of gas oil were obtained and 82% of the hexadecane converted was in the naphtha fraction. KC2600 catalyst with hexadecane in the absence of nitrogen has very good selectivity for naphtha. Little conversion was observed above 100 ppm N in both reactions. These results show that the hydrocracking activity of KC2600 is completely poisoned by amounts of nitrogen around 100 ppm and nitrogen removal from the high nitrogen containing feeds such as coal derived liquids is required prior to the hydrocracking process. The catalytic cracking and hydrogenation functions of KC2600 (NiMo/zeolite) can be examined by two reaction pathways of cumene hydrocracking.

1: cumene → benzene + propylene → other products
2: cumene → iso-propylcyclohexane → other products

Pathway 1 is cumene cracking to benzene (B) and propylene (PP) by acid sites mainly on the zeolite. In pathway 2, cumene is hydrogenated to iso-propylcyclohexane (IPCH) by metal sites (Ni and Mo) followed by cracking to other compounds such as cyclohexane (CH), PP, etc. From these experiments, the concentrations of cumene, B, and IPCH from cumene reactions as a function of nitrogen content are shown in Figure 2. The concentration of B was about 0.7% at 0 ppm N and decreased to 0 at about 33 ppm N. IPCH was observed to appear at about 13 ppm N. Below 13 ppm, IPCH is probably cracked to form CH and PP. The IPCH concentration increased to a maximum around 33 ppm N and decreased to about 0 above 100 ppm N. These observations show the following. Below 10 ppm N, cracking reactions by acid sites are dominant. As nitrogen content increases from 10 ppm, however, acid sites are poisoned. On the other hand, metal sites have substantial activity in the range of 10-100 ppm N with IPCH being the main product identified. This activity was also poisoned above 100 ppm N. It can be concluded that the acid function for reaction pathway 1 is severely poisoned around 33 ppm N, while the hydrogenation function (Ni and Mo) still has some activity up to

about 100 ppm N.

Coal Liquids Experiments. Figure 3 shows the lumped boiling range distribution of the hydrocracking liquid products from continuous reactor. The feed had a nitrogen content of 230 ppm (Feed B in Table 1), and the reaction conditions have been described previously. It is seen that there is a significant deactivation of the catalyst, and it is completely deactivated in 24 hours on stream, as reflected by the gas oil content. However, very high hydrocracking activity was observed in a TBMR run with fresh catalyst, which is also shown in Figure 3. It is probable that, during the first few hours in the continuous reactor, the liquid produced might contain low gas oil fraction (high naphtha fraction) because of initially high cracking activity. The gas oil content then increased gradually due to catalyst deactivation. As a result, the sample collected in the first 24 hours, which is actually a mixture produced during this period, exhibited some gas oil conversion, but not as high as that in TBMR in which the reaction time was only 2 hours. The rapid deactivation of the catalyst is speculated to be due to nitrogen or polyaromatics in the feed. Therefore, as a follow on to this study, several deactivation runs were performed in TBMRs with different feed nitrogen contents.

Figure 4 shows the experimental runs made to examine the effect of feed hydrotreating conditions on the hydrocracking reactions. In the following, the feed N content is used as a measure of hydrotreating severity, although other feed characteristics, e.g. polyaromatics content, are also important in catalyst activity behavior. Figure 4 shows that the gas oil conversion decreases with the increase of nitrogen in the feed. The deactivation rate also increases with the increase of nitrogen content, except for the 1800 ppm N feed, where gas oil conversion was low. This is consistent with previous results in the literature. Yan[3] reported that for the hydrocracking of heavy gas oil over NiW/REX-NiW/silica-alumina, when the nitrogen content was increased from 1 ppm to 12 ppm, the reactor temperature had to be increased by 16.7°C to maintain the same catalyst activity. Bouchy et al[4] studied the hydrocracking of a model light cycle oil with 480 ppm N in the feed. They found that the inhibiting effect of nitrogen led to a decrease of the reaction rate of about 30%. It is generally agreed that nitrogen compounds will irreversibly adsorb on acidic sites of hydrocracking catalysts and thus reduce their effectiveness and activity maintenance. It thus appears that a more active hydrotreating catalyst must be developed or more severe hydrotreating conditions should be employed for HDN to reduce the nitrogen content to even lower levels. Another option lies in the development of new hydrocracking catalysts which are more resistant to nitrogen poisoning. Yet it should be noticed that the yield of desired product, e.g., naphtha formation, also might be greatly affected by the catalyst activity and reaction conditions, as is seen in Figure 5 where considerable gas formation was accompanied with gas oil conversion. It seems that some nitrogen in the feed may function to temper the catalyst activity towards gas formation. Therefore, it appears that quantitative determination of the hydrocracking rate constant and the nitrogen effect would be meaningful for the optimal design of hydrocracker for the coal liquid.

To quantify the effect of N content on the initial hydrocracking rate, an empirical power-law kinetic model, as shown in equation (2) was used to describe the gas oil conversion.

$$-\frac{dy_A}{dt} = \frac{W_{cat}}{W_{liq}} k y_A^{\ a} p_H^{\ b} \qquad (2)$$

In equation (2), y_A is the weight fraction of gas oil, p_H is the partial pressure of hydrogen which is directly proportional to the weight fraction of dissolved hydrogen, W_{cat} is the weight of catalyst, and W_{liq} is the weight of liquid feed. The term $W_{cat}t/W_{liq}$ is equivalent to the reciprocal of WHSV generally used in flow reactors.

Figure 6, plotted as weight fraction vs. reaction time, suggests that the reactions can be adequately described using the following consecutive reaction scheme, because the initial rate of gas formation is zero, and the reaction rate of naphtha to gases is much slower than that of gas oil to naphtha.

Gas Oil ——> Naphtha ——> Gases

In Figure 6, the data were obtained with catalyst loading from 0.1 to 1g, three particle sizes (16-25, 60-80, 80-200), and reaction time from 20 to 120 min. There was no discernable effect of catalyst loading, particle size, or reaction time, therefore, it is believed that, in our experiments, there is neither internal nor external mass transfer limitation and the data represent the results of reaction kinetics. At $W_{cat}t/W_{liq}$ larger than 0.15 hour, the percentage of naphtha

is essentially stable, but more gas was generated with time at the expense of gas oil. Thus, it appears that a value of $W_{cat}t/W_{liq}$ of no more than 0.15 (or WHSV in flow reactor larger than 6) would be appropriate for the hydrocracking of coal liquid, if the desired product is naphtha. In practice, the value of WHSV in a flow reactor is typically less than 6 because the catalyst will be deactivated somewhat in the initial reaction period.

Since the TBMR is a batch reactor, the hydrogen partial pressure decreases with gas oil conversion. For this reason, the rate constant was evaluated using the low gas oil conversion data. The hydrogen concentration in the liquid, which is approximately directly proportional to its partial pressure, was also assumed constant during this initial stage. Therefore equation (2) is reduced to equation (3).

$$-\frac{dy_A}{d\left(\frac{W_{cat}}{W_{liq}}t\right)} = k' y_A^{\alpha} \qquad (3)$$

The linear plots of Figure 7, $\ln (y_{A0}/y_A)$ vs. $W_{cat}t/W_{liq}$ according to equation 3, indicate that gas oil hydrocracking can be described as a first order reaction. The effect of feed nitrogen content is significant. The reaction rate is approximately inversely proportional to nitrogen content. Since this study considered only the initial reaction rate of gas oil conversion, no quantitative effect of feed nitrogen content on catalyst activity towards gas formation was determined as it was generally less than 1%.

REFERENCES

1 Song, C., Schobert, H.H., and Matsui, H., ACS Fuel Chem. Prepr., 36(4), 1892-1899, 1991.

2. Zhan, X., Joo, H.S., and Guin, J.A., paper in preparation for Energy and Fuels.

3 Yan, T.Y., Ind. Eng. Chem. Res., 28(10), 1463-1466, 1989.

4 Bouchy, M., Peureux-Denys, S., Dufresne, P., and Kasztelan, S., Ind. Eng. Chem. Res., 32(8), 1592-1602, 1993.

Table 1. Properties of Feeds for Hydrocracking

Feed	A	B	C	D
Nitrogen Content (ppm)	50	230	820	1800
Naphtha (-205°C) (wt %)	14.1	11.3	10.5	10.3
Gas Oil (+205°C) (wt %)	85.9	88.7	89.5	89.7
Molecular Type Distribution (wt%)				
Paraffins	17.3	15.3	14.4	11.4
Naphthenes	26.2	24.0	22.6	21.1
Monoaromatics	34.8	37.4	39.3	42.3
Polyaromatics	21.7	23.3	23.7	25.2

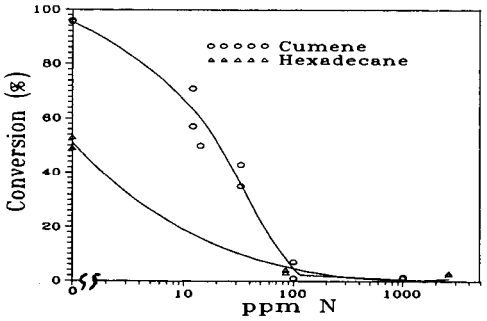

Figure 1 Effect of Nitrogen Content on Cumene and Hexadecane Conversion.

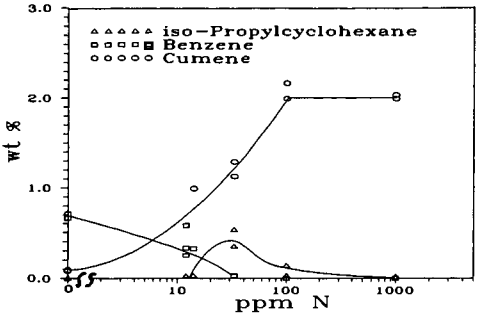

Figure 2 Product Distribution of Cumene Reactions as a Function of Nitrogen Content.

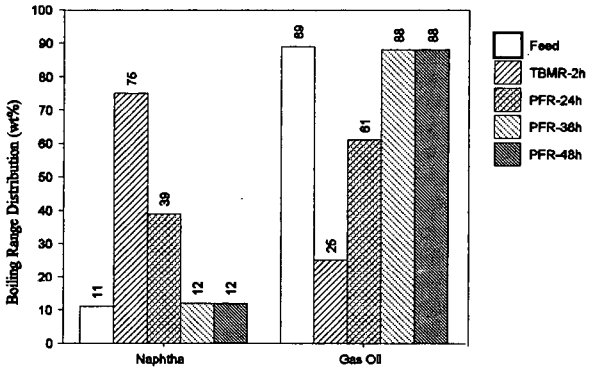

Figure 3 Hydrocracking Catalyst Deactivation in Continuous Reactor with Feed Nitrogen Content of 230 ppm.

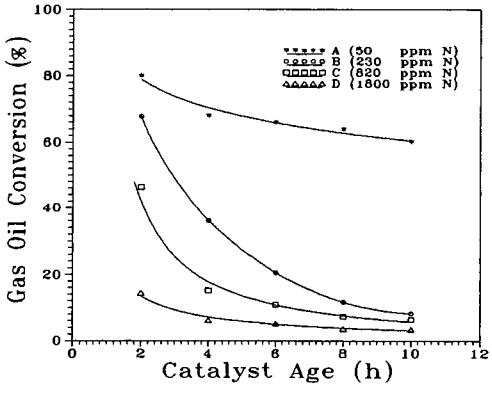

Figure 4 Effect of Feed Nitrogen Content on the Catalyst Deactivation Behavior and Gas Oil Conversion in Successive 2h TBMR Experiments.

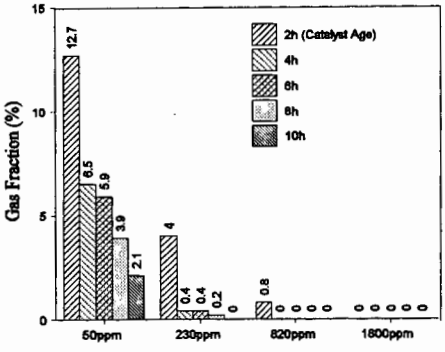

Figure 5 Effect of Feed Nitrogen Content on the Gas Make for Hydrocracking Reactions in TBMR

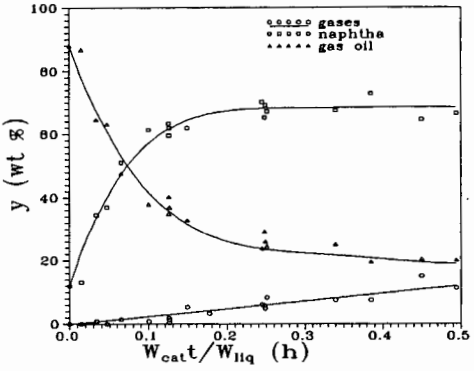

Figure 6 Hydrocracking Product Distribution at 400°C with Feed Nitrogen Content of 230 ppm

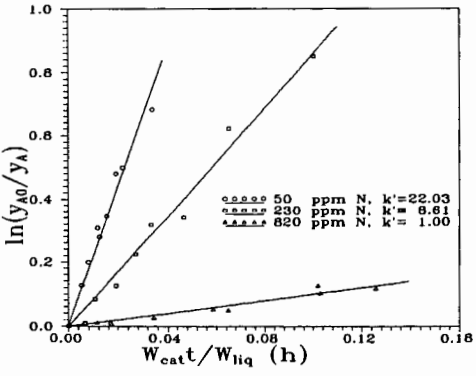

Figure 7 First Order Plots of Gas Oil Conversion with Different Feed Nitrogen Contents

EFFECT OF IRON CATALYSTS ON HYDROGENATION PATHWAYS IN DIRECT COAL LIQUEFACTION

Richard K. Anderson, William J. Clements, Edwin N. Givens and Frank J. Derbyshire
University of Kentucky, Center for Applied Energy Research
3572 Iron Works Pike, Lexington, KY 40511-8433

Keywords: Coal liquefaction, iron catalyst, hydrogenation

Abstract

The effect of a commercially available, high surface area nanometer size iron oxide (SFIO) catalyst on the pathway by which hydrogen is added to a subbituminous coal during direct liquefaction was studied under a variety of conditions. This unique iron oxide, prepared by pyrolyzing volatilized iron carbonyl to produce a finely divided product, is characterized as γ-Fe_2O_3 having a surface area of ~300 m^2/g and particle size of 1-3 nm. Liquefying Wyodak coal in tetralin (0.5 hrs, 415 °C, 2.3 tetralin/dry coal, 6.89 MPa H_2 cold) containing 1.2 wt % Fe as SFIO resulted in an increase in overall coal conversion (77 to 83%) with most of the increase in product being in formation of THF soluble-pentane insoluble product. Adding an excess of sulfur to convert the iron to pyrrhotite further increases conversion to 85% along with a decrease in the THF soluble-pentane insoluble fraction. The presence of catalyst increases the amount of hydrogen added to the product as dihydrogen (H_2) relative to the amount from tetralin via the H-donor pathway. In the absence of catalyst, 60% was added as H_2; adding 1.2% Fe increased H_2 addition to 67%; adding 3 mol S/mol Fe to 1.2% Fe further increased H_2 addition to 82%.

Introduction

Through the use of various types of catalysts, high yields of distillate fuels have been produced in pilot plants from lower-cost subbituminous coal.[1,2,3] The use of high surface area, small particle catalysts has been one area that has been extensively explored in an effort to maximize yields and reduce the cost of catalyst. Fe has been of particular interest as a dispersed catalyst because of its abundance, low cost and its environmental acceptability. Various approaches have been used for preparing disposable nanometer size Fe catalysts, among which are microemulsions,[4,5] aerosols,[6,7,8,9] hydrothermal disproportionation of sulfides,[10] and precipitation of sulfated oxyhydroxides.[11] Highly dispersed iron particles, in various forms as oxides and oxyhydroxides, have been shown to retain their small size upon conversion to pyrrhotite under coal hydroliquefaction conditions.[6,7,12]

In our laboratory, a specially prepared, commercially available superfine Fe oxide (SFIO) was found to have high activity for coal conversion and excellent selectivity for producing distillate product.[13] In the study reported here, the activity of this catalyst for conversion of a Wyodak coal in tetralin was compared with a much lower surface area Fe oxide prepared from Aiusruther spray roast processing of spent acid from steel pickling.[14] The effect of these catalysts on the pathways by which hydrogen (H) is added to the coal and its products was investigated.

Experimental

Samples of the subbituminous coal and powdered iron oxides used at the Wilsonville Advanced Coal Liquefaction Facility in Run 263J[14] were supplied by CONSOL, Inc. The Wyodak coal from the Black Thunder mine in Wright, Wyoming was ground to -200 mesh, riffled and stored under nitrogen at 4 °C. Proximate and ultimate analyses are presented in Table I. The average moisture content measured at the beginning of each run was 21.9 ± 0.72 wt % of as-received coal.

Two iron oxide catalysts were used. One, a sample of SFIO provided by MACH I, Inc., King of Prussia, PA, contained 63 wt % Fe with a γ-Fe_2O_3 structure, average particle size of 1-3 nm, and nitrogen BET surface area of 300 m^2/g.[15] The second, from Bailey Engineers, Fairfield, AL, (IO) was 99% Fe_2O_3 with 0.35 wt % manganese oxide being the largest impurity. The material had a structure of α-Fe_2O_3, nitrogen BET surface area of 8.6 m^2/g, an average particle size of ~140 nm, and bulk density 26 times greater than SFIO (1.37 vs. 0.052 g/ml). Carbon black (CB) was purchased from UIC, Inc. and had a fixed carbon content of 93% with a nitrogen BET surface area of 90 m^2/g.

Liquefaction experiments were conducted by adding 3 grams of coal, 5.4 grams of tetralin, and catalyst to a 50 mL microautoclave. When used, dimethyl disulfide (DMDS) was added at a ratio of 3.0 moles S per mole Fe. The reactor was sealed, pressurized with H_2 to 6.89 MPa, and immersed in a fluidized sand bath set at the specified temperature while continuously agitating at a rate of 400 cycles per minute. After the specified reaction period, the microautoclave was rapidly cooled in a sand bath at room temperature. Gaseous products

were collected and analyzed by gas chromatography. Solid-liquid products were washed from the reactor using tetrahydrofuran (THF) and extracted in a Soxhlet apparatus for 18 hours. The THF-insoluble material (IOM), comprising unconverted macerals and mineral matter, was dried (80 °C/0.1 atm). A pentane insoluble-THF soluble fraction (PA+A) was precipitated from the concentrated THF soluble fraction by adding pentane. The pentane soluble material (Oils) was analyzed with a Hewlett-Packard 5890 gas chromatograph fitted with a DB-5 column to determine the naphthalene-tetralin ratio. Product yields were calculated assuming complete recovery of the inorganic mineral matter plus catalyst, which was demonstrated independently. Fe in the catalyst precursor is presumed to convert to pyrrhotite ($Fe_{0.9}S$) and report to the ash fraction. Oils are calculated by difference, which includes water produced during the reaction and any experimental error. The net product yield equals the amount of maf coal in the feed and coal conversion equals 100 minus the yield of IOM. The average standard deviations for each product fraction were calculated: hydrocarbon gases, 0.1; $CO+CO_2$, 0.4; IOM, 1.4; PA+A, 2.4; Oils, 2.8.

Discussion

The dominant phase of the SFIO, as determined by X-ray absorption fine structure (XAFS) analysis, is $FeOOH{\cdot}xH_2O$ with bulk iron coordinated to six oxygen or hydroxyl groups along with a significant additional fraction of the iron located at the particle surfaces at sites with lower coordination.[16] Extended heating at temperatures >400 °C produces α-Fe_2O_3. Considerable particle growth occurs upon sulfidation in the presence of H_2S and tetralin at 380 °C, with the formation of pyrrhotite having a particle size of several hundred nanometers.[17] However, in the presence of coal, sulfiding produces a much smaller particle size pyrrhotite[6] which has also been observed on Fe-impregnated carbon black.[18]

Approximately 95% of the Fe contained in the residue isolated from runs to which 1.2 wt % Fe was added as SFIO was present as the oxide, even though the amount of sulfur present in the coal (0.39%) was sufficient to convert ~70% of the added Fe to pyrrhotite. However, pyrrhotite would only form when sulfur was added to the reaction mixture. In runs to which a 3-fold excess of sulfur was added along with 1.2 wt % Fe, >95% of the Fe was converted to pyrrhotite within 7.5 min, indicating that when sulfur was present pyrrhotite formed rapidly and was present during almost all of the reaction period. Since particle size of the resulting pyrrhotite was previously reported to be related to the size of the original oxide, SFIO should provide pyrrhotite having a smaller size with correspondingly higher surface area than IO.

As seen in Table II, THF conversion increased when Fe oxides were added to the reaction mixture, while adding sulfur along with the Fe oxides further increased conversion. In the absence of sulfur at 30 minutes runtime, adding SFIO and IO resulted in conversions of 83.4 and 80.2%, respectively, relative to a conversion of 76.7% in the absence of added Fe oxides. The increase was greater for SFIO suggesting a response to the higher surface area. Reactions in which sulfur was added follow the same pattern with SFIO giving higher conversion. At 30 min, addition of sulfur to SFIO and IO increased conversions to 85.4 and 83.6%, respectively, while at 60 min, conversions were 88.8 and 87.0%, respectively.

Oils yields responded quite differently to addition of Fe oxide in the absence of added sulfur. In both cases shown, they actually decreased somewhat, resulting in a buildup of PA+A. When SFIO and IO were present in the 30 min runs, Oils yields decreased to 29.7 and 26.2%, respectively, relative to a yield of 31.8% in the absence of added Fe. When sulfur was added, oil yields increased for both Fe oxides. After 30 min, yields upon addition of SFIO and IO were 36.7 and 37.0%, respectively, while after 60 min, yields were 46.2 and 46.8%, respectively, compared to 42.6% in the absence of added Fe. The sulfided catalyst is clearly better than the oxide for promoting Oils yield.

Adding sulfur to the reaction at the same level as in the other experiments but in the absence of any added Fe oxide caused an increase in conversion from 76.7 to 79.1% and a decrease in Oils yield from 31.8 to 28.2%. At this level of sulfur addition, the calculated initial H_2S partial pressure in the reactor at reaction temperature was 25 psig. The effect on conversion and Oils yield was similar, though less effective than adding Fe oxides in the absence of added sulfur. Since the combined addition of sulfur and Fe oxides was superior to the addition of the Fe oxides alone, the direct contribution from adding sulfur at this level (equivalent to ~1% H_2S in H_2) is small relative to its effect on the chemistry of the Fe in the reaction.

Total H consumption in these reactions was determined from analysis of dihydrogen (H_2) in the gaseous product and the H remaining in the solvent. The latter was calculated from a determination of the change in ratio of naphthalene to tetralin in the pentane soluble fraction. Total H consumption appeared not to increase upon addition of SFIO or IO in the absence of sulfur. Adding sulfur with the Fe oxide had little effect on hydrogen consumption using IO, but a significant effect on hydrogen consumption with SFIO. Total H consumption, based upon maf coal, in the presence of SFIO in the 30 min runs increased from 36 mg/g in the

absence of sulfur to 45 mg/g when sulfur was added. The consumption of H_2 from the gas phase reflected this increased activity. In the 30 min runs, reaction of coal in the absence of additives and in the presence of SFIO gave H_2 consumptions of 23 and 24 mg/g, respectively. Adding sulfur to the SFIO increased H_2 consumption to 37 mg/g. Similar activity changes were observed for the 60 min runs.

The effect of adding 14% of a high surface area carbon (90 m^2/g) on conversion, product yields and H consumption was negligible. Even though the available N_2 BET surface area was more than double the surface area from adding SFIO at a 1.2% Fe level, the reaction did not change. Clearly, the catalytic effect of adding SFIO is not merely a response to added surface area.

Conclusions

Conversion of Wyodak coal to THF soluble product increases in the presence of added Fe oxide, regardless of the presence of sulfur. The higher surface area SFIO is more active than IO for conversion. Both SFIO and IO increase Oils yields when sulfur is added but have little effect in its absence. Since addition of sulfur to coal in the absence of added Fe oxides had little effect on the reaction, the mechanism by which sulfur affects the reaction is presumed to be through sulfiding the Fe. Total H consumption was affected only when both SFIO and sulfur were added to the reaction. The other cases showed little response. The contribution of tetralin to the amount of H consumed in the reaction appears to be relatively constant for reaction times of 30 and 60 min suggesting the reaction pathway involving H-transfer from solvent to coal is important early in the reaction sequence. The effect of SFIO with sulfur, the catalyst that significantly improved H consumption, is to increase direct H_2 addition to the product. The absence of any effect of adding high-surface area carbon indicates that surface area alone is not responsible for the improvement from adding the Fe-oxides.

Acknowledgement

The authors gratefully acknowledge the support of the Department of Energy under contract DE AC22-91PC91040. We also thank Frank Huggins for contributing Mössbauer studies of the liquefaction residues and Z. Feng for her TEM work.

References

1. Southern Electric International, Inc., Technical Progress Report, "Run 262 with Black Thunder Mine Subbituminous Coal" *Document No. DOE/PC/90033-22*, September, 1992.
2. Bauman, R. F.; Coless, L. A.; Davis, S. M.; Poole, M. C.; Wen, M. Y. Continuous Bench-Scale Slurry Catalyst Testing- Direct Coal Liquefaction of Rawhide Sub-bituminous Coal. Proceedings: Coal Liquefaction and Gas Conversion Contractors Review Conference. Pittsburgh, PA. Aug. 1995, p91.
3. Pradhan, V. R.; Lee, L. K.; Stalzer, R. H.; Johanson, E. S.; Comolli, A. G.; Catalytic Multi-stage Liquefaction of Coal at HTI- Bench-scale Studies in Coal/ Waste Plastics Coprocessing. Proceedings: Coal Liquefaction and Gas Conversion Contractors Review Conference. Pittsburgh, PA. Aug. 1995, p75.
4. Wilcoxon, J. P.; Sylwester, A.; Nigrey, P.; Martino, A.; Quintana, C.; Baughman, R. J. *Proceedings, Eighth Annual Inter. Pittsburgh Coal Conf.* 1991, 703.
5. Darab, J. G.; Fulton, J. L.; Linehan, J. C. *Prepr. Pap.- Am. Chem. Soc., Div. Fuel Chem.* 1993, *38(1)*, 27.
6. Andres, M.; Charcosset, H.; Chiche, P.; Davignon, L.; Djega-Mariadassou, G.; Joly, J. P.; Pregermain, S.; *Fuel* 1983, *62*, 69.
7. Andres, M.; Charcosset, H.; Chiche, P.; Djega-Mariadassou, G.; Joly, J-P.; Pregermain, S. *Preparation of catalysts III* (Eds. G. Poncelet and P. Grange), Elsevier: Amsterdam, 1983, pp 675-682.
8. Dadyburjor, D. B.; Stiller, A. H.; Stinespring, C. D.; Zondlo, J. W.; Wann, J.; Sharma, R. K.; Tian, D.; Agarwal, S.; Chadha, A. *Prepr. Pap.- Am. Chem. Soc., Div. Fuel Chem.* 1994, *39(4)*, 1088.
9. Rice, G. W.; Fiato, R. A.; Soled, S. L. 05/26/87. Iron carbide-based catalyst produced in the presence of laser radiation. U. S. Patent 4668647.
10. Dadyburjor, D. B.; Stewart, W. R.; Stiller, A. H.; Stinespring, C. D.; Wann, J. P.; Zondlo, J. W. *Energy Fuels* 1994, *8(1)*, 19.
11. Pradhan, V. R.; Tierney, J. W.; Wender, I. *Energy and Fuels* 1991, *5*, 497-507.
12. Djega-Mariadassou, G.; Besson, M.; Brodzki, D.; Charcosset, H.; Huu, T. V.; Varloud, J. *Fuel Processing Tech.* 1986, *12*, pp 143-145.
13. Quarterly Technical Progress Report, Advanced Direct Liquefaction Concepts for PETC Generic Units, July 1994 through September 1994, DOE/PC/91040-48.
14. Southern Electric International, Inc., Technical Progress Report, "Run 263 with Black Thunder Mine Subbituminous Coal and Dispersed Molybdenum Catalysts" *Document No. DOE/PC/90033-*

23, December, 1992.
15. Srinivasan, R.; Keogh, R. A.; Davis, B. H. "Characterization of Sulfided Iron Catalysts" *Prepr. Pap.-Am. Chem. Soc., Div. Fuel Chem.* 1993, *38(1)*, pp 203-210.
16. Zhao, J.; Feng, Z.; Huggins, F. E.; Shah, N.; Huffman, G. P. "Structure and Phase Transition of an Ultrafine Iron Oxide Catalyst" *Prepr. Pap.- Am. Chem. Soc., Div. Fuel Chem.* 1993, *38(1)*, pp 196-202.
17. Srinivasan, R.- personal communication.
18. Cugini, A.V.; Krastman, D.; Martello, D. V.; Frommell, E. F.; Wells, A. W.; Holder, G. D. *Energy Fuels* 1994, *8(1)*, pp 83-87.

Table I. Black Thunder Coal Analysis

Proximate Analysis	(wt%, as-determined)	Ultimate Analysis	(wt%, dry)
Moisture	21.2	Carbon	68.68
Ash	5.15	Hydrogen	4.76
Volatile Matter	34.4	Nitrogen	1.21
Fixed Carbon	39.3	Sulfur	0.56
Sulfur Types	(wt%, dry)	Oxygen (diff)	18.25
Total	0.39	Ash	6.54
Pyritic	0.07	Ash, SO_3-free	5.42
Sulfate	0.09		
Organic	0.23		

Table II. Product distribution from liquefaction of Wyodak coal in tetralin[a]

Catalyst	none				SFIO			IO			CB[b]
Added Fe, wt% mf Coal	0	0	0	0	1.2	1.2	1.2	1.2	1.1	1.2	0
S/Added Fe mol/mol	0	0	-	-	0	3.0	3.2	0	3.0	3.0	0
H_2S Partial Pressure at temperature, psi			25	24							
Reaction time, minutes	30	60	30	60	30	30	60	30	30	60	30
Products, wt% maf Coal											
HC Gases	0.7	1.0	1.1	1.3	0.8	1.4	2.0	0.8	1.4	1.7	0.7
$CO+CO_2$	5.3	5.2	6.7	5.7	5.3	5.1	7.1	6.1	5.1	4.9	5.2
Oils	31.8	42.6	28.2	34.0	29.7	36.7	46.2	26.2	37.0	46.8	32.4
PA+A	38.9	35.4	43.1	42.2	47.6	42.2	33.5	47.1	40.1	33.6	38.2
IOM	23.3	15.8	20.9	16.8	16.6	14.6	11.2	19.8	16.4	13.0	23.5
THF Conversion	76.7	84.2	79.1	83.2	83.4	85.4	88.8	80.2	83.6	87.0	76.5
n:t ratio	0.26	0.26	0.32	0.40	0.19	0.14	0.16	0.29	0.20	0.24	0.25
Hydrogen consumed, mg/g maf Coal											
from gas	23	30	19	21	24	37	52	22	28	35	20
from solvent	15	15	18	21	12	8	10	16	12	14	16
Total	38	45	37	42	36	45	62	38	40	49	36

a. Liquefaction experiments at 415°C using 3 g Black Thunder coal, 5.4 g tetralin, 6.89 MPa H_2 cold. SO_3-free ash basis.
b. 14% carbon black added (mf coal basis, no Fe).

THE EFFECT OF H_2 PARTIAL PRESSURE AND TEMPERATURE ON CATALYTIC HYDROGENATION WITH MoS_2 CATALYSTS

A. V. Cugini, K. S. Rothenberger, M. V. Ciocco, G. A. Veloski, and D. V. Martello
U.S. Department of Energy, PETC
Pittsburgh, PA 15236

Keywords: Coal Liquefaction, Catalytic Hydrogenation, Molybdenum Catalysts.

INTRODUCTION

Molybdenum-based catalysts have been used extensively for catalytic hydrogenation[1-3]. The type of catalyst, either supported or unsupported, and the preparation and activation procedures can impact catalytic behavior for hydrogenation and coal conversion reactions. This study compared the catalytic hydrogenation and coal conversion observed with preactivated forms of supported and unsupported catalysts. The objective was to utilize model compounds to compare the catalytic hydrogenation activity of these two types of catalysts. The effect of catalyst type, supported or unsupported, on catalytic hydrogenation with and without coal present was studied over a range of pressures, 1.4 MPa (200 psig) - 11.0 MPa (1600 psig) H_2. The results indicated that catalytic hydrogenation activity was observed at H_2 partial pressures as low as 4.8 MPa (700 psig) with both catalyst types.

EXPERIMENTAL

Materials. ACS grade 1-methylnaphthalene from Fisher Scientific Company, found to be 99% pure by gas chromatography, was used without further purification. Blind Canyon coal, (DECS-6) from the U.S. Department of Energy's Coal Sample Program, was used in these studies. The Blind Canyon coal was a low pyrite bituminous coal with 6.3% ash and 3.7% moisture. A unique, high surface area, molybdenum catalyst was prepared at the U.S. Department of Energy's Pittsburgh Energy Technology Center (PETC). The catalyst consisted of the recovered solid from a semi-batch 1-L stirred autoclave reaction of ammonium heptamolybdate, hydrogen sulfide, and Panasol (a mixture of alkylated naphthalenes) under 17.2 MPa (2500 psi) hydrogen at 700 °K [2-4]. The catalyst contained 50% C, 30% Mo, and 20% S by weight, and possessed a BET surface area of approximately 260 m^2/g. Supported molybdenum/nickel catalysts, AKZO AO-60 obtained from HTI, Inc. and Shell-324, were also used. Other catalysts tested included two prepared by impregnating carbon black with Mo or Fe (Mo-C-1 and Fe-C-1, respectively), sulfated Fe_2O_3[5], and carbon black (BET surface area of 490 m^2/g) obtained from Columbian Chemicals Co.

Reactions. Reactions were conducted in a stainless steel batch microautoclave reactor system constructed at PETC. The cylindrical reactor portion has a volume of 43 mL, and the total internal volume, including all tubing and connections, is 60 mL. The reactor was mounted on a rocker arm, which extends into an electrically heated sand bath. In typical experiments, the reactor was charged with various combinations of solvent, coal, catalyst, a sulfur source, and then was pressurized with hydrogen. Unless otherwise stated, a full charge consisted of 6.6 g solvent, 3.3 g coal, 0.1 g catalyst, 0.1 g elemental sulfur, and 6.9 MPa (1000 psi) ambient temperature hydrogen gas. The reactor was then attached to the rocker arm (180 cycles / minute) and plunged into a preheated sand bath, where it was heated up to 700 °K in 2 to 4 minutes. It was held at temperature in the sand bath for 30 minutes, removed and allowed to air cool, typically in less than 5 minutes, to room temperature. The reactor was vented and the gas collected for analysis.

Sample Work up Procedure and Coal Conversion Calculation. During work up, the reactor (including tubing) was cleaned and rinsed with tetrahydrofuran (THF). The material collected was combined and filtered through a 0.45 micron filter under nitrogen gas pressure, yielding the "THF solubles" and "THF insolubles." Coal conversion was calculated based on the mass of MAF coal from the measured mass of THF insolubles adjusted for catalyst and coal mineral matter[6].

Gas and Pressure Analyses. At the completion of each run, product gases were collected and analyzed at PETC by a previously published method [7]. The product gaseous mixture composed mainly of H_2, C_1-C_4, CO_2, and H_2S, was corrected for non-ideal behavior using an equation of state, and the amount of H_2 consumed was then calculated.

Solvent Hydrogenation Analysis. Low-Voltage, High-Resolution Mass Spectrometry (LVHRMS) data were used to calculate solvent hydrogenation. LVHRMS data were obtained on a Kratos MS-50 high-resolution mass spectrometer interfaced to a personal-computer-based data system developed at PETC. Further details on the LVHRMS technique and data reduction routines are provided in references 8 and 9.

RESULTS AND DISCUSSION

The catalytic hydrogenation of 1-methylnaphthalene using various catalysts was investigated in microautoclave reactors. The results from the catalytic hydrogenation experiments are compared in Table 1. The results in Table 1 seem to indicate that supporting the catalyst (either Fe or Mo) is beneficial for solvent hydrogenation. This is somewhat surprising for the Mo system since as shown in Table 2, the dispersion (physical) for the MoS_2 catalyst is about the same or slightly greater for the unsupported than the supported catalyst. Also shown in Table 1 is the synergistic effect of having both the sulfated Fe_2O_3 and carbon black present during solvent hydrogenation. The H_2 consumption is much higher with both the sulfated Fe_2O_3 and carbon black present than with either used alone and is twice the sum of the H_2 consumed for the sulfated Fe_2O_3 and carbon black each employed separately. In addition, hydrogen consumption using the mixed pair of sulfated Fe_2O_3 and carbon black was equal to that of the highly dispersed MoS_2. A possible explanation is that the sulfated Fe_2O_3 may associate with the carbon black allowing absorbed hydrogen to migrate to the carbon surface (i.e., spillover[10]). This hydrogen could be active and could increase the amount of solvent hydrogenated and the H_2 consumption. A second possibility is that the presence of the carbon black resulted in a more dispersed form of pyrrhotite. Experiments are being conducted in order to test these possibilities.

TABLE 1. Effect of Catalyst Type on Solvent Hydrogenation, 6.9 MPa (1000 psig) H_2 cold / No coal)

Catalyst[a]	H_2 Consumed (mMol)	Solvent Hydrogenation (%)
MoS_2 (unsup.)	28	28
Mo-C-1	55	48
AO-60	54	53
Shell-324	52	53
Fe-C-1	38	19
Sulfated Fe_2O_3	10	na
Sulfated Fe_2O_3 + Carbon Black[b]	28	na
Carbon Black[b]	4	1
None	5	1

[a]3000 ppm active metal loading used with respect to solvent weight.
[b]1.0 g of Carbon Black added.

TABLE 2. Catalyst Dispersion

Catalyst	XRD size (002 plane of Mo, Å)	BET Surface Area (m^2/g)
MoS_2 (unsup.)	<25	260
AO-60	30	162
Mo-C-1	47	na

TABLE 3. Effect of Catalyst Type on Coal Liquefaction Experiments

Catalyst[a]	Coal Conversion (%maf coal)	H_2 Consumed (mMol)	Solvent Hydrogenation (%)
MoS_2 (unsup.)	95	55	13
AO-60	87	32	10
Shell-324	81	39	9

[a]1000 ppm active metal loading used with respect to maf coal weight.

In the presence of a complex system, such as coal, the trends are altered, as shown in Table 3. There does not appear to be a significant difference between the supported and unsupported catalysts. If anything, the unsupported catalysts appear to outperform the supported catalysts. This is not surprising in that the effect of the addition of coal on the suppression of catalytic

hydrogenation activity of both the unsupported and supported catalysts has been previously reported [11,12]. The unsupported MoS_2 and supported AO-60 catalysts are compared with respect to the effect of H_2 pressure on H_2 consumption and coal conversion in Figures 1 and 2 respectively. Figure 1 shows that the H_2 consumption for the MoS_2 with no coal present was lower than that of the supported catalyst at all the pressures tested. However, as shown in Figures 1 and 2, the H_2 consumptions and coal conversions, with coal present, are similar for both catalysts.

SUMMARY

The focus of this study was to compare the catalytic hydrogenation observed with supported and unsupported catalysts. In the tests with the 2-ring aromatic solvent (1-methylnaphthalene), the supported catalysts showed superior catalytic hydrogenation performance. Even the case where the support and catalyst precursor were added separately (Sulfated Fe_2O_3 + Carbon Black), the hydrogen consumption was greater than the unsupported catalyst alone. However, the performance of supported and unsupported catalysts in hydrogenation and conversion were comparable when coal was added to the system. Also, at an initial H_2 pressure of 6.9 MPa (1000 psig) cold with coal present, the H_2 consumptions and coal conversions are slightly higher for the unsupported catalyst experiments.

DISCLAIMER

BIBLIOGRAPHY

1. Derbyshire, F. J., Catalysis in Coal Liquefaction: New Directions for Research, IEA CR/08 June (1988).
2. Cugini, A. V., Krastman, D., Lett, R. G., and Balsone, V. D., *Catalysis Today*, **19**(3), pp. 395-408 (1994).
3. Cugini, A. V., Martello, D. V., Baltrus, J. P., and Holder, G. D., *Proceedings of the 17th International Conference on Coal Utilization and Slurry Technologies*, Clearwater, FL, April 28-May 1, (1992).
4. Cugini, A. V., *Ph. D. Dissertation*, University of Pittsburgh (1993).
5. Pradhan, V. R., Herrick, D. E., Tierney, J. W., and Wender, I., "Finely Dispersed Iron, Iron-Molybdenum, and Sulfated Iron Oxides as Catalysts for Coprocessing Reactions," *Energy and Fuels*, **5**(5), pp. 712-720 (1991).
6. Ciocco, M. V., Cugini, A. V., Rothenberger K. S., Veloski, G. A., and Schroeder, K. T., "Effect of Pressure on First Stage Coal Liquefaction with Dispersed Catalysts," Proceedings of the Eleventh Annual International Pittsburgh Coal Conference, Pittsburgh, PA, pp. 500-505, (1994).
7. Hackett, J. P. and Gibbon, G. A. In Automated Stream Analysis for Process Control, Manka, D. P., ed., Academic Press, pp. 95-117, (1982).
8. Schmidt, C. E., Sprecher, R. F., and Batts, B. D., Anal Chem., **59**, pp. 2027-2033, (1987).
9. Schmidt, C. E. and Sprecher, R. F., In Novel Techniques in Fossil Fuel Mass Spectrometry, ASTM STP 1019, Ashe, T. R. and Wood, K. V., eds., American Society for Testing and Materials: Philadelphia, PA, pp. 116-132, (1989).
10. Boudart, M. and Djega-Mariadassou, G., In Kinetics of Heterogeneous Catalytic Reactions, Princeton University Press, Princeton, NJ, pp. 205-206, (1982).
11. Rothenberger, K. S., Cugini, A. V., Schroeder, K. T., Veloski, G. A., Ciocco, M. V., "The Effect of Coal Addition on Solvent Hydrogenation and Coal Conversion in a Model Alkylnaphthalene Solvent," Proceedings; ACS Div. of Fuel Chem., 39(**1**), (1994).
12. Ciocco, M. V., Cugini, A. V., Rothenberger K. S., Veloski, G. A., and Schroeder, K. T., "The Effect of Hydrogen Pressure on First-Stage Coal Liquefaction with Dispersed and Supported Catalysts; the Role of Catalyst in Hydrogen Transfer," Presented at the American Institute of Chemical Engineers, 1995 Annual Meeting, November 12-17, (1995).

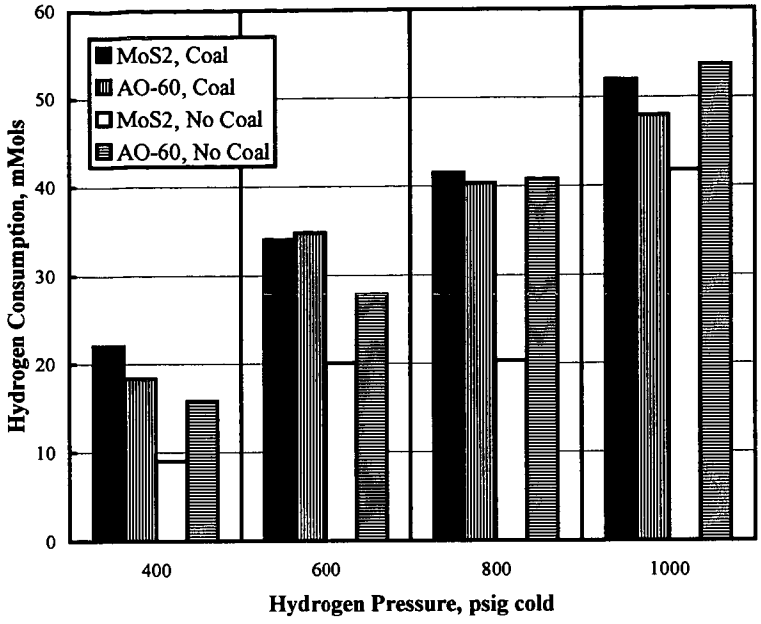

Figure 1. Effect of Pressure on Hydrogen Consumption

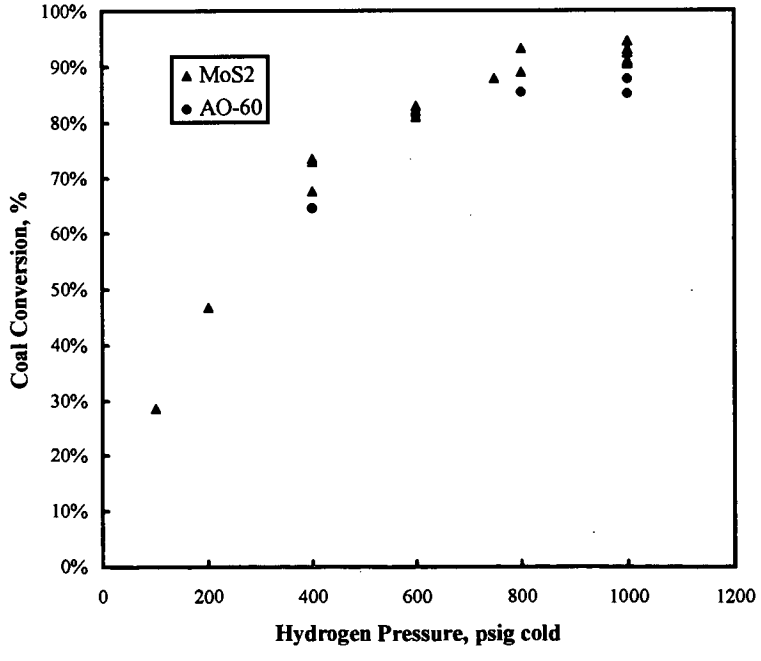

Figure 2. Effect of Pressure on Coal Conversions

COMPONENTS OF OIL DERIVED FROM LIQUEFACTION OF HYDROCARBON-RICH MICROALGAE

Seiichi INOUE, Shigeki SAWAYAMA and Tomoko OGI
National Institute for Resources and Environment, 16-3 Onogawa, Tsukuba, Ibaraki 305, Japan

Keywords: *Botryococcus braunii*, liquefaction, components

ABSTRACT

Botryococcus braunii is a colonial green microalga that produces and accumulates oily hydrocarbons called botryococcenes(C30-36). Liquefaction was applied to *B. braunii* for recovery of hydrocarbons. The liquefied oil was obtained with yield of 64% at 300°C. The oil was fractionated into three fractions by silica gel column chromatography and analyzed to determine its composition. The yields of three fractions were 5% of low molecular weight hydrocarbons, formed by degradation of botryococcenes, 27.2% of botryococcenes and 22.2% of polar substances, produced from organic materials other than hydrocarbons through liquefaction. Further analysis using GC-MS identified some components of the oil. Main components of low molecular hydrocarbons and polar substances were C17-22 hydrocarbons and C14-20 fatty acids, respectively.

INTRODUCTION

The use of biomass for energy is largely motivated from the standpoint of global environmental issues. Biomass-derived fuels would reduce greenhouse gas concentrations to the extent that they could replace fossil fuels currently being used. *Botryococcus braunii* is a unique colonial green microalga that produces and accumulates oily hydrocarbons, called botryococcenes (C30-36), with a dry weight range of 17-86%.[1] These hydrocarbons can be upgraded to transport fuels by hydrocracking[2] or catalytic cracking[3] after being recovered from the algal cells.

On a laboratory scale, the hydrocarbons of algal cells are separated by extraction with organic solvent after their freeze-drying and sonicating. However, this method is not suitable for large scale separations due to the high cost. Therefore, an effective method is needed for separating hydrocarbons from algal cells. We have proposed a new method for separating hydrocarbons from algal cells by direct liquefaction. Applying this process to *B.braunii*, a greater amount of oil than that obtained from *B.braunii* was achieved with yields of 57-64% at 300°C compared to our previous work.[4] Liquefaction could be an effective method for converting the algal cells of *B.braunii* into oil.

The analysis of the oil is important for providing preliminary information about the conversion of organic materials and for the recovery of hydrocarbons produced from the algal cells. In this paper, we analyzed the components of the liquefied oil and determined the suitable reaction conditions needed for the recovery of botryococcenes from *B.braunii*.

EXPERIMENTAL

Algal strain and botryococcenes extraction

The Berkeley strain of *B.braunii* was used for the liquefaction. This strain produces mainly $C_{34}H_{58}$.[5] The algal cells of *B.braunii* were filtered using a 20 μm nylon mesh and then freeze-dried. The algal cells (943 g) were ultrasonically extracted with 50 ml of hexane for 30 min. It gave an oil as hexane extracts (50% of dry cell weight). The extract was chromatographed on a silica gel column with hexane as the eluent in order to obtain Botryococcenes (36% of dry cell weight).

Liquefaction

Liquefaction of *B.braunii* was performed in a 300 ml autoclave at 200, 300 or 340°C, with or without Na_2CO_3 as the catalyst. Liquefied oil was extracted from the reaction mixture with CH_2Cl_2. Details of the liquefaction procedure were reported in a previous study.[4]

Fractionation

The liquefied oil was separated into three fractions. The procedure for fractionation is provided in Fig. 1. The liquefied oil was chromatographed on a silica gel column with 200 ml hexane and 200 ml diethylether. The first 100 ml of the hexane eluate gave F1. The next 100 ml of the hexane eluate was F2, and the 200 ml of the diethylether eluate was F3.

Analysis

The mean molecular weight of the respective fractions was measured using the 117 Molecular Weight Apparatus (Corona, Japan). Elemental composition of the respective fractions was analyzed using a 2400 CHN Elemental Analyzer (Perkin-Elmer, USA). The GC analysis was carried out using a capillary column (DB-1, 30 m x 0.25 mm, Hewlett-Packard, USA). The initial oven temperature was held at 100°C for 10 min, then heated to 220°C at 3 °C min^{-1}. The temperatures of the injector and FID were 220°C and 240°C, respectively. The GC-MS (DB-1, 30 m x 0.25 mm, Hewlett-Packard, USA) analysis was carried out under the same condition.

RESULTS AND DISCUSSION

The properties of F1, F2 and F3 and of botryococcenes extracted from the algal cells are shown in Table 1. The mean molecular weight of F2 was in the range of 438-572, and that of

botryococcenes in the algal cells was 472. The elemental composition of F2 was in good agreement with that of botryococcenes. In addition, the GC retention time of F2 coincided well with the retention time of the botryococcenes. From these results, F2 was identified as the botryococcenes. Elemental analysis showed that F1 was hydrocarbons and the mean molecular weight of F1 was in the range of 197-281. These results suggest that F1 is some kind of degraded product of the botryococcenes. F3 contained oxygenated compounds. Since F3 contained oxygen compounds, they may be produced from organic materials except for the hydrocarbons through liquefaction. From these results, we could confirm that F1, F2 and F3 were low molecular weight hydrocarbons, botryococcenes and polar substances, respectively.

Figure 2 shows the yield of each fraction of the liquefied oil and hexane extracts from the algal cells. The recovery (75%) of the botryococcenes in the liquefied oil was obtained when the liquefaction was carried out at 300°C in the presence of a catalyst (5% sodium carbonate). The yields of the three fractions based on an organic basis were 5% low molecular weight hydrocarbons, 27.2% botryococcenes, and 22.2% polar substances.

The recovery of the botryococcenes was improved with the use of a catalyst at the reaction temperatures of 200 and 300°C (Fig. 2). The quantitative difference in the recovery of the botryococcenes between 200°C and 300°C with a catalyst was very small, but recovery at 340°C decreased. The reaction temperature of 200°C is a preferable reaction temperature from the standpoint of energy use. The liquefaction process can be used for recovery of the botryococcenes as well as the conversion of the algal cells into oil. The total recovery of the fractions (F1, F2 and F3) was in the range of 70-88 wt% for the liquefied oils. The liquefied oil of *B. braunii* had a small amount (1%) of nitrogen, but the fractions (F1, F2 and F3) from the silica gel column contained no nitrogen. The loss is most likely due to the strong adsorption of highly polar components in the liquefied oil onto the silica gel.

Further analysis using GC-MS identified some components of the liquefied oil obtained at 300°C with a catalyst. Table 2 shows the main components of low molecular hydrocarbons and polar substances. The main components of low molecular hydrocarbons were C17-22 hydrocarbons. It is thought that these compounds were formed by degradation of botryococcenes in the algal cells. On the other hand, the main components of the polar substances were C14-20 fatty acids. Except for these compounds, many compounds were identified. From the standpoint of the reaction mechanism during the liquefaction of *B.braunii*, it is very interesting that a methoxyl compound was identified. Ether compounds were found in some strains of *B.braunii*.[6,7] The methoxyl compound may be produced during the liquefaction. Phenol and pyrrolidine compounds, which are absent in the cell, were also identified. They are formed by the degradation and combination of the constituents, such as proteins, in the algal cell.

CONCLUSION

The oil derived from the liquefaction of *B.braunii* consisted of three fractions: low molecular hydrocarbons, botryococcenes and polar substances. From an analysis using GC-MS of the oil obtained at 300°C with a catalyst, the main components of the low molecular hydrocarbons and polar substances were C17-22 hydrocarbons and C14-20 fatty acids, respectively. The recovery of botryococcenes was 75%. The recovery of the botryococcenes was improved using a catalyst at reaction temperatures of 200 and 300°C.

REFERENCES

1. T.G. Tornabene, Microorganisms as hydrocarbon producers *Experientia* **38**, 43-46 (1982).
2. L.W. Hillen, G. Pollard, L.V. Wake and N. White, Hydrocracking of oils of *Botryococcus braunii* to transport fuels. *Biotechnol. Bioeng.* **XXIV**, 193-205 (1982).
3. H. Kitazato, S. Asaoka and H. Iwamoto, Catalytic cracking of hydrocarbons from microalgae. *Sekiyu Gakkaishi* **32**(1), 28-34 (1989).
4. Y. Dote, S. Sawayama, S. Inoue, T. Minowa and S. Yokoyama, Recovery of liquid fuel from hydrocarbon-rich microalgae by thermochemical liquefaction. *Fuel* **73**, 1855-1857 (1994)
5. J. R. Maxell, A. G. Douglas, G. Eglinton, and A. McCormick, The botryococcenes-hydrocarbons of novel structure from the alga Botryococcus braunii, Kützing. *Photochemistry* **7**, 2157-2171 (1968).
6. P. Metzger and E. Casadevall, Botryococcoid ethers, ether lipids from *Botryococcus braunii*. *Photochemistry* **30**, 1439 (1991).
7. P. Metzger and E. Casadevall, Ether lipids from *Botryococcus braunii* and their biosynthesis. *Photochemistry* **31**, 2341 (1992).

Table 1 Properties of the fractionated oil and botryococccenes

	Mean molecular weight	Elemental composition			GC retention time
		C(%)	H(%)	O(%)	(sec)
Fraction 1	197-281	84.5-85.5	14.6-15.5	0.0	-3540
Fraction 2	438-572	85.0-86.5	13.2-14.0	0.0-1.0	4140-4380
Fraction 3	867-2209	73.3-77.3	12.2-13.3	10.1-14.3	4680-
Botryococcenes	472	85.7	14.3	0.0	4140-4380

Table 2 Components of liquefied oil

Low molecular weight hydrocarbon
5-Octadecene
Heptadecane
$C_{19}H_{38}$
$C_{20}H_{40}$
Octadecane
Tetramethyl hexadecene
Docosane
Polar substances
Mesityl oxide
Diacetone alcohol
Phenol
Methyl phenol
Ethyl phenol
2,6-Bis(1,1-dimethylethyl)-4-ethyl phenol
Tetradecanoic acid
Trimethyl pentadecanone
Methyl tetradecanoic acid
Hexadecanoic acid
9-Octadecenoic acid
Octadecanoic acid
Eicosanoic acid
1-(7-Methyl-1-oxopentadecyl)pyrrolidine

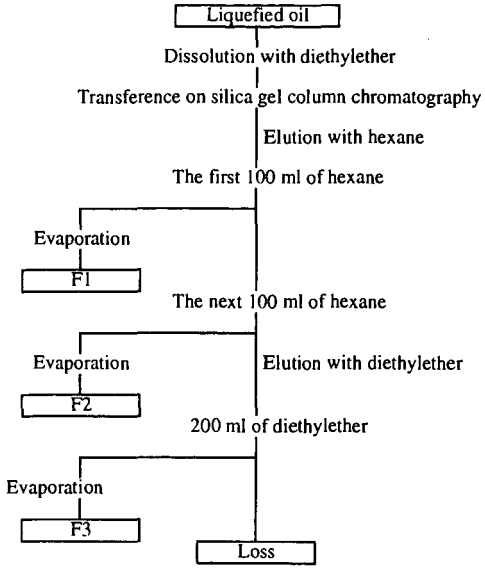

Fig. 1. Procedure for fractionation of liquefied oil

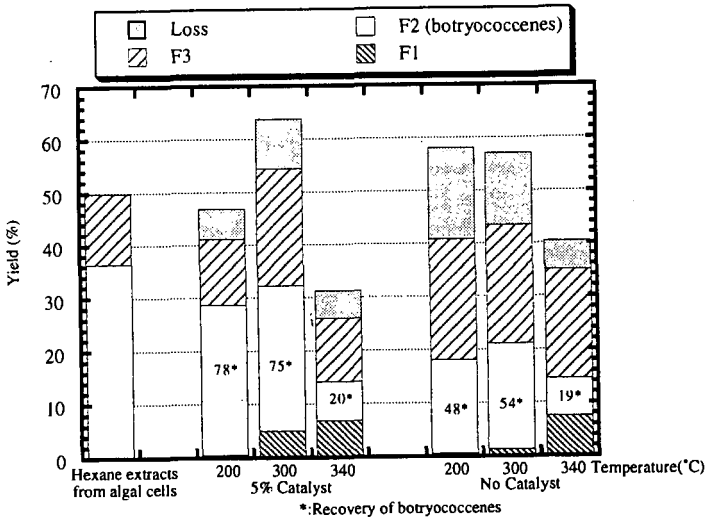

Fig. 2 Yield of each fraction of liquefied oil and hexane extracts from algal cells.

DEMETALLATION OF WASTE OIL WITH COAL

Edward C. Orr, Lian Shao, Edward M. Eyring
Department of Chemistry, University of Utah, Salt Lake City, UT 84112

KEYWORDS: Demetallation, Waste Oils, Coprocessing

INTRODUCTION

The breakdown of coal into liquid fuels has been researched extensively in order to improve upon the economics of the process. To produce liquid fuels from hydrogen deficient coal, hydrogen must be added. Weisz noted that for the most hydrogen deficient coals, it would be necessary to add 8 % by weight hydrogen to produce quality hydrocarbons.[1] One way to decrease the cost of coal liquefaction would be to minimize the need for expensive hydrogen. By coprocessing coal with heavy petroleum resids, the resid may act as a hydrogen donor for the coal diminishing the need for additional costly hydrogen gas.[2] In coprocessing resids with coal it has also been shown that some of the nickel and vanadium that are naturally abundant in the resid reside in the coal char and ash after coprocessing.[3]

More recently, it has been shown that coprocessing waste materials (plastics, rubbers, and waste lubricants) with coal can decrease the cost of coal liquefaction.[4] In addition, coprocessing of coal with waste materials has also been shown to enhance coal conversion to liquids.[5] The addition of waste materials to coal liquefaction reactions also means the addition of heavy metals. Waste rubber tires contain zinc[6] and waste lubricants can contain a variety of heavy metals such as iron, manganese, and zinc.[7] Recent results indicate trace heavy metals found in waste automotive oil will reside in coal char and ash after coprocessing.[7] Demetallation of the trace heavy metals in waste automotive oils was not found to be dependent upon the rank of coal. Out of six different coals used in the demetallation experiments, Illinois #6 coal showed the best demetallation effect. The Illinois #6 has a high content of inorganic matter which has been suggested to have influence on the degree of demetallation. The present paper reports further experiments carried out with Illinois #6 and demineralized Illinois #6 in order to determine the effect of the inorganic portion of the coal on demetallation of waste automotive oil. The extent of the demetallation of the produced oil is reported. X-ray photoelectron spectroscopy (XPS) was used to analyze the surface of the coals before and after demineralization.

EXPERIMENTAL

Illinois #6 was obtained from the Pennyslvania State Coal Sample Bank. The Illinois #6 was used as received (-60 mesh). At all times the coal was stored under a nitrogen atmosphere. The waste automotive oil was obtained from Interline Resources Inc. (Salt Lake City, Utah). The waste automotive oil was stored under ambient conditions and used as received. Demineralization of the Illinois #6 coal was carried out by mixing 500 mL of 6 N HCl with 20 g of Illinois #6 at approximately 45 °C for 1 hour. The coal was then filtered. The filtered coal was then mixed with 250 mL of concentrated HF at ambient conditions for 1 hour. The coal was again filtered. The coal was then treated with 250 mL of 12 N HCl at 45 °C for 1 hour. The coal was then filtered and washed with deionized water until no chloride was precipitated by addition of silver nitrate. The demineralized coal and the untreated coal were dried at 100 °C under vacuum for 2 hours. The dried demineralized and dried untreated coal were then mixed with waste automotive oil in a 1:1 ratio determined by weight. Samples were placed in stainless steel tubing reactors which have volumes of 27 cm^3. Tubing reactors were sealed and then purged with nitrogen gas and finally pressurized to 1000 psig (cold) of hydrogen. Tubing reactors were placed in a fluidized sandbath and shaken vertically at a rate of 160 rpm. The temperature of the sandbath was maintained at 430 °C for 1 hour. After liquefaction the tubing reactor was removed from the sandbath and cooled at room temperature for 5 minutes and finally quenched in cold water. The sample was scraped out of the tubing reactor and placed in a Soxhlet extraction thimble. The internal surfaces of the

tubing reactor were washed with tetrahydrofuran (THF). The THF wash was then placed in the before mentioned extraction thimble. The material was then extracted with THF using a Soxhlet extractor for 48 hours. The nonsoluble portion was dried and weighed in order to calculate the total conversion on a dry ash free. The THF soluble portion was run through a rotary evaporator to remove the THF. The THF soluble portion was then dried under vacuum at 430 °C for 2 hours. The THF soluble portion was extracted with cyclohexane. The portion that is insoluble in cyclohexane is referred to as asphaltenes. The cyclohexane was removed from the cyclohexane soluble portion with a rotary evaporator. The residue was then dried under vacuum at 100 °C for 2 hours. The cyclohexane soluble portion is referred to as oil. The ICP analyses were completed by Data Chem Laboratories, Salt Lake City, UT. The XPS results were obtained from a FISONS ESCALAB 220i-XL using a six channel detection system. Samples were mounted upon double sided 3M tape on top of a metallic sample holder. Charging effects were countered by using an electron flood gun.

RESULTS

Proximate and ultimate analyses of the untreated Illinois #6 coal are given in Table 1.[8] The Illinois #6 coal is a high volatile C bituminous coal. Table 2 shows a comparison of ICP analyses of untreated coal and demineralized coal. There is a significant difference in the amount of inorganic matter present in the untreated coal and the demineralized coal. Table 2 shows a substantial decrease in naturally abundant metals such as aluminum, calcium, iron, and sodium for the demineralized coal. This indicates that the demineralization process was effective in removing a substantial fraction of the inorganic constituents.

XPS analysis of the untreated and the demineralized Illinois #6 coal indicates a decrease in inorganic matter at the surface of the demineralized coal. The XPS analysis of the untreated Illinois #6 coal detected sodium, aluminum, silicon, sulfur, and calcium. XPS analysis of the demineralized coal detected only sulfur and calcium. This indicates that some of the inorganics on the surface of the coal were effectively removed by the demineralization process. From the ICP result, iron makes up over 2 % by weight of the total Illinois #6 coal. Detection of the iron by XPS was not achieved. Past investigators have also reported that detection of iron on the surface of coal is difficult.[9,10] We assume that most of the iron present resides in the bulk coal structure and not upon the coal surface.

The waste automotive oil was analyzed by ICP to determine the type of trace heavy metals present. The results are shown in Table 3. The phosphorous and zinc are present due to an antiwear lubricant, zinc dialkyldithiophosphate, added to the motor oil.[11]

Table 4 shows the liquefaction conversion data for reacting untreated Illinois #6 and demineralized Illinois #6. The untreated Illinois #6 showed better total conversion than the demineralized coal probably because of the decrease in iron in the demineralized coal. Decreasing the iron content decreases the pyrrhotite formation. Pyrrhotites are known to act as coal liquefaction catalysts.[12]

The last two columns of Table 3 shows the ICP analysis of the product oils or the cyclohexane soluble portion of the coal and waste automotive oil reactions. The product oil from both the untreated and the demineralized coal are free of all the elements detected in the untreated waste automotive oil except for some sodium detected in the oil sample from the demineralized coal.

Demineralization of the Illinois #6 decreased the inorganic portion of the coal substantially. The iron content was decreased from 2.3 % to 1.5 % yet the presence of 1 % iron or more would still be sufficient enough for catalytic effects.[13] The remaining iron in the form of iron sulfide will function as a catalyst aiding in dissolution of the coal forming gas, oil, asphaltenes, and char. In coprocessing experiments conducted with resids, Miller et al. concluded that new char formation was responsible for demetallation.[14] In past studies completed in this laboratory, trace heavy metals initially in the automotive oil were found to be more abundant in

asphaltenes.[7] The asphaltenes are precursors to char. Retrogressive reactions allow asphaltenes, laden with heavy metals, to form char which may then trap or embed the heavy metals. Therefor, iron sulfide enhances formation of asphaltenes and indirectly char which traps heavy metals. Thus the iron inherent in the coal may aid in demetallation of the waste automotive oil.

CONCLUSION

Demineralized Illinois #6 coal showed no detectable difference for demetallation of waste automotive oil in coprocessing reactions when compared to untreated Illinois #6 coal. The inorganic portion of the coal, except the iron, seems to have little effect upon the demetallation characteristics of the coal.

ACKNOWLEDGMENTS

We gratefully acknowledge the donation of waste automotive crankcase oil by Professor Larry L. Anderson (Department of Chemical and Fuels Engineering, University of Utah, Salt Lake City, UT) and Interline Resources Inc., (Salt Lake City, UT). Financial support by the U.S. Department of Energy, Fossil Energy Division, through the Consortium for Fossil Fuel Liquefaction Sciences, Contract No. UKRF-4-21033-86-24, is also gratefully acknowledged.

REFERENCES

1 Weisz, P.B., Chemtech, **1982**, 12, 114.
2 Shen, J.; Curtis, C.W., Prepr. Pap. Am. Chem. Soc. Div. Fuel Chem., **1995**, 40 (3), 622.
3 Cugini, A.V.; Lett, R.G., Energy & Fuels, **1989**, 3, 120.
4 Gray, D.; Tomlinson, G., Prepr. Pap. Am. Chem. Soc. Div. Fuel Chem., **1995**, 40 (1), 20.
5 Orr, E.C.; Tuntawiroon, W.; Ding, W.B.; Bolat, E.; Rumpel, S.; Eyring, E.M.; Anderson, L.L., Prepr. Pap. Am. Chem. Soc. Div. Fuel Chem., **1995**, 40 (1), 44.
6 Orr, E.C.; Tuntawiroon, W.; Anderson, L.L.; Eyring, E.M., Prepr. Pap. Am. Chem. Soc. Div. Fuel Chem., **1994**, 39 (4), 1065.
7 Orr, E.C.; Shi, Y.; Liang, J.; Ding, W.; Anderson, L.L.; Eyring, E.M., Prepr. Pap. Am. Chem. Soc. Div. Fuel Chem, **1995**, 40 (3), 633.
8 Pennyslvania State Coal Sample Bank
9 Weitzacker, C.L.; Gardella, Jr., J.A., Anal. Chem., **1992**, 64, 1068.
10 Kelemen, S.R.; Gorbaty, M.L.; George, G.N.; Kwiatek, P.J., Energy & Fuels, **1991**, 5, 720.
11 Tarrer, A.R., Technical Report on DOE Contract No. DE-FC22-93PC93053, Period: May 1, 1994-October 31, 1994, pp. 150.
12 Pradhan, V.R.; Hu, J.; Tierney, J.W.; Wender, I., Prepr. Pap. Am. Chem. Soc. Div. Fuel Chem., **1993**, 38 (1), 8.
13 Sommerfeld, D.A.; Tuntawiroon, W.; Anderson, L.L; Eyring, E.M., Prepr. Pap. Am. Chem. Soc. Div. Fuel Chem., **1993**, 38 (1), 211.
14 Miller, T.J.; Panvelker, S.V.; Wender, I.; Tierney, J.W., Fuel Processing Technology, **1989**, 23, 23.

Table 1 Proximate and Ultimate Analysis of Coals From Pennyslvania State Coal Sample Bank

	Illinois #6
Proximate	
% Ash	16.16
% Volatile	38.14
% Fixed Carbon	45.70
Ultimate	
% Carbon	78.11
% Hydrogen	5.44
% Nitrogen	1.32
% Sulfur	5.39
% Oxygen	9.73
Iron	
% Iron	2.3

Table 2 ICP analyses of untreated Illinois #6 coal and demineralized Illinois #6 coal

Metal	Illinois #6 µg/g	Demineralized Illinois #6 µg/g
Aluminum	1,300	330
Antimony		
Arsenic		
Barium	17	6.6
Beryllium	1.1	.8
Cadmium	1.2	.6
Calcium	6100	320
Chromium	14	15
Cobalt	5.6	
Copper	10	11
Iron	23,000	15,000
Lead	10	
Lithium		
Magnesium	220	42
Manganese	58	13
Molybdenum		
Nickel	14	14
Phosphorous		
Potassium	460	
Selenium		
Silver		
Sodium	770	160
Strontium	24	12
Thallium		
Vanadium	19	20
Zinc	74	4.3

Table 3 First column contains ICP analysis of the received waste automotive oil. The second and third columnss are ICP analyses of oils produced from reacting waste automotive crankcase oil with untreated Illinois #6 coal and demineralized Illinois #6 coal at 430 °C under a 1000 psig (cold) hydrogen for 1 hour.

Metal	Waste Automotive Oil μg/g	Untreated Illinois #6 Coal Oil μg/g	Demineralized Illinois #6 Coal Oil μg/g
Aluminum			
Antimony			
Arsenic			
Barium	11		
Beryllium			
Cadmium			
Calcium	990		
Chromium	2.7		
Cobalt			
Copper	44		
Iron	130		
Lead	47		
Lithium			
Magnesium	410		
Manganese	10		
Molybdenum			
Nickel			
Phosphorous	780		
Potassium			
Selenium			
Silver			
Sodium	450		76
Strontium			
Thallium			
Vanadium			
Zinc	690		

Table 4 Percent conversion of untreated Illinois #6 and demineralized Illinois #6 coal reacted with waste automotive oil mixed in a 1:1 ratio by weight. Liquefaction was carried out in tubing reactors at 430 °C under a 1000 psig (cold) hydrogen for 1 hour.

	Untreated Illinois #6	**Demineralized Illinois #6**
Gas + Oil	38.8	40.2
Asphaltenes	22.1	13.2
Total Conversion	60.9	53.4

VARIABLE TEMPERATURE EPR STUDIES OF ILLINOIS NO. 6 COAL TREATED WITH DONOR AND ACCEPTOR MOLECULES

Robert L. Thompson, Kurt S. Rothenberger, and Herbert L. Retcofsky
U. S. Department of Energy
Pittsburgh Energy Technology Center
P. O. Box 10940
Pittsburgh, PA 15236

Keywords: charge-transfer, EPR spectroscopy, coal extracts

INTRODUCTION

The structure of coal is believed to consist of extended networks of polyaromatic hydrocarbons linked by a wide variety of bonding interactions. In addition to covalent bonds, these networks contain non-covalent interactions, such as hydrogen bonding and charge-transfer interactions. Charge transfer, which can be studied by electron paramagnetic resonance (EPR) spectroscopy,[1] involves the association of electron donors and acceptors. Both donor and acceptor sites are known to exist in coal, although acceptor sites are probably far less common. Such intermolecular associations may play an important role in determining the relaxation behavior of the coal matrix in certain solvents, an important consideration in coal liquefaction.

Charge-transfer interactions between strong donors and acceptors can lead to paramagnetic products, which can be observed by EPR spectroscopy. Any unpaired electrons in the sample can interact to give coupled singlet-triplet states, or they can remain independent of each other to give doublet states. In the former case, if the triplet state lies above the singlet state, it may be too high in energy to be populated at ambient temperature; however, when the interaction lies within the appropriate range, the triplet state can become populated such that the product gives an EPR signal.[1]

Most evidence to date supports the interpretation of EPR results of coal as arising from non-interacting doublet states, but some evidence in support of the existence of thermally accessible triplet states, such as temperature-dependent EPR intensities and the observation of $\Delta M_s = \pm 2$ transitions, has been reported as well.[2,3] In this work, we have studied by variable-temperature EPR spectroscopy, Illinois No. 6 coal, its pyridine extract, and chromatographic fractions of the pyridine extract that have been treated with strong electron donors and acceptors.

The intensity of an EPR signal arising from a doublet-state spin system (I_D) is inversely proportional to temperature according to the Curie Law, whereas the intensity of an EPR signal arising from a ground-state singlet system with a thermally accessible triplet state (I_{ST}) obeys a more complex relationship. Non-Curie Law behavior is often used as a diagnostic for the latter case. We have found that a useful test for non-Curie behavior is to measure the ratio of sample intensity to that of a known doublet state sample under identical conditions. Plots of this ratio versus temperature are useful in illustrating the variable temperature EPR results, as well as accounting for changes within the spectrometer cavity and sample during the experiment.

$$\frac{I_{ST}}{I_D} = \frac{\left[\frac{C_{ST}}{T}\right]\left[\frac{4}{\exp(J/k_BT)+3}\right]}{\left[\frac{C_D}{T}\right]} = \left[\frac{4\ C'}{\exp(J/k_BT)+3}\right] \qquad (1)$$

Equation 1 shows the ideal ratio I_{ST}/I_D as a function of temperature,[1] where J is the energy gap between the singlet and triplet states and k_B is Boltzmann's constant.

EXPERIMENTAL PROCEDURES

The coal used in this work was a high-volatile bituminous coal from the Illinois No. 6 seam in Franklin County, IL (MF analyses: 72.7 %C, 4.7 %H, 1.6 %N, 1.2 %S, 8.0 %ash). The pyridine extract of this coal was obtained by Soxhlet extraction after the coal had been ground to -100 mesh. The pyridine extract was separated into functionality enriched fractions containing aromatics, bases, and acids on an activated Al_2O_3 column according to an adaptation of the procedure developed by Schiller.[4] The yields for samples obtained from these procedures are listed in Table 1.

Samples of the coal, pyridine extract, and chromatographic fractions were treated with donors or acceptors by refluxing a mixture of coal material and reagent (in amounts ranging from 2.5:1 to 5:1) in chlorobenzene for 1 to 2 days, followed by evaporation of solvent and vacuum drying at 50°C until constant weight. Among the donors and acceptors added were tetrathiafulvalene (TTF), tetracyanoquinodimethane (TCNQ), tetracyanoethylene (TCNE), *p*-chloranil (CA), and iodine. EPR measurements were conducted as described elsewhere.[5]

RESULTS AND DISCUSSION

The treated coal and pyridine extract samples were studied by variable temperature EPR spectroscopy. Their EPR intensities were measured over a temperature range from -171°C to 23°C, then adjusted by dividing by the EPR intensities of DPPH obtained at identical temperatures.[5] DPPH is a well-studied, stable, non-interacting doublet-state free radical that obeys the Curie Law over a wide temperature range.[6] This method accounts for any experimental errors due to changes in sample or cavity characteristics with temperature.[7]

In every case, the EPR intensities of the coal, extract, and extract fractions increased upon treatment with the donor or acceptor, although the increase was not commensurate with a new spin for every molecule of reagent added. Neither was the magnitude of increase a function of the donor or acceptor strength of the added reagent; the acceptor with the largest electron affinity did not always give the largest intensity increase.

Only the addition of TTF, a strong donor, resulted in any discernable change in the shape of the EPR spectrum. It gave rise to a another feature at lower field to the original broad, featureless, first-derivative lineshapes of the coal and extract; all other reagents failed to alter the original lineshape. A more definitive spectrum was obtained from the CH_2Cl_2 extract taken from the TTF-pyridine extract sample. The hyperfine structure shown in Figure 1 is strikingly similar to that in the EPR spectrum of $(TTF)_3(BF_4)_2$.[8] In Figure 1, both spectra are centered at a field corresponding to $g = 2$. This spectrum is assigned to the radical cation of TTF; its detection in the extract sample implies that there are acceptor sites in the coal capable of completely removing an electron from TTF.

Variable temperature EPR studies were made of all of the treated coal samples, the results of which are shown in Figure 2. The straight, horizontal plots of I_{sample}/I_{DPPH} as a function of temperature imply that all of the coal samples obey the Curie Law at least as strictly as does DPPH, establishing them as consisting predominantly of doublet-state spins. The temperature range covered was sufficiently wide to have observed any thermally accessible triplet spins, if such had existed. Because the Curie Law was so strictly observed, the newly induced spins must either be doublet state spins or have interactions so weak that they are indistinguishable from doublet state spins.

Similar EPR results were obtained for the pyridine extract samples, shown in Figure 3, and are again indicative of adherence to the Curie Law for all samples. It is significant that coal extracts have a lower spin concentration than the whole coal; thus, were a small portion of thermally accessible triplet spins present in the treated coal, but obscured by a larger portion of native doublet spins, we would expect to observe them more readily in the extract. Because we do not see any deviation from Curie Law even in the extract samples, it is clear that thermally accessible triplet spins play no important role in the EPR behavior of whole coal.

Studies supporting the deviations from Curie Law in coal samples[2,3] have relied upon the mathematical deconvolution of EPR spectra, which is by nature artificial and rests on the questionable assumption that the lineshapes of coal signals are Lorentzian. These studies also observe forbidden $\Delta M_s = \pm 2$ transitions for certain coals. We have observed similar EPR signals in many of our samples under similar spectrometer conditions, but evidence does not support the assignment of these signals to $\Delta M_s = \pm 2$ transitions. The EPR spectra of Illinois No. 6 coal at a field corresponding to $g = 4$ are shown in Figure 4. These signals resonate at the appropriate field, but are extremely weak and their intensities do not vary with temperature. In fact, in some cases the observed signal was larger at -171°C than at 23°C, in contradiction to assignment to a thermally accessible triplet state. The location of these signals suggests that they are due to iron-bearing impurities such as kaolinite, which has been shown to possess a variety of low field signals from Fe(III) substituting in the lattice for Al(III) and Si(IV).[9]

The only non-Curie Law behavior we have observed was associated with certain minor sub-fractions from coal extract. The fractions obtained from the pyridine extract displayed weak EPR signals similar in shape to that of the coal and extract. Variable temperature EPR results for the acidic fraction revealed that it obeys the Curie Law, but the results for the aromatic and basic fractions show some slight deviation. As seen in Figure 5, their EPR intensity ratios are no longer horizontal, but slanted lines. This behavior is indicative of the presence of thermally accessible triplet spins. These fractions represent a minuscule portion of the whole coal and are likely overshadowed by the preponderance of doublet state spins.

The yields of individual fractions from the chromatographic separation were small. With this limited amount of sample, the donors and acceptors added to the fractions were limited to TTF and TCNE only. The EPR results for these treated fractions were surprising in that the aromatic sample obeyed Curie Law after treatment with TTF or TCNE, whereas the untreated aromatic fraction deviated from Curie Law. The acidic samples obeyed the Curie Law both before and after treatment with TTF or TCNE. The intensities of the treated basic samples deviated as strongly after treatment as before, particularly TTF-base, which had a curved rather than linear relationship to temperature, as shown in Figure 6.

The samples treated with TCNQ and TCNE were also studied by IR spectroscopy to monitor changes in the stretching frequency of the nitrile group, which has a frequency located in a region of the spectrum that is relatively free of absorptions for most coals. Larsen and co-workers[10] have shown the location of the stretching frequency for coals treated with these two electron acceptors to be very sensitive to the amount of electron density accepted. The nitrile

stretching frequencies of these samples are summarized in Table 2, which includes TCNQ and TCNE and shows the distinct shift to lower frequencies for all of the treated coal samples.

The IR results imply that electron density is being transferred from the coal to the acceptor, but the EPR results indicate that charge-transfer complexes having thermally accessible triplet states are not being formed in any detectable quantity. Similar results have been obtained by others for coal samples treated with TCNQ.[10] They have demonstrated that, although the IR frequencies of these samples were shifted, the EPR spectra did not show any evidence of formation of the TCNQ radical anion and the intensity increase was much less than would be expected if every added molecule of TCNQ resulted in an additional spin. These results were attributed to the formation of extended electronic valence bands between the coal and TCNQ.

It is possible that the frequency shifts in our samples reflect a distinct donation of electron density to TCNQ and TCNE, but the donations occur in such a way that the electrons remain paired. Alternatively, the formation of charge-transfer complexes may indeed be taking place, but with the EPR active triplet state so high in energy as to be essentially unpopulated at room temperature and below.[5]

We have found that a very small fraction of the spins present in Illinois No. 6 coal deviates from the Curie Law due to the population of thermally accessible triplet states. The vast majority of spins observable by EPR in the whole coal behaves as non-interacting doublet state spins, effectively obscuring the weak non-Curie Law behavior. We have also observed that Curie Law behavior persists even in samples treated with reagents capable of inducing charge transfer. Deviation from Curie Law finally becomes observable in the aromatic and basic fractions of the pyridine extract of the coal, as well as in some of the treated fractions. IR spectra reveal that electron density is indeed donated from the coal to the acceptors TCNQ and TCNE, and the EPR intensities are increased relative to the untreated coal samples, but treatment does not result in any noticeable deviation from Curie Law. Finally, while weak EPR signals are observed at half-field for many of the samples studied above, these signals are believed to arise from Fe(III)-containing impurities rather than from $\Delta M_s = \pm 2$ transitions.

REFERENCES

1. Bijl, D., Kainer, H., Rose-Innes, A.C. *J. Chem. Phys.* 1959, **30**, 765.
2. Duber, S., Więckowski, A.B. *Fuel* 1984, **63**, 1474.
3. Duber, S., Mikosz, J. *Fuel* 1993, **72**, 267.
4. Schiller, J.E., Mathiason, D.R. *Anal. Chem.* 1977, **49**, 1225.
5. Rothenberger, K.S., Sprecher, R.F., Castellano, S.M., Retcofsky, H.L. in 'Magnetic Resonance of Carbonaceous Solids' (Eds. R. Botto, Y. Sanada), ACS Adv. Chem. Ser. 229, Washington, DC, 1992, 581.
6. Singer, L.S., Spencer, E.G. *J. Chem. Phys.* 1953, **21**, 939.
7. Castellano, S., Chisolm, W., Sprecher, R.F., Retcofsky, H.L. *Anal. Chem.* 1987, **59**, 1726.
8. Wudl, F., Kaplan, M.L. *Inorg. Synth.* 1979, **19**, 27.
9. Angel, B.R., Hall, P.L. *Proc. Int. Clay Conf., Madrid* 1973, 47.
10. Flowers, R.A., Gebhard, L.A., Larsen, J.W., Sanada, Y., Sasaki, M., Silbernagel, B. *Energy Fuels* 1994, **8**, 1524.

Table 1. Extraction and Chromatographic Yields
(each value an average of 3 runs)

pyridine extraction yield	16.8	
chromatographic yields:	based on extract	based on coal
aromatics	4.2	0.7
bases	7.4	1.2
acids	17.3	2.9

Table 2. Infrared Frequency Changes for Samples Treated with TCNQ and TCNE

sample	ν(CN)	$\Delta\nu$(CN)	sample	ν(CN)	$\Delta\nu$(CN)
TCNQ	2227	----	TCNE	2236	----
coal-TCNQ	2179	-48	coal-TCNE	2200	-36
extract-TCNQ	2182	-45	extract-TCNE	2201	-35
			aromatics-TCNE	2206	-30
			bases-TCNE	2206	-30
			acids-TCNE	2213	-23

Figure 1. EPR Spectra of (a) CH_2Cl_2 Soluble Portion of Pyridine Extract + TTF and (b) $(TTF)_3(BF_4)_2$.

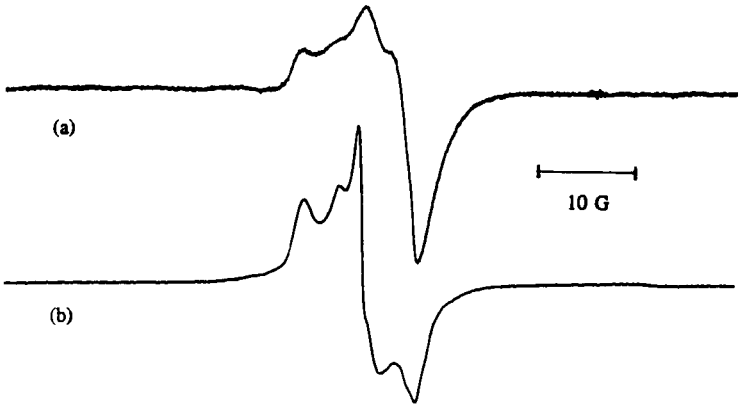

Figure 2. VT-EPR Results for Treated Illinois No. 6 Coal Samples.

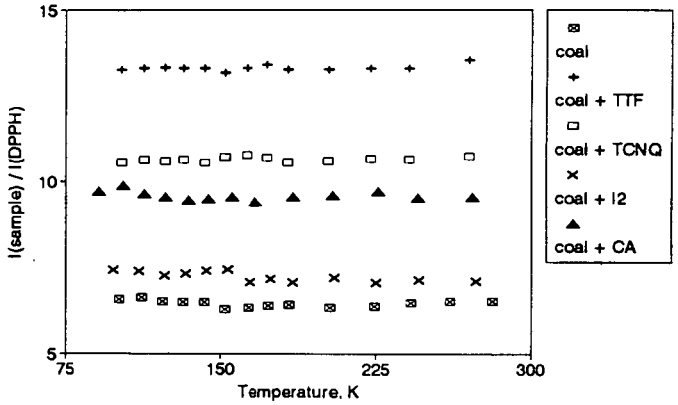

Figure 3. VT-EPR Results for Treated Pyridine Extract Samples.

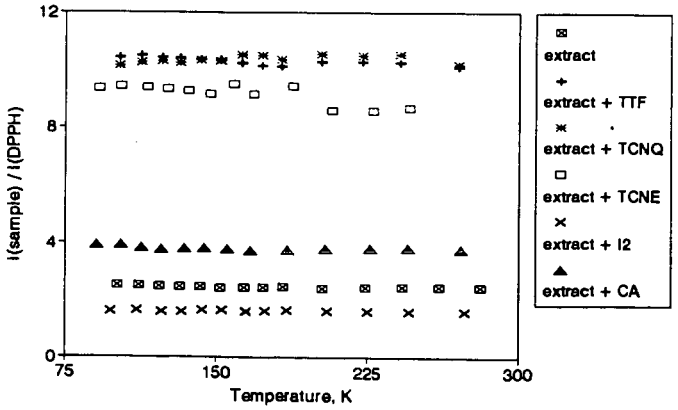

Figure 4. Half Field EPR Spectra of Illinois No. 6 Coal.

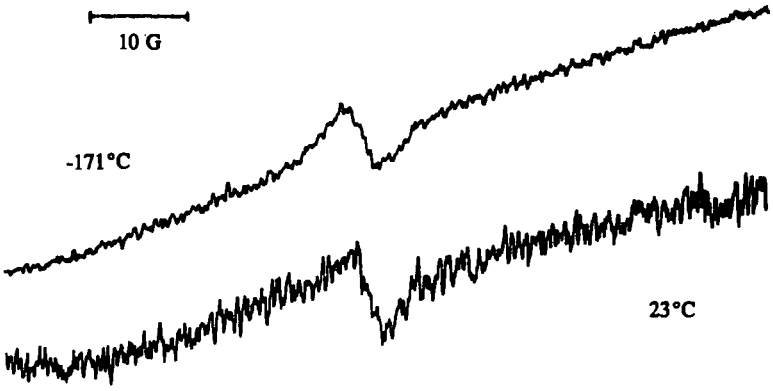

Figure 5. VT-EPR Results for Pyridine Extract Fractions.

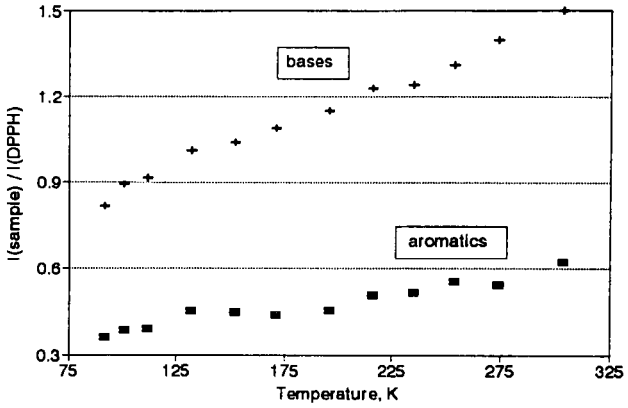

Figure 6. VT-EPR Results for Treated Base Fraction Samples.

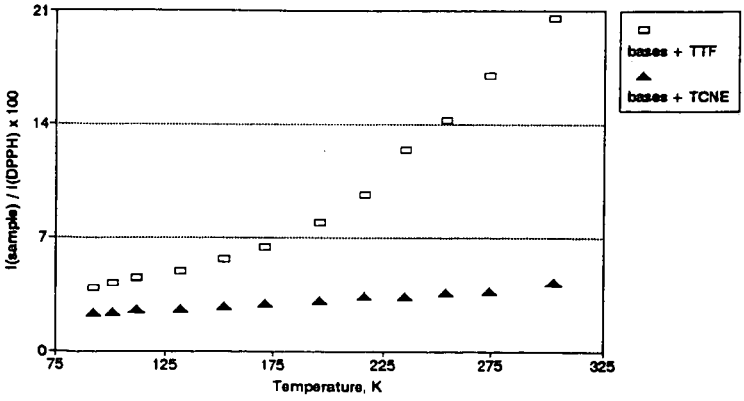

PRODUCTION OF ORGANIC ACIDS IN HIGH YIELDS FROM BROWN COALS THROUGH THE LIQUID PHASE OXIDATION WITH H_2O_2 AT LOW TEMPERATURE

Kouichi Miura, Kazuhiro Mae, Hajime Okutsu and Nori-aki Mizutani
Department of Chemical Engineering, Kyoto University,
Kyoto 606 JAPAN

Key words: Liquid phase oxidation of coal, Fatty acids from coal, H_2O_2 oxidation

INTRODUCTION

Low rank coals such as brown coal and lignite are most abundant fossil resources, but they have not been utilized in a large amount because of their low calorific values. They will not be utilized widely without some method that merits the utilization of such coals. Production of valuable chemicals, such as fatty acids *via* liquid phase oxidation may be a possible way to utilize the coals, judging from their structure.

Many attempts have been performed for decades to obtain organic acids from coal through the oxidation in alkali or acid medium. Kamiya et al. [1,2], Kapo et al.[3] and Bimer et al.[4] oxidized coals by oxygen in an aqueous NaOH or Na_2CO_3 solution at 110 to 270 °C under the pressure of 4.0 to 7.5 MPa. Water-soluble organics could be obtained in 50% yield on carbon basis, but CO_2 was produced in 40 to 50% yield. Montgomery et al.[5] performed the oxidation of a bituminous coal at 150 °C using H_2O_2 as an oxidizing agent, but CO_2 was produced in 60 to 90% yield. Deno et al.[6,7] oxidized four kinds of coals including lignite and several aromatic compounds at 50 to 70 °C using a mixture of trifluoroacetic acid and H_2O_2. They reported that fatty acids and methanol were produced in 5 to 15 % yield.

Thus the attempts for obtaining fatty acids from coal through liquid phase oxidation have not been so successful. A large amount of CO_2 were produced when increasing the decomposition rate by employing severe oxidation conditions such as high temperature, high pressure, and strong acids. A much milder oxidation method seemed to be favorable to produce fatty acids in high yield and in high selectivity. Selection of a suitable coal that is easily degraded in oxidizing agents seemed to be important also.

We have recently found that an Australian brown coal oxidized by H_2O_2 for 2 h at 60°C was extracted by 84 wt% in a mixed solvent of methanol and 1-methylnaphthalene at room temperature[8]. We also analyzed these extracts in detail, then clarified that 40% of carbon in the oxidized coal was aliphatic carbon.[9] This result suggests that a large amount of fatty acids can be recovered if the coal is further oxidized in liquid phase by H_2O_2.

In this paper we show that the liquid phase oxidation of brown coal with H_2O_2 under mild conditions produces water-soluble fatty acids in high yields. We also examine the mechanism by which the organic acids are produced from coal through a detailed study on the product distribution and the coal properties during the H_2O_2 oxidation.

EXPERIMENTAL

Three kinds of coals, an Australian brown coal (Morwell, MW), a Canadian brown coal (Highvale, HV), and a Japanese sub-bituminous coal (Taiheiyo, TC) were used as raw coals. The analyses of the coals are listed in Table 1. The coals were ground into fine particles of less than 74 μm, and dried in vacuo at 110 °C for 24 h before use. Morwell coal as received, which contains more than 60% of moisture, was also used without drying. This was performed to examine the possibility of utilizing the coal without energy-consuming drying process. The oxidation of the coals were performed as follows: 0.5 g of coal particles were mixed with 10 ml of 30% aqueous hydrogen peroxide in a 500 ml flask with a plug. After treating the mixture for several hours in an water bath kept at a constant temperature of 40 °C, 60°C or 80 °C, all the gas in the flask was purged by 10 litre of nitrogen gas and was collected in a gas bag. The gaseous product was analyzed for CO_2, CO and hydrocarbon gases by a gas chromatograph. Next, an excess of cold water was added to the mixture to terminate the oxidation reaction, then the mixture was filtrated to separate it into the solid residue and the aqueous solution. The solid residue was evacuated at 60 °C for 24 h, and was served to the CHN analysis, the F.T.i.r. analysis, and the ^{13}C-n.m.r. analysis. The solid yield on carbon basis was calculated from the CHN analysis. The aqueous solution was served to the TOC, the GPC, and the HPLC analyses. The HPLC analysis detected low molecule fatty acids using a sulfonated polystyrene gel column with an electric conductivity

detector. The content of total organic carbon, the molecular weight distribution, and the composition of fatty acids were estimated from these measurements.

RESULTS AND DISCUSSION

Oxidation of dried MW coal

First, the dried MW coal was oxidized at 60 and 80 °C for different reaction times to examine the validity of the proposed oxidation method. Figure 1 shows the changes in the solid yield with the progress of the oxidation. The height of each bar corresponds to the solid yield at a certain reaction time. Elemental composition at each reaction time is given in the bar. At 60 °C the solid yield decreased to 55% in 2h, and decreased gradually to 19% at 24 h. At 80 °C the coal was decomposed rapidly, and the solid yield was only 15 % at 4 h. The water-soluble oraganics were analyzed by the HPLC and the GPC as stated above. Figure 2 shows a typical chromatogram for low molecule fatty acids obtained using the HPLC. Five components, malonic acid, glycolic acid, formic acid, acetic acid, and a C_2-calboxyl acid, which could not be identified, were separated distinctly and could be quantified. As an another low molecule component methanol was quantified using the GC-MS method. From these analyses the components whose molecular weights (M_w) are smaller than 104 were quantified. Figure 3 shows the change in the number basis molecular weight distribution (MWD) with the progress of the oxidation at 60 °C. Components larger than 60 in molecular weight were detected by the GPC. It is clearly shown that each MWD has two distinct peaks, and that the MWD shifts to smaller molecule region with the increase of the oxidation time. The components detected were separated into two fractions: one is the fraction ranging M_w=105 to 400 and the other is the fracion of M_w>400. The former fraction was quantified by subtracting the amount of the components ranging Mw=60 to 104, which were quantified by the HPLC. The content of the total organic carbon in the water-soluble product was measured separately. Only CO_2 was detected as the gaseous product, and it was quantified by the gas chromatograph. Using these measurements, we could establish the carbon balance during the oxidation.

Figure 4a shows the changes in the product distribution of carbon basis with the progress of oxidation. At 60 °C the yield of water-soluble components increased gradually with the oxidation time, and reached 52 % at 24 h. The yield of the smallest molecule fraction (M_w<104) was surprisingly 28 %. The yield of CO_2 was less than 30 % even at 24 h. At 80 °C the yield of water-soluble components reached 54 % only in 1 h, but the yield decreased gradually with the increase of the oxidation time and CO_2 was produced in 50 % yield at 4 h. Figure 4b shows the product distribution of the smallest molecule fraction (M_w<104) on coal basis. At 60 °C the yield of this fraction increased monotonously with the oxidation time and reached surprisingly 52% at 24 h. At 80 °C, on the other hand, the yield increased little with the increase of the oxidation time, and it was less than 30% at 4 h. The above results clearly indicate that the oxidation of the dried MW coal by H_2O_2 at around 60 °C is a promising method to produce valuable chemicals in high yield and in high selectivity.

Test of the validity of the proposed method for other coals

It was clarified that the proposed oxidation method is very effective to produce valuable chemicals from the dried MW coal under mild conditions. Then the validity of the method was tested for several low rank coals and the wet MW coal (coal as received). The coals were oxidized for 24 h at 40, 60, and 4 h at 80 °C. Figure 5a shows the product distribution on carbon basis for the coals. All the coals were decomposed rapidly and a large amount of water-soluble organics were produced at 40 °C and 60°C. For the MW dried coal, the solid yield was 19 % and the yield of the water-soluble organics reached 52 % at 60°C as stated above. The product distributions for the wet MW coal were similar to the distributions for the dried MW coal, although the decomposition rate of the wet coal was slightly smaller than that of the dried coal. This result shows that the drying process of the low rank coal, which consumes a large amount of energy, can be eliminated when the coal was oxidized by the proposed method. For HV, the solid yield was smaller than that of the dried MW coal, but larger amount of CO_2, 40% in yield, was produced at 60 °C. The main components of the water-soluble organics were high molecular weight compounds. On the other hand, the solid yield was large and the water-soluble organics yield was small for TC coal. This is probably because TC coal (subbituminous coal) consist of more condensed aromatic components as compared with MW coal.

Figure 5b shows the yields of the smallest molecule fraction on coal basis. Only five kinds of fatty acids and methanol were involved in the fraction for all the coals. Such high selectivities for the fatty acids were judged to derive from the structure of coal. Deno et al.[7] performed the H_2O_2-TFA-H_2SO_4 oxidation of model compounds such as toluene and dibenzofuran, and they found that one or two kinds of

particular fatty acids which reflect the structure of the model compound were produced from each compound. The structure of brown coal consists of one or two aromatic rings connected by short chain linkages such as ether, methylene and ethylene bridges. Then the five fatty acids would be produced by the decomposition of the short chains. The total yields of the fatty acids were 10 to 20 wt% at 40°C for all the coals, and they increased to 30 to 50% at 60 °C except for TC coal. The largest yields was obtained for the dried MW coal at 60 °C. It reached surprisingly 52 % as stated earlier, and consisted of 13.1% of malonic acid, 7.8% of glycolic acid, 6.5% of acetic acid, and 19.3 % of formic acid.

Figure 6 shows the MWDs (M_w>60) of the water-soluble compounds for the coals oxidized at 60 °C. They all showed bimodal distributions having peaks at around 200 and 1000. The components of the smaller molecular weight region probably consist of aromatics of one or two aromatic rings. This suggests that much larger amount of fatty acids can be recovered under proper oxidation conditions. Thus it was clarified that the proposed oxidation method is effective to produce valuable chemicals in high yield and in high selectivity especially from the brown coal.

Mechanism of the H_2O_2 oxidation of coal

It is worth while to examine the oxidation mechanism of brown coal for searching optimum oxidation conditions. This was performed by tracing in detail the changes in the solid properties and the product distributions during the oxidation of the dried MW coal. Figure 7 shows the change in the atomic ratios of oxygen to carbon (O/C) and hydrogen to carbon (H/C) with the oxidation time at 60°C and 80°C. The O/C value increased at first, then decreased with the increase of oxidation time. The H/C value increased significantly with the oxidation time at both temperatures. This clearly shows that hydrogen atoms were introduced into the coal by the H_2O_2 oxidation. Figure 8 shows the change in the F.T.i.r. spectra of the dried MW coal during the oxidation. The intensities of the peaks at 1710 cm^{-1} and 1170 cm^{-1}, which are, respectively, assigned to carboxyl groups and alcoholic OH groups, increased with the progress of oxidation. The intensity of the peak at 2890 cm^{-1}, which is assigned to the aliphatic C-H stretching vibration, increased significantly at 24 h. We clarified that the ratio of aliphatic carbon to total carbon of MW coal is 0.43 from the ^{13}C-n.m.r. spectrum[9]. The sum of the yields of CO_2 and the smallest molecule fraction (M_w<104) in Fig. 4a exceeded 0.43 at the oxidation time of 12 and 24 h at 60 °C. This clearly indicates that a part of the aromatic rings of the coal are ruptured by the H_2O_2 oxidation even at 60 °C. The oxidation of coal by air is known to reduces the H/C ratio and the aliphatic proportion in the coal.[10] The above discussion clearly shows that the mechanism of the H_2O_2 oxidation is completely different from the mechanism of the air oxidation. The H_2O_2 oxidation in acid aqueous solutions contains the proton donating reaction.[11] The pH in the mixture of the dried MW coal in the H_2O_2 aqueous solution was below 4.0, so the proton donating reaction surely proceeded to change the coal and the larger molecules of the water-soluble components into aliphatic rich structure. This will surely increase the yields of smaller molecules with the progress of oxidation.

Summarizing the above discussion, the high yield and the high selectivity for the fatty acids were judged to be achieved by the structure of MW coal itself and the proton donating reaction which is realized by H_2O_2 in acid aqueous solutions.

CONCLUSION

A new and effective method for utilizing the low rank coal as chemical resources was presented, in which the coal was oxidized with 30%-H_2O_2 at below 80 °C under ambient pressure. Oxidizing an Australian brown coal for 24 h at 60 °C, five kinds of fatty acids were recovered surprisingly in 52 % in yield. We are expecting that the proposed method will change the conversion technology of brown coal dramatically.

REFERENCES

1. Kamiya, Y., *Kogyo Kagaku Zasshi*, **1956**, 59, 197-202.
2. Kamiya, Y., *Fuel*, **1963**, 42, 353-358.
3. Kapo, G.; Calvert, S.; *Ind. Eng. Chem. Des. Dev.*, **1966**, 5, 97-104.
4. Bimer, J.; Salbut, P. D.; Berlozecki, S., *Fuel*, **1993**, 72, 1063-1068.
5. Montgomery, R.S.; Bozer, K.B., *Fuel*, **1959**, 38, 400-402.
6. Deno, N.C.; Gregger, B.A.; Stroud, S.G., *Fuel*, **1978**, 57, 455-459.
7. Deno, N.C.; Gregger, B.A.; Messer, L.A.; Meyer, M.P.; Stroud, S.G., *Tetrahedron Lett.*, **1977**, 1703.
8. Miura, K.; Mae, K.; Maki, T.; Araki, J., *Chem. Lett.*, **1995**, 901.
9. Mae, K.; Miura, ; K. Maki, T.; Inoue, S., *Proc. Int. Conf. on Coal Sci.*, **1995**, 365-368.
10. Song, C.; Saini, A.K.; Schobert, H.H., *Energy & Fuels*, **1994**, 8, 301-312.
11. Schumb, W.C.; Satterfield, C.N., "Hydrogenperoxide", 1955, Reinhold (New York).

Table 1 Properties of coals

Coal(Abbrev.)	Proximate analysis(wt%)			Ulimate anaysis(wt%,daf)				
	FC	VM	Ash	C	H	N	S	O
Morwell(MW)	48.2	50.3	1.5	64.8	4.5	0.6	0.3	29.8
Highvale(HV)	52.6	35.4	12.0	67.0	4.3	1.0	0.2	27.5
Taiheiyo(TC)	43.2	45.8	11.0	74.5	6.0	1.3	0.4	17.8

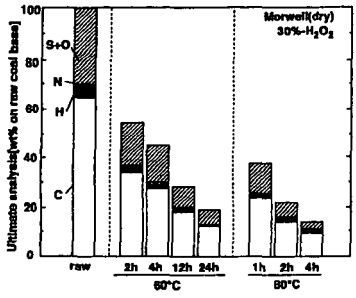

Figure 1 Changes in the solid yield and the elemental composition through the H_2O_2 oxidation of the dried MW coal

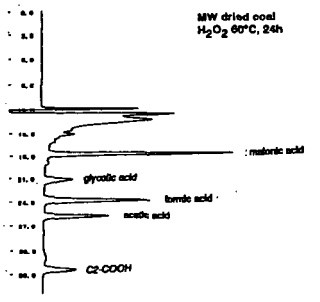

Figure 2 A typical HPLC chart for the organic acid analysis

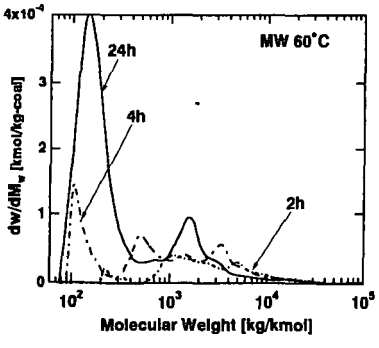

Figure 3 Change in the molecular weight distributions of the water-soluble organics produced through the H_2O_2 oxidation of the dried MW coal

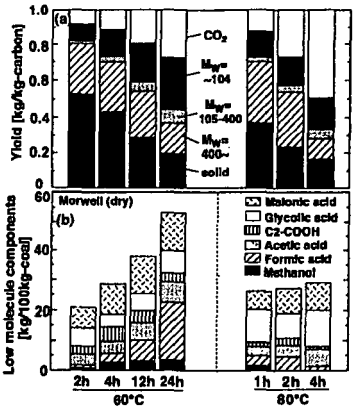

Figure 4 Change in the product distributions through the H_2O_2 oxidation of the dried MW coal

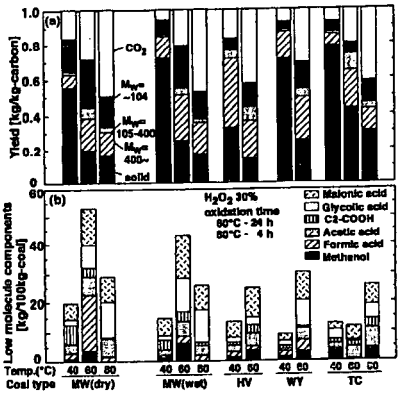

Figure 5 Product distributions through the H_2O_2 oxidation for low rank coals

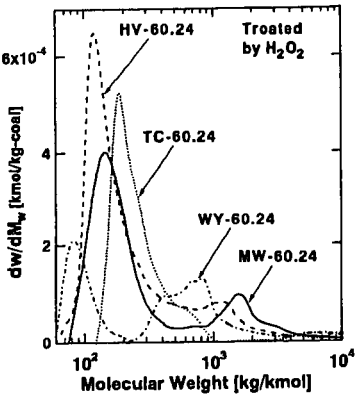

Figure 6 Molecular weight distributions of the water-soluble organics produced through the H_2O_2 oxidation for low rank coals

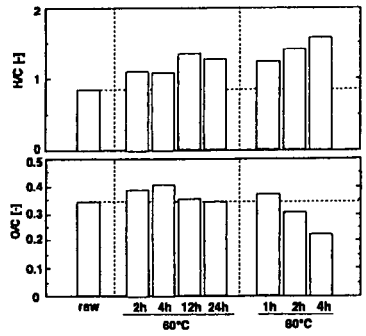

Figure 7 Change in the H/C and O/C atomic ratios through the H_2O_2 oxidation of the dried MW coal

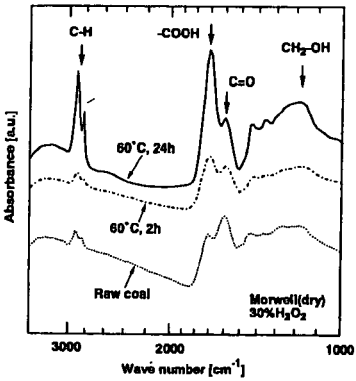

Figure 8 Change in the F.T.i.r. spectra through the H_2O_2 oxidation of the dried MW coal

PYROLYSIS OF SIMPLE COAL MODEL COMPOUNDS CONTAINING AROMATIC CARBOXYLIC ACIDS: DOES DECARBOXYLATION LEAD TO CROSS-LINKING?*

Thomas P. Eskay, Phillip F. Britt, and A.C. Buchanan, III
Chemical and Analytical Sciences Division, Oak Ridge National Laboratory
P.O. Box 2008, MS-6197, Oak Ridge, Tennessee 37831-6197

Keywords: Pyrolysis, Decarboxylation, Cross-Linking, Model Compounds.

Introduction

In recent years, it has been proposed that oxygen functional groups, prevalent in low rank coals, are major actors in retrograde reactions which inhibit their efficient thermochemical processing. In the pyrolysis and liquefaction of low-rank coals, low temperature cross-linking reactions have been correlated with the loss of carboxyl groups and the evolution of CO_2 and H_2O [1,2]. Pretreatments such as methylation, demineralization, or ion-exchange of the inorganic cations reduce cross-linking and CO_2 evolution in pyrolysis, while the exchange of Na^+, K^+, Ca^{++}, and Ba^{++} into demineralized coal increases cross-linking and CO_2 evolution in pyrolysis and liquefaction [3,4]. These results suggest, in part, that decarboxylation pathways in coal may play an important role in the cross-linking of the coal polymer. However, the reaction pathways associated with the decarboxylation and cross-linking events in low rank coal are currently unknown. Furthermore, it is not known whether the reaction pathway that leads to decarboxylation also leads to cross-linking. Radical recombination or addition reactions have been suggested as being involved in retrograde reactions. However, the involvement of radical pathways in thermal decarboxylation reactions has recently been brought into question by the observation that decarboxylation of benzoic acid derivatives under coal liquefaction conditions yielded only small amounts of aryl-aryl coupling products [5]. Therefore, to gain a better understanding of the role decarboxylation plays in cross-linking reactions in low rank coals, we have studied the pyrolysis of several bibenzyls containing aromatic carboxylic acids. The structures currently under investigation are 1,2-(3,3'-dicarboxyphenyl)ethane (**1**) and 1,2-(4,4'-dicarboxyphenyl)ethane (**2**). These compounds are capable of forming reactive free-radical intermediates at *ca.* 400°C through homolysis of the weak bibenzylic bonds. This provides a constant source of free-radicals to potentially assist in the decarboxylation reaction.

Experimental

1,2-(3,3'-dicarboxyphenyl)ethane (1). Into a 1 L oven-dried flask, containing a magnetic stirbar, equipped with an oven-dried addition funnel and kept under positive argon pressure, was placed 3-bromobenzyl bromide (13.0 g, 5.22 x 10^{-2} moles) and dry THF (500 mL). The solution was cooled to -78°C, and the addition funnel was charged with 2.5 M *n*-butyllithium in hexane (54 mL, 1.35 x 10^{-1} moles). The *n*-butyllithium was added dropwise over a period of 20 min and the solution was stirred for 30 min at -78°C. Carbon dioxide, produced from warming dry ice and passing it through two separate drying tubes of $CaSO_4$ and $CaSO_4/CaCl_2$, was bubbled into the solution for 1.5 h. The reaction was warmed to room temperature and quenched with saturated aqueous $NaHCO_3$ (100 mL). The solution was transferred to a separatory funnel and diluted with H_2O (700 mL) and Et_2O (700 mL). The aqueous layer was collected and acidified with concentated H_2SO_4 to precipitate **1**. The white precipitate was collected by vacuum filtration and air dried giving 6.884 g (98 %, GC purity 97 %). Further purification by 4 recrystallizations from isopropyl alcohol and drying over P_2O_5 in a vacuum desicator yielded the product in 99.9 % purity by GC analysis.

1,1,2,2-tetradeutero-1,2-(3,3'-dicarboxyphenyl)ethane (1-d_4) was synthesized by the procedure described above for the synthesis of **1** using 3-bromobenzyl bromide-d_2 which was synthesized as described below. The deuterium content of the product was 97 % d_4 by GC-MS analysis.

3-bromobenzyl bromide-d_2 Into a 1L oven-dried 2-neck flask, containing a magnetic stirbar, equipped with a reflux condenser and an addition funnel, was placed $LiAlD_4$ (Aldrich 98 % deuterium content, 5.00 g, 0.12 moles) and dry Et_2O (300 mL). The solution was stirred and

* This research was sponsored by the Division of Chemical Sciences, Office of Basic Energy Sciences, U.S. Department of Energy under contract DE-AC05-840R21400 with Lockheed Martin Energy Systems, Inc.

3-bromobenzoic acid (20.0 g, 0.10 moles) in dry Et_2O (300 mL) was added from the addition funnel over a period of 30 min. The solution was refluxed for 1 h and was quenched with the cautious addition of H_2O (100 mL). The solution was poured into H_2O (200 mL) containing concentrated H_2SO_4 (16 mL) and stirred until all the solid dissolved. The Et_2O layer was collected and the aqueous layer was extracted with Et_2O (2 x 100 mL). The combined Et_2O extract was washed with dilute aqeous $NaHCO_3$, dried over Na_2SO_4, and the Et_2O was removed to yield 19.4 g of liquid, 3-bromobenzyl alcohol (100 %, crude yield). The deuterium content of the product was 99 % d_2 by GC-MS.

The crude 3-bromobenzyl alcohol (10.1 g, 53.7 mmol) was then placed into a 1-neck (100 mL) flask containing concentrated HBr (26 mL) and concentrated H_2SO_4 (4.0 mL). The solution was refluxed for 6 h, cooled to room temperature, and extracted with hexane (2 x 50 mL). The hexane was passed through a plug of Merck grade 60 silica gel in a (2.5 cm diameter x 2.5 cm long) column and the hexane was evaporated to produce a white solid (11.75 g, 89 % based on crude 3-bromobenzyl alcohol). By GC-MS analysis, the product was 99 % d_2.

1,2-(4,4'-dicarboxyphenyl)ethane (2) was synthesized as described previously [7].

Pyrolyses. Pyrolyses were performed in sealed pyrex tubes (sealed at ca. 10^{-5} Torr) in a Tecam fluidized sandbath at 400 $\pm$ 1.5 °C. Following pyrolysis, the samples were quickly removed from the sandbath and cooled in liquid N_2. The tubes were then cracked open and the solid products were removed with a 2:1 mixture of pyridine:N,O-bis(trimethylsilyl)trifluoroacetamide (BSTFA). Internal standards (2,4,6-trimethylbenzoic acid and 2-phenylbenzoic acid) were added and the reaction mixtures analyzed by GC and GC-MS. Gas chromatography analysis was performed using a Hewlett-Packard 5890 Series II gas chromatograph equipped with a J&W Scientific 30 m x 0.25 mm id, 0.25 μm film thickness DB-1 column and a flame ionization detector. Mass spectra were obtained at 70 eV on a Hewlett-Packard 5972 GC/MS equipped with a capillary column identical to that used for GC analysis. The identities of products from the thermolysis of **1** and **2** were determined by GC-MS analysis and were further confirmed by comparison with commercially available or synthesized authentic materials.

Results and Discussion

Thermolysis of **1** and **2** was conducted at 400 °C in sealed pyrex tubes and analyzed by GC and GC-MS. The major products from the thermolysis of **1** are shown in equation 1 and account for $\geq$ 95 % of the mass balance at conversions of **1** up to 22 %. Several other

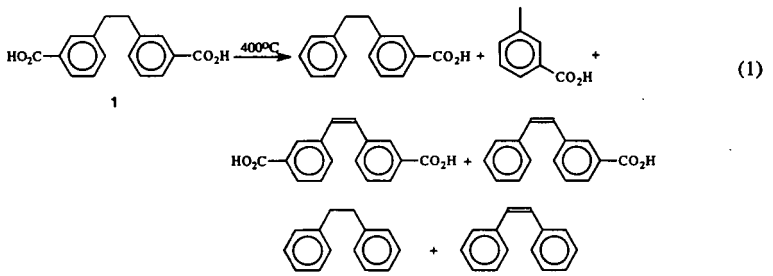

(1)

products are formed in the pyrolysis that have not been identified, but based upon the GC peak area and the good mass balance, the amount of these products are small (< 2 %). The results obtained for the thermolysis of **1** at 400 °C at various time intervals are given in Table 1, entries 1-5. A similar product distribution and mass balance (> 96 %) was obtained in the thermolysis of **2**.

The major product from the thermolysis of **1** and **2** is decarboxylation to 3-carboxybibenzyl and 4-carboxybibenzyl respectively. The good mass balances ($\geq$95 %) suggest that the decarboxylation reaction does not lead to significant quantities of high molecular weight products that might not be observed by GC analysis. Analysis of the methylated (via diazomethane) reaction mixture from the thermolysis of **2** by reverse phase high performance liquid chromatography showed no new products. This result supports the premise that no non-volatile, high molecular weight products are formed. The rate constant for C-C homolysis of the bibenzylic bond was calculated to be 1.8 $\pm$ 0.1 x 10^{-6} s^{-1} for **1** and

$3.8 \pm 0.6 \times 10^{-6}$ s^{-1} for **2** based on the amount of HO_2CPhCH_3 formed at conversions of less than 10 %. The rate constant is slightly lower than reported for homolysis of bibenzyl in tetralin (8.0×10^{-6} s^{-1}) [6]. The apparent first-order rate constant of decarboxylation of **1** and **2** has also been calculated to be $3.7 \pm 0.2 \times 10^{-5}$ s^{-1} and $6.6 \pm 0.2 \times 10^{-5}$ s^{-1}, respectively. The rate constant for decarboxylation of **1** is roughly a factor of 2 slower than that of **2**, suggesting that the decarboxylation mechanism is influenced by the position of the carboxy group on the aryl ring.

On the basis of the product distribution and rate of decarboxylation, the decarboxylation of **1** and **2** is proposed to proceed by an ionic pathway as shown in equation 2. Although the reaction order has not been determined, it is proposed that a second

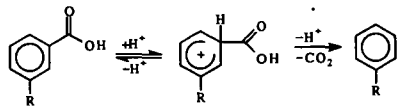

(2)

equivalent of starting material is the source of the acid. Catalysis by residual mineral acid, used to precipitate the diacid during its synthesis, is unlikely based on the similar thermolysis results obtained from the thermolysis of **2** prepared by simple precipitation from mineral acid, and **2** purified by dissolving in NH_4OH, titrating with HCO_2H, and washing with water, ether, and acetone. The difference in the decarboxylation rates of **1** and **2** also supports an ionic pathway. If the rate determining step is protonation of the aromatic ring, the *para*-substituent in **2** would stabilize the carbocation intermediate while the *meta*-substituent in **1** would not. The toluic acid and stilbene derivatives are formed by a free-radical reaction analogous to that reported for the thermolysis of bibenzyl [6,9]. Homolysis of **1** produces 2 (HO_2CPhCH_2•) followed by hydrogen abstraction from **1** to form $HO_2CPhCH_2CH(•)PhCO_2H$ (**3**) and toluic acid (Scheme 1). It is predicted that hydrogen abstraction by HO_2CPhCH_2• or

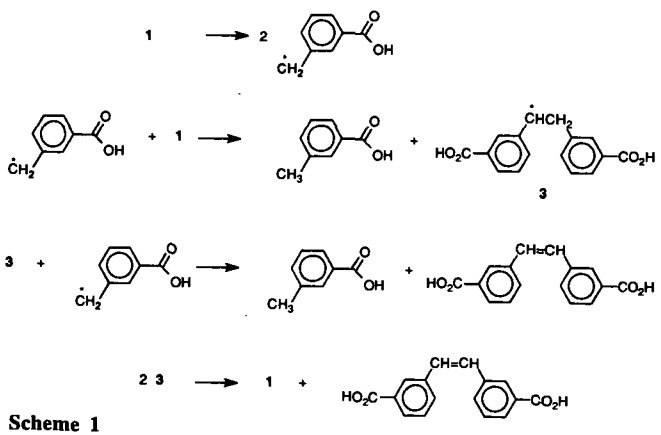

Scheme 1

3 would favor the benzylic C-H bond (86 kcal/mole) over the stronger O-H bond of the carboxylic acid (estimated as 101 kcal/mole). The stilbene derivatives are formed from the disproportionation of **3**, but no products from the coupling of **3** are observed, in contrast to the thermolysis of bibenzyl in which tetraphenylbutane is a major product [9], .

The decarboxylation and cross-linking of aromatic carboxylic acids has been assumed to arise from a free-radical pathway (eq 3), since free-radicals are known to be formed as the

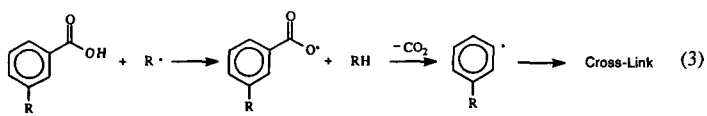

(3)

reactive intermediates in the thermolysis of coal. Aryl radicals are known to add to aromatic rings to form biaryls [6]. The data obtained from decarboxylation of **1** and **2** is inconsistent with a free-radical mechanism. Moreover, it is predicted that the hydrogen abstraction from the carboxylic acid in equation 3 should be the rate determining step in this decarboxylation, since it is known that aryl carboxy radicals undergo decarboxylation at rapid rates (*ca.* 10^6 s^{-1} at 23 °C [8]). Thus a free-radical mechanism should not show a difference in the rate of decarboxylation of **1** and **2**, because the carboxy radical is not in conjugation with the aromatic ring.

To further investigate the mechanism for the decarboxylation of **1**, the thermolysis of **1** containing deuterium in the ethylene bridge (**1-d_4**) was investigated. This molecule should allow us to distinguish if decarboxylation is occuring by an ionic pathway (eq 2) or free-radical pathway (eq 3). Decarboxylation by an ionic pathway would place a hydrogen at the 3-position while the free-radical pathway would place a deuterium at the 3-position of the aromatic ring from D abstraction of the aryl radical (Scheme 2). Preliminary data from a 30

Ionic Pathway

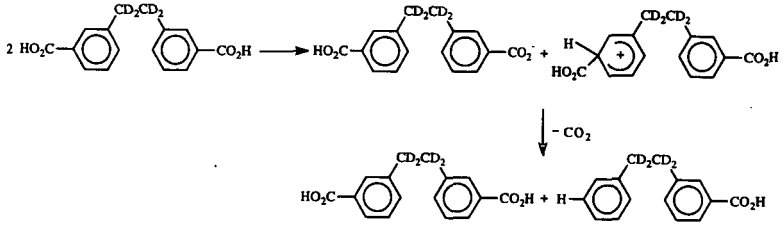

Radical Pathway

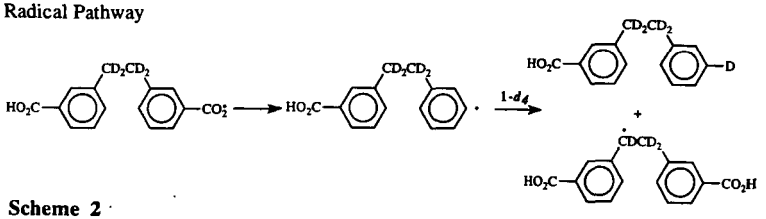

Scheme 2

min thermolysis of **1-d_4** are given in Table 1, entry 6. Analysis of the deuterium content of the major product, 3-carboxybibenzyl, by GC-MS showed that > 97 % of the product was d_4. No d_5 was detected, which strongly supports our assertion that decarboxylation of **1** is occuring by an ionic pathway. The deuterium content of the *m*-toluic acid is currently under investigation to determine if the benzylic radical can abstract hydrogen from the carboxylic acid to give *m*-toluic acid-d_2 as well as from the ethylene bridge to give *m*-toluic acid-d_3.

Summary and Conclusion

The thermolysis of two aromatic carboxylic acids **1** and **2** have been investigated at 400 °C as models of carboxylic acids in low rank coals. The major decomposition pathway observed is decarboxylation, which mainly occurs by an ionic pathway. This decarboxylation route does not lead to any significant amount of coupling or high molecular weight products that would be indicative of cross-linking products in coal. The pyrolysis of **1** and **2** will be investigated under a variety of conditions that better mimic the environment found in coal to further delineate the role that decarboxylation plays in coal cross-linking chemistry.

References

1. Suuberg, E.M.; Lee, D.; Larsen, J.W. *Fuel* **1985**, *64*, 1668.

2. (a) Solomon, P.R.; Serio, M.A.; Despande, G.V.; Kroo, E. *Energy and Fuels* **1990,** *4,* 42. (b) Ibarra, J.V.; Moliner, R.; Gavilan, M.P. *Fuel* **1991,** *70,* 408.
3. (a) Serio, M.A.; Kroo, E.; Chapernay, S.; Solomon, P.R. *Prepr. Pap.-Am. Chem. Soc. Div., Fuel Chem.* **1993,** *38(3),* 1021. (b) Serio, M.A.; Kroo, E.; Teng, H.; Solomon, P.R. *Prepr. Pap.-Am. Chem. Soc., Div. Fuel Chem.* **1993,** *38(2),* 577.
4. Joseph, J.T.; Forria, T.R. *Fuel* **1992,** *71,* 75.
5. Manion, J.A.; McMillien, D.F.; Malhotra, R. *Prepr. Pap.-Am. Chem. Soc., Div. Fuel Chem.* **1992,** *37(4),* 1720.
6. Stein, S.E.; Robaugh, D.A.; Alfieri, A.D.; Miller, R.E. *J. Am. Chem. Soc.* **1982,** *104,* 6567.
7. Britt, P.F.; Buchanan, A.C., III, Hoenigman, R.L. *Coal Science* Pajares, J.A. and Tascon, J. M. D. Eds.; Coal Science and Technology 24; Elsevier Science B.V.: Amsterdam, Netherlands, 1995, 437.
8. Wang, J.; Tsuchiya, M; Sakuragi, H.; Tokumaru, K. *Tetrahedron Letters* **1994,** *35,* 6321.
9. Poutsma, M. L. *Fuel* **1980,** *59,* 335.

Table 1 Product Distributions Observed from the Thermolysis of *m,m*-$HO_2CPhCH_2CH_2PhCO_2H$ at 400°C for Various Time Intervals.

Entry	1	2	3	4	5	6[c]
Products (mole %)	10 min	30 min	60 min	90 min	120 min	30 min
m-CH_3PhCO_2H	8.2	9.9	10.1	10.3	14.1	9.0
m-$CH_3CH_2PhCO_2H$	0.93	1.6	1.4	1.4	1.7	1.3
$PhCH_2CH_2Ph$	b	1.2	2.4	3.2	4.8	1.2
PhCH=CHPh	b	b	0.1	0.1	0.4	b
m-$HO_2CPhCH_2CH_2Ph$	83.7	80.3	76.4	73.3	82.3	84.6
m-HO_2CPhCH=CHPh	0.7	0.6	1.9	2.5	5.6	0.8
m,m-HO_2CPhCH=$CHPhCO_2H$	5.3	5.9	11.2	9.1	11.2	3.2
Conversion[a]	2.6	9.6	17.3	22.3	33.8	8.1
Mass Balance	97.8	96.0	93.0	94.7	90.0	98.4

a-Based on products identified. b-product not detected. c-1-d_4.

RELIABLE CHEMICAL DETERMINATION OF OXYGEN-CONTAINING FUCTIONALITIES IN COAL AND COAL PRODUCTS. CARBOXYLIC ACID AND PHENOLIC HYDROXYL FUNCTIONALITIES

Tetsuo Aida, Yukinari Tsutsumi, and Teiji Yoshinaga
Department of Industrial Chemistry
Faculty of Engineering, Kinki University at Kyusyu
11-6 Kayanomori, Iizuka, Fukuoka 820, JAPAN

Keywords: Coal, chemical determination, oxygen-containing fuctionality

INTRODUCTION

Coal contains various chemical functionalities. Particularly, the oxygen-containing functionalities are considered to play an important role to controle its physical and chemical properties. Recent developement of sophisticated instrumentaion such as FT-ir, ^{13}C-CP-MAS-NMR, XPS, etc., for the direct non-destructive chacterization of a solid coal has made it possible to provide quite reliable information about such hetero-atom-fuctionalites as sulfur-(1), nitrogen-(2) and oxygen-containing fuctionalities. However there still seems to be a problem concerning the selectivity between delicate functiomalities, i.e., a carboxylic, phenolic and alcoholic hydroxyl functionalities.

About 40 years ago, Blom et al.(3) developed chemical determination methods for various ogygen-containing functionalities in coal and coal products, which have often been used in the literatue with some minor modifications. In the course of our studies concerning the solvent swelling of coal, we have learned that this classical method may involve serious experimenntal errors based on the accessibility, particuraly the determination of the carboxylic acid functionality in coals, which used to be carried out in an aqueous solution by using calcium acetate. In general, the coal does not swell very much in a water, furthermore the coals exibit significant steric requirments for the penetrant molecules(4), and its extent of swelling widely varied depending upon the coal rank(5). Usually, a higher rank coal like a bituminous coal exhibits serious penetration restriction. Thus, if one wants to use a chemical reaction on coals, in order to obtain reasonable accessibility of chemical reagent to the functionality in solid coals it is critical to pay maximum attention to the arrangement of the reaction conditions, i.e., reagents and solvents.

Based on our experimental results of coal swelling, we have developed a quite reliable chemical determination method for carboxylic acid and phenolic hydroxyl fuctionalities in coal and coal products. The principle of this method is described as follows: Chemical reactions using various borohydrides were adopted for the determination of these functionalities as shown below, which have very different reactivities and give us a stoichiometric amount of hydrogen gas for each functionality in a pyridine solvent. Thus, we can discriminate each functionalities based upon the difference of thier reactivities to the borohydrides:

$$\text{R-OH} + \text{MBH}_4 \longrightarrow \text{R-OM} + \text{BH}_3 + \text{H}_2$$

(R = Aryl, Alkyl, -CO-, H, etc. ; M = Li, Na, K, n-Bu_4N etc.)

EXPERIMENTAL

The chemical reagents were commercial products(Aldrich's gold label grade) which were used without further purifications. Pyridine was dried over calcium hydride and distilled before use. Coals from the Ames Coal Library were ground, seized, dried at 110°C under vacuum overnight, and stored under a dry nitrogen atmosphere. The pyridine extractions of coals were carried out by using excess amount of pyridine under an ultrasonic irradiation. In order to remove trace amounts of pyridine in the pyridine-extract it was washed by THF/H_2O(30vol%) solution saturated by CO_2, then dried at 110°C overnight , and stored under a dry nitrogen atmosphere.

Volumetric measurements of hydrogen gas evolved through the reactions were carried out by using a gas-buret under hydrogen atmosphere at 25°C. A typical procedure was as follows: Pyridine-extract(0.1g) was throughly groung by using an agate mortar in a dry-box, and placed into a 30ml reaction vessel. Dry pyridine(5ml) was added and the mixture stirred for 30-60minutes prior to start the reaction with excess amount of pyridine/tetra-n-butylammonium borohydride solution. The volume of hydrogen gas generated from the reaction mixture was measured by a gas-buret.

RESULTS AND DISCUSSION

1. Reactivities of various borohydrides toward hydroxyl fuctionalities

In order to evaluate the chemical reactivity of borohydrides, 1-naphthol was chosen as a standard model compound of a phenolic hydroxyl functionality. In Figure 1, the effects of the counter cations of borohydrides are demonstrated. This Figure shows the rate of completion of the reaction vs. reaction time in minute, which were calculated from the volume of the hydrogen gas evolved. Very interestingly, a lithium borohydride reacted very rapidely(completed within 5 minutes under these reaction conditions), compared to the others which were finaly complete only after a prolonged reaction time. Among the experimental data shown in this Figure, it is also quite interesting to note that tetra-n-butylammmonium borohydride reacted with 1-naphthol slowly and stoichiometrically, since the affinity of these types of tetra-alkyl ammmounium compunds for the macromolecular network structure of coals had been well-known to be quite high, i.e., Liotta Methylation(6). There will be a good chance to distinguish kinetically between a phenolic hydroxyl functionality and more stronger hydroxyl functionalities like a carboxylic acid in a solid coal.

2. Reactions of lithium borohydride with various hydroxyl model compounds

The reactivities of various hydroxyl fuctionalities toward lithium borohydride were examined by using model compounds, such as a water, benzyl alcohol, 1-naphthol, catechol and benzoic acid. Figure 2 summerizes the results.

Very interestingly, the reactions with carboxylic acid(benzoic acid) and phenolic compounds(1-naphthol and catechol) proceeded significantly faster than those of others(benzyl alcohol and water), which means that the amount of hydrogen gas evolution within 60 minutes under this reaction condition represents the amount of both carboxylic acid and phenolic hydroxyl functionalities.

3. Reactions of tetra-n-butylammonium borohydride with various hydroxyl model compounds

Figure 3 shows the results obtained from the experiments to examine the reactivities of various model compounds toward tetra-*n*-butylammonium borohydride.

Compared to the previous experiments with lithium borohydride, the reaction rate of benzoic acid was significant. Most of the hydrogen gas evolution at the ininitial stage of the reaction is considered to come from the reaction with a carboxylic acid functionality. Even if it was a mixture of those, we can obtain reasonable analytical values of the acid functionality by a treatment of an extraporation of the curve in the Figure.

4. Quantitative determination of carboxylic acid and phenolic hydroxyl functionalities in the mixture of various hydroxyl model compounds

Coal is believed to contain various hydroxyl functionalities, such as a water, alcoholic, phenolic and carboxylic hydroxyl functionalities. Based on the results described above, we have tried to evaluate the proposed method, "Metal hydride method" using a mixture of the model compound which was prepared with an equivalent amount of the functionalities. Figure 4 exhibits the hydrogen gas evolution from reaction mixtures for both the case of the lithium salt and tetra-n-butyl ammmonium salts. The data shown in this Figure seem to be consistent. The equiliblium value of the reaction(hydrogen gas evolution) with lithium salt must represent the sum of carboxylic acid and phenolic hydroxyl functionalities, meanwhile in the case of tetra-n-butylammmonium salt the extraporated value must be the amount of carboxylic acid functionality. Obviously, the data shown in this Figure seems to be consistent.

5. Quantitative determination of carboxylic acid and phenolic hydroxyl functionalities in the pyridine-extract of coal

In order to minimize the complications of the accessibility of the borohydride molecule to the active sites buried into the macromolecular network structure of coal and inorganic components in coal, we have started the quantitative determination of these functionalities by using pyridine-extract which gives us a homogenenous reaction system. In Figure 5, a typical measurement is demonstrated, in which Illinois No.6 coal was used. Although the rate of the hydrogen evolution seems to be slow compared to those of the model compounds, the pattern was quite similar. The calculated values of the contents of carboxylic acid and phenolic hydroxyl functionalities from the Figure 5 were 0.82 mmol/g amd 2.03 mmol/g which corresponded to 8 units/660-carbon atom and 24 units/660-carbon atom. Although we have no reason to believe that the content of these functionalities in the pyridine-extract is exactly same as the raw coal, it is quite interesting that the content of phenolic hydroxyl functionality was almost equal to the number(25 units/660-carbon atom) of phenolic hydroxyl functionality described in the Shinn Model(7) of Illinois No.6 coal. But there was 8 fold differences in the carboxylic acid functionality(1 unit/ 660 carbon atom in Shinn Model vs. 8 units/660 carbon atom by present work).

Table 1 summarizes the analytical data obtained by this new method for the pyridine-extracts of different rank of coals. The coal-rank dependency of each functionalities appearing in this Table seem to be unusual, based on our previous understanding. The carboxylic acid functionality(which had been believed to be so reactive that it would not survive metamorphism and be detectable in higher ranks of coal) seems to exist significantly in a wide range of coals. On the other hand, the phenolic hydroxyl functionality in coal is reasonably stable over the coal-rank range used in this study. The contradictions on these data revealed here are thought to prove very serious and important problems in reviewing our understanding of the physical and chemical properties of coals.

The accumulation of the experimental data concerning the content of these functionalities in the raw coals is now underway in our laboratory. We are now developing the method for the detemination of an alcoholic hydroxyl functionality in coal.

CONCLUSION

Based on the experimental results of solvent swelling of coal, a reliable chemical determination method both carboxylic acid and phenolic hydroxyl functionalities has been developed by using the reactions of borohydride salts in pyridine solvent. Advantages of this method are considered to be (a) better accessibility of chemical reagent into the macromolecular network of coal (in pyridine solvent), (b) quantitative and direct(one-step) reaction, and (c) accuracy and easiness(volumetric determination of hydrogen gas).

AKNOWLEDGEMENTS

A part of this research was supported by the grant from the Nihon Shigaku Shinkoh Zaidan through The Institute of Environmental Science of Kinki University during 1990-1992.

REFERENCES
(1) Gorbaty, M.L., George, G.N., and Kelemen, S.R., Fuel, **69**, 1065(1990)
(2) Burchill, P., and Welch, L.S., Fuel, 68, 100(1989)
(3) Blom, L., Edelhausen, L., and van Krevelen, D.W., Fuel, **36**, 135(1957)
(4) Aida, T., Fuku, K., Fujii, M., Yoshihara, M., Maeshima, T., and Squires, T.G., Energy & Fuels , **5**, 79(1991)
(5) T. Aida, submitted to Fuel
(6) Liotta, R., Rose, K., and Hippo, E., J. Org. Chem., **46**, 277(1981)
(7) Shinn, J.H., Fuel, **63**, 1187(1984)

Table 1. Contents of carboxylic acid and phenolic hydroxyl functionalities in pyridine-extract of coals

Coal	Carbon content(%,dmmf)		Content of functionality(mmol/g)	
	Raw coal	Pyridine-extract	-COOH	Ar-OH
Hanna No.80	73.1	77.4	0.96	2.04
Adaville No.11	76.6	76.0	1.02	2.08
Illinois No.6	80.6	79.7	0.82	2.03
West Kentucky No.9	82.5	79.9	0.65	1.45
Pittsburgh No.8	85.1	77.8	0.52	1.58

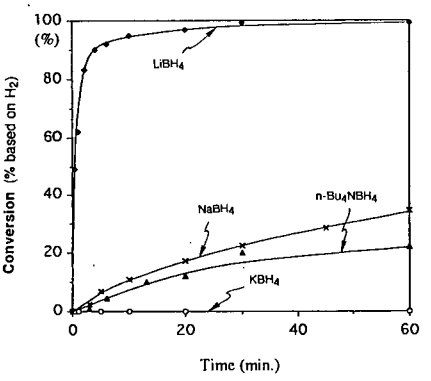

Figure 1. Reactions of 1-naphthol with various borohydrides

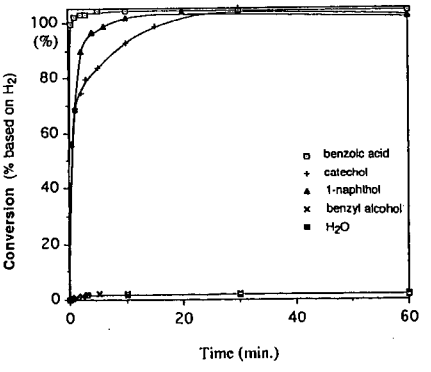

Figure 2. Reactions of $LiBH_4$ with various model compounds

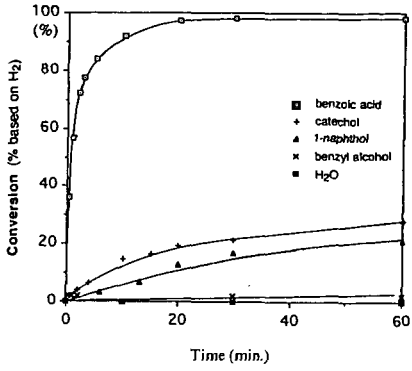

Figure 3. Reactions of n-Bu_4NBH_4 with various model compounds

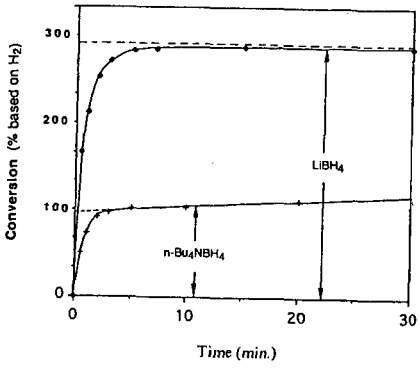

Figure 4. Reactions of $LiBH_4$ and n-Bu_4NBH_4 with model compounds mixture
(benzoic acid / catechol /1-naphthol /benzyl alcohol / H_2O = 1 / 0.5 / 1 / 1 / 1 mol.)

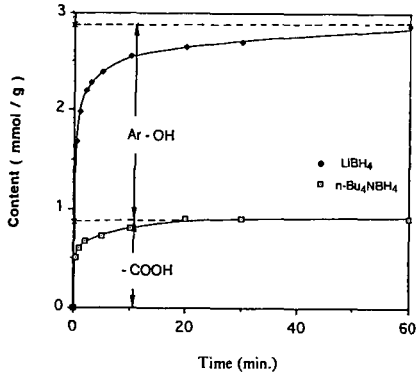

Figure 5. Determination of carboxylic acid and phenolic hydroxy functionalities in pyridine-extract of Illinois No. 6 coal

INTERMOLECULAR INTERACTIONS FOR HYDROCARBONS ON WYODAK COAL

Amy S. Glass and Damon S. Stevenson
Department of Chemistry
University of Dayton
Dayton, OH 45469-2357

(Keywords: Wyodak coal, ionic forces, coal surface interactions)

INTRODUCTION

Low rank coals are abundant in the U.S.[1] Although their calorific values, mineral matter contents, and coking properties make them less desirable than higher rank coals in some industrial applications, low rank coals are used as feedstocks in coal liquefaction and are coprocessed with higher rank coals for other applications.[2-5] The desire to use these coal resources more effectively would be aided by an understanding of the intermolecular and surface interactions at mineral-organic and organic-organic coal interfaces.

Studies of intermolecular forces in low rank coals have concentrated on the coals' ionic properties.[6-10] Schafer quantified the ion-exchange groups in various low rank coals.[6] From swelling studies Nishioka concluded that ionic forces play a role in determining the macromolecular structures of low rank coals.[7] Ahsan et al. studied Wyodak coal's interactions with organic acids before and after the coal was demineralized by citric acid washing (CAW).[8] They found that interactions with aromatic acids increased while those with aliphatic acids decreased as a result of demineralization. From pH studies of coal slurries Vorres found that a range of different ion-exchange sites exist in Wyodak coal.[9] Martinez-Tarazona et al. showed that low rank coals possess ion-exchange sites in the form of both organic (carboxylate and phenolate) and inorganic (clay) components.[10]

In the present work, inverse gas chromatography (IGC) has been used to quantify the intermolecular forces of Wyodak subbituminous coal from the Argonne Premium Coal Sample Bank. It has been found that saturated and unsaturated hydrocarbons experience different intermolecular forces at the coal surface and that these molecules can be used to probe both specific and nonspecific forces in Wyodak coal.

EXPERIMENTAL

The procedure for IGC of coal surfaces has been described previously.[11] About 3g of coal of 40/60 mesh fraction is packed into a 1/8 inch O.D. stainless steel tube ~1.5m in length. GC columns are conditioned at the highest temperatures at which IGC experiments will be performed (150°C, 200°C, or 250°C). Experiments involve obtaining at least 5 peaks every 5-10 degrees over a column temperature range of at least 30 degrees.

Wyodak coal from the Argonne Premium Coal Sample Bank was used as the stationary phase.[12] The coal was extracted in tetrahydrofuran (THF) in a Soxhlet extractor for several days. Citric acid washing and HF-HCl demineralization procedures were those used previously.[13] The alkylation procedure was that of Liotta et al.[14] Adsorbate liquids and reagents were obtained from Aldrich at the highest purities available and used without additional purification. Adsorbate gases were obtained from Aldrich or from Matheson at purities of at least 99.99%.

RESULTS AND DISCUSSION

Figure 1 shows isosteric adsorption heats, q_{st}, for hydrocarbons interacting with Wyodak coal which has been heated to 150°C or 200°C.[15] The data are plotted vs. molecular polarizability of the adsorbates, α'. The molecular polarizability is related to the electron distribution of the adsorbate molecule.[16] For a given class of adsorbate molecules (eg., n-alkanes, chloroalkanes, 1-alkenes), α' increases linearly with increasing adsorbate size or increasing number of carbon atoms in the adsorbate molecule.[16]

The lower plot in Figure 1 shows data for n-alkanes on Wyodak coal. These types of adsorbates can interact with the coal by nonspecific van der Waals dispersion forces only. The adsorption heats for n-alkanes increase linearly with increasing adsorbate polarizability as expected for van der Waals interactions. The slope of the plot for n-alkanes in Figure 1 is a measure of the increase in dispersive van der Waals force with increasing adsorbate size.[16] This information (the slope of the plot) is analogous to a dispersive surface tension, γ_s^d, which gives the strength of the van der Waals interaction normalized to the adsorbate area at a surface.[17] The slope of the plot for n-alkanes in Figure 1 translates into a dispersive surface tension of 25 mJ/m^2. This is a fairly low dispersive surface tension, demonstrating that Wyodak coal presents a low energy surface to saturated hydrocarbons, similar to those found for hydrocarbon oils and bitumens.[18,19]

The two upper plots in Figure 1 show data for 1-alkenes on Wyodak coal that has been heated at 150°C or at 200°C. Comparison of the upper plot, for the 150°C-heated coal, with the plot for n-alkanes demonstrates that alkenes have ~2-4 kcal/mol stronger interaction with the coal than n-alkanes. This difference is most likely the result of a specific interaction between alkenes and the coal, discussed below. The steeper slope of the plots for alkenes (upper plots) compared to the slope for alkanes (lower plot) reflects the stronger nonspecific van der Waals force experienced by alkenes at this surface.[16] On oxidized carbon surfaces which contain polar functional groups, alkenes have more exothermic adsorption enthalpies than alkanes.[20] The stronger nonspecific interactions of alkenes on Wyodak coal likely involve interactions with polar groups on the coal.

As seen by comparing the two upper plots in Figure 1, heating the coal to 200°C causes a constant decrease in the adsorption heat exothermicities for 1-alkenes. The constant decrease in exothermicities of the alkenes' adsorption heats after heating the coal to 200°C suggests that a *specific* interaction between alkenes and the coal has been lost as a result of heating. Heating has caused the adsorption heats for all 1-alkenes to decrease by the same amount, ~1.2 kcal/mol, while it has not changed the slope of the alkenes plot. A specific alkene-coal interaction, as opposed to a nonspecific van der Waals interaction, would be characterized by a constant change in adsorption heat for a particular adsorbate functional group-coal interaction. All of the 1-alkenes in Figure 1 possess a single double bond. Loss of a specific interaction between the double bond of alkenes with the coal surface would result in a constant decrease in the adsorption heat exothermicity. It is likely that a specific interaction is occurring between the double bond of the alkenes and ionic or polar groups on the coal surface. An interaction between the double bond of the hydrocarbon with a positive charge at a surface, a so-called "cation-π" interaction, could be responsible for the specific interactions between unsaturated hydrocarbons and Wyodak coal.[16] Cation-π interactions occur in biological systems and at the surfaces of inorganic solids such as clays and silica.[16,21] When the coal is demineralized by CAW or HF-HCl treatment, the same decrease in adsorption heat exothermicities (~1.2 kcal/mol; data not shown) occurs.[15] This result provides evidence that removing ion-exchangeable cations from Wyodak coal results in the loss of a specific cation-π interaction which involves ion-exchange cations on the coal surface and the unsaturated bond of the hydrocarbon adsorbate.

Figure 2 shows data for n-alkanes and 1-alkenes interacting with the surface of Wyodak coal that has been heated at 250°C. It is seen that heating to 250°C results in the same plot of adsorption heat vs. polarizability for n-alkanes and 1-alkenes. Unlike the case for the 150°C-heated coal (Figure 1) where the different slopes of the plots show that alkanes and alkenes have different nonspecific interactions with the coal, the result in Figure 2 says that heating to 250°C gives the same nonspecific interaction for both types of hydrocarbons on Wyodak coal. Furthermore, a comparison of the data for alkenes on 200°C-heated Wyodak coal

(Figure 1) with data for alkenes on 250°C-heated Wyodak coal (Figure 2) shows that the adsorption heats for alkenes are similar on these two heated coals. These two heated coals have lost their specific interactions with the coal; therefore, this result says that the nonspecific component of the adsorption heat for alkenes is similar for 200°C-heated and 250°C-heated coals. On the other hand, the nonspecific component of the adsorption heat for alkanes has increased in exothermicity as a result of heating the coal to 250°C. The same result (same plot for alkanes and alkenes) is obtained by extracting or alkyating the coal (results not shown).[15] The slope of the plot in Figure 2 corresponds to a dispersive surface tension of ~50 mJ/m². This value is similar to dispersive surface tensions found for flat carbonaceous surfaces.[22] It was shown previously that extracting Illinois No. 6 coal or heating to 250°C gave a dispersive surface tension of ~50 mJ/m² for that coal as well.[23] These treatments cause changes in the concentration and/or polarizabilities of atoms at the coal surface.[16,23] Changes in bulk coal properties have been reported to result from these treatments and it is possible that changes in the bulk are reflected as changes in the coal's dispersive surface tension.[24]

CONCLUSION

In conclusion, IGC data show that three types of forces are experienced by hydrocarbons at the Wyodak coal surface: a nonspecific force experienced by n-alkanes, a nonspecific force experienced by 1-alkenes, and a specific force experienced by 1-alkenes. The nonspecific force felt by n-alkanes gives a dispersive surface tension of ~25 mJ/m² for this coal. The nonspecific force felt by 1-alkenes is stronger and likely involves interactions with polar groups at the coal surface. The specific interaction between alkenes and Wyodak coal is most likely due to an interaction of the unsaturated bond with ionic groups at the coal surface; i.e., a cation-π interaction. Heating the coal to 250°C increases the interactions with n-alkanes so that both types of hydrocarbons, alkanes and alkenes, have the same nonspecific interaction with the 250°C-heated coal. The nonspecific interaction with the 250°C-heated coal gives a dispersive surface tension of ~50 mJ/m².

REFERENCES

1. Van Krevelen, D. W. *Coal*, 3rd. ed.; Elsevier: New York, 1993; Chapter 1.
2. Van Krevelen, D. W. *Coal*, 3rd. ed.; Elsevier: New York, 1993; Chapter 24.
3. Neavel, R. C. In *Coal Structure*, ACS Adv. Chem. Series No. 192; Gorbaty, M. L.; Ouchi, K., Eds.; ACS: Washington, DC, 1981; Chapter 1.
4. Neavel, R. C. In *Coal Science*, vol. 1; Gorbaty, M. L.; Larsen, J. W.; Wender, I., Eds.; Academic: New York, 1982; pp. 1-19.
5. Berkowitz, N. *An Introduction to Coal Technology*; Academic: New York, 1979; Chapter 13.
6. Schafer, H. N. S. *Fuel* 1970, *49*, 271-280.
7. Nishioka, M. *Fuel* 1993, *72*, 1725-1731.
8. Ahsan, T.; Wu, J. H.; Arnett, E. M. *Fuel* 1994, *73*, 417-422.
9. Vorres, K. S. *Prepr. Pap.-Am. Chem. Soc. Div. Fuel Chem.* 1993, *38*, 1045-1057.
10. Martinez-Tarazona, M. R.; Martinez-Alonso, A.; Tascon, J. M. D. *Fuel* 1990, *69*, 362-367.
11. Glass, A. S.; Larsen, J. W. *Energy Fuels* 1993, *7*, 994-1000.
12. Vorres, K. S. *Energy Fuels* 1990, *4*, 420-426.
13. Silbernagel, B. G.; Gebhard, L. A.; Flowers, R. A.; Larsen, J. W. *Energy Fuels* 1991, *5*, 561-568.
14. Liotta, R.; Rose, K.; Hippo, E. *J. Org. Chem.* 1981, *46*, 277-283.
15. Glass, A. S.; Stevenson, D. S. *Energy Fuels*, submitted.
16. Kiselev, A. V.; Yashin, Y. I. *Gas-Adsorption Chromatography*; Plenum: New York, 1969; Chapter 2.
17. Doris, G. M.; Gray, D. G. *J. Coll. Int. Sci.* 1980, *77*, 352-362.
18. Zisman, W. A. In *Contact Angle, Wettability, and Adhesion*,

ACS Adv. Chem. Ser. No. 43; ACS: Washington, DC, 1964; Chapter 1.
19. Drelich, J.; Bukka, K.; Miller, J. D.; Hanson, F. V. *Energy Fuels* 1994, *8*, 700-704.
20. Elkington, P. A.; Curthoys, G. *J. Phys. Chem.* 1969, *73*, 2321-2326.
21. Dougherty, D. A.; Kearney, P. C.; Mizoue, L. S.; Kumpf, R. A.; Forman, J. E.; McCurdy, A. In *Computational Approaches in Supramolecular Chemistry*, Wipff, G., Ed.; Kluwer: New York, 1994; pp. 301-309.
22. Lopez-Garzon, F. J.; Pyda, M.; Domingo-Garcia, M. *Langmuir* 1993, *9*, 531-536.
23. Glass, A. S.; Larsen, J. W. *Energy Fuels* 1994, *8*, 629-636.
24. Brenner, D. *Fuel* 1984, *63*, 1324-1328.

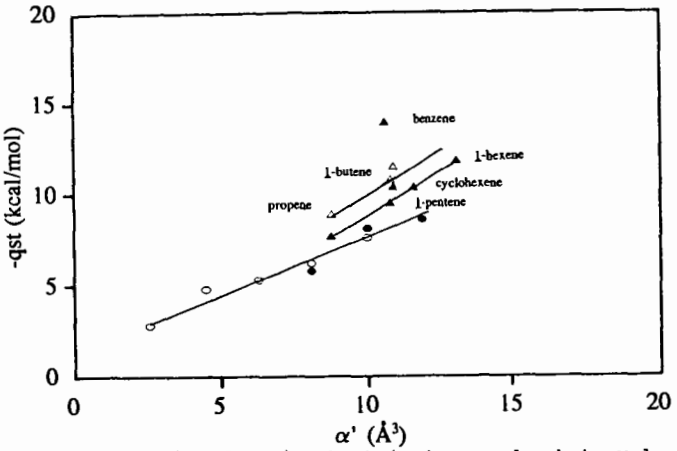

Figure 1. Isosteric adorption heat (q_{st}) vs. adsorbate volume molecular polarizability (α') for n-alkanes, alkenes, and benzene on Wyodak coal heated in helium at 150°C and at 200°C.[15] ○=n-alkanes (methane, ethane, propane, n-butane, and n-pentane) on 150°C-heated coal; ●=n-alkanes (n-butane, n-pentane, n-hexane) on 200°C-heated coal; △=1-alkenes on 150°C-heated coal; ▲=alkenes and benzene on 200°C-heated coal.

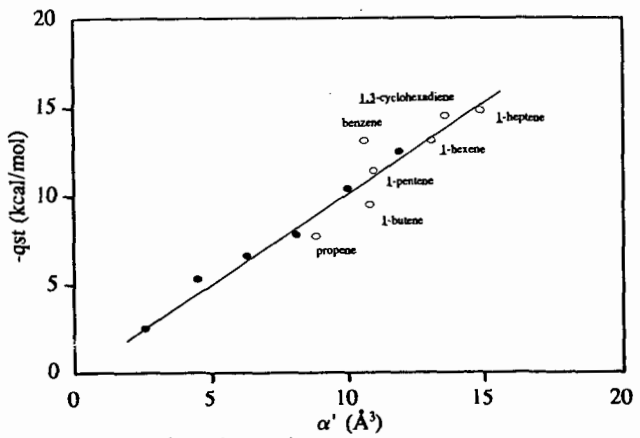

Figure 2. Isosteric adsorption heat (q_{st}) vs. molecular volume polarizability (α') for alkanes and unsaturated hydrocarbons on Wyodak coal heated to 250°C. ●=n-alkanes in order of increasing exothermicity: ethane, propane, n-butane, n-pentane, n-hexane, and n-heptane; ○=alkenes and aromatics on Wyodak coal heated at 250°C.

CHEMICAL STRUCTURE OF COAL TAR DURING DEVOLATILIZATION

T. H. Fletcher[1], M. Watt[1], S. Bai[2], M. S. Solum[2], and R. J. Pugmire[3]

[1]Department of Chemical Engineering Brigham Young University, Provo, Utah 84602
Departments of Chemistry[2] and Chemical and Fuels Engineering[3], University of Utah, Salt Lake City, Utah 84112

Keywords: coal, pyrolysis, ^{13}C NMR

Introduction

Enormous progress has been made in coal pyrolysis research during the last two decades. Models of coal devolatilization have progressed from simple rate expressions based on total mass release[1, 2] to empirical relationships based on the elemental composition of the parent coal[3] to models that attempt to describe the macromolecular network of the coal.[4-6] In the last several years, advancements in chemical analysis techniques have allowed quantitative investigations of the chemical structure of both coal and its pyrolysis products, including the nature of the resulting char. A prominent research goal is to accurately predict the rates, yields, and products of devolatilization from measurements of the parent coal structure. The prediction of nitrogen species evolved during devolatilization is of current interest. These goals necessitate modeling the reaction processes on the molecular scale, with activation energies that relate to chemical bond breaking rather than to the mass of products released from the coal. Solid-state ^{13}C NMR spectroscopy has proven particularly useful in obtaining average values of chemical structure features of coal and char, while liquid phase ^{1}H NMR spectroscopy has been used to determine some of the chemical features of coal tar.[7-10] Pyridine extract residues from coal and partially-pyrolyzed coal chars have also been analyzed by solid-state ^{13}C NMR spectroscopy, and the extracts have been analyzed by ^{1}H NMR spectroscopy.[11]

Several current devolatilization models use some kind of network approach to describe the parent coal structure and subsequent devolatilization behavior.[4-6] Coal is modeled as an array of aromatic clusters connected by labile bridges. Kinetic expressions are postulated for the rate of bridge scission, and statistical representations are used to determine the number of clusters liberated from the coal matrix as a function of the number of bridges cleaved. The vapor pressure of liberated clusters are calculated and used to determine yields of tar versus metaplast. Crosslinking reactions eventually connect the remaining metaplast to the char matrix. Such models require knowledge of the average size of the aromatic clusters in the coal, the number of attachments (bridges and side chains) per cluster, the ratio of bridges to side chains, and the average size of the bridges or side chains. Several reviews of these models have been published.[12, 13] All three of these models use the solid-state ^{13}C NMR data to some extent to guide selection of coal-dependent input parameters to describe the coal matrix. One model demonstrated success in using the solid-state ^{13}C NMR data directly as the only coal-dependent structural input parameters.[6] One of the common assumptions in these models is that the aromatic clusters are not broken during the pyrolysis process, and hence the bridge breaking rate largely controls the devolatilization rate. Therefore, the average number of aromatic carbons per cluster in the coal is equal to that in the char and in the tar.

In a recent paper, Niksa[14] postulated that nitrogen evolution during pyrolysis could be modeled assuming that the mass of nitrogen per aromatic cluster in the coal tar was equal to that in the parent coal. A theoretical analysis was performed using tar data reported in the literature to determine the validity of Niksa's assumption. Elemental analyses of tar samples were reported by Freihaut, et al.[15, 16] and by Chen.[17] It has been shown that the carbon aromaticity of the pristine tar (as estimated from ^{1}H NMR spectroscopy) is similar to that of the parent coal for both lignites and bituminous coals .[8, 9] Assuming that the number of aromatic carbons per cluster in the tar is equal to that in the coal, the mass of nitrogen per cluster $M^{N}_{cluster}$ can be calculated as follows:

$$M^{N}_{cluster} = \frac{x_N}{x_C} MW_C \frac{C_{cl}}{f_{a'}} = MW_{cl}\, x_N \qquad (1)$$

where x_N = wt% N in coal (daf), x_C = wt% C in coal (daf), MW_C = molecular weight of carbon, C_{cl} = # of aromatic carbon per cluster, $f_{a'}$ = carbon aromaticity, and MW_{cl} = molecular weight per aromatic cluster. Results of this analysis are shown in Fig. 1, indicating that the mass of nitrogen per cluster in the tars do not equal the mass of nitrogen per cluster in the parent coal. The results shown in Fig. 1 are pieced together from data reported in several experiments, which may have caused errors. It may also be possible that (a) the number of aromatic clusters in the tar does not equal that in the coal, or that (b) the carbon aromaticity of the tar does not equal that of the coal. This paper describes experiments and analyses of *one* set of coal tars and chars. This is the first time that this high resolution ^{13}C NMR spectroscopy techniquw has been applied to coal tars, and data regarding the number of aromatic carbons per cluster and carbon aromaticities in coal tars are presented.

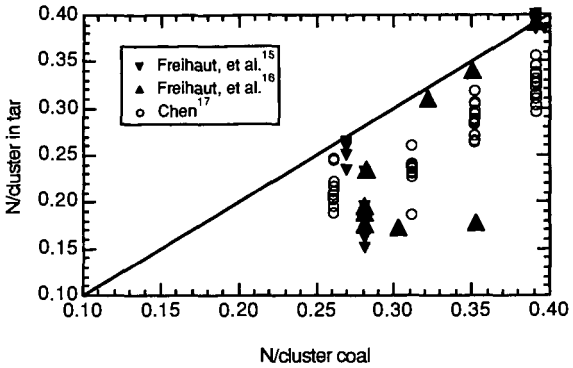

Figure 1. Comparison of the calculated nitrogen per cluster in the tar and in the parent coal.

Experimental Apparatus

Samples of tar and char were produced at atmospheric pressure in the High Pressure Controlled-Profile (HPCP) drop tube reactor.[18] The HPCP drop tube furnace is a laminar flow furnace with a computer-controlled wall temperature profile to create isothermal conditions for reactivity tests. Particles are fed with the primary gas through a water-cooled injector, which can be moved in order to vary particle residence times. The secondary gas flows into a preheater prior to entering the reactor. Wall heaters control the temperature profile in the drop tube furnace. The collection probe collects the entire mass flow and quenches all particle reactions. The collection probe is water-cooled with gas quench jets in the probe tip. A permeable liner inside the main probe tube allows quench gas to be injected radially along the length of the probe to reduce particle and tar deposition. A virtual impactor follows the collection probe to aerodynamically separate the gases from the heavier particles. A cyclone separates char particles from tars and aerosols, and the tars and aerosols are eventually collected on filters.

Table I
Coal Properties

Coal	PSOC ID	Rank	%C (daf)	%H (daf)	%N (daf)	%Ash (dry)
Illinois #6 (IL)	1493D	hvc bituminous	77	5.0	1.5	15.1
Blue #1 (NM)	1445D	sub-bituminous	77	5.7	1.3	3.6
Pittsburgh #8 (PA)	1451D	hva bituminous	84	5.5	1.7	4.1

The HPCP was used to pyrolyze coal samples in 100% nitrogen, at moderate gas temperatures of 930 K, and at residence times of 230 ms and 420 ms. Relatively low temperatures were used in these experiments to minimize possible secondary reactions in the evolved coal tars. Properties of the three coals examined are shown in Table 1. The 63-75 μm size fraction was used in all of these experiments, resulting in heating rates of approximately 10^4 K/s. The "D" on the Penn State coal identification number signifies coals from a suite selected by the DOE Pittsburgh Energy Technology Center's Direct Utilization/AR&TD program. These coals have been well characterized and studied by many other researchers, including those referenced in Figure 1.

^{13}C NMR Analysis

Solid state ^{13}C NMR techniques (CP/MAS and dipolar dephasing) have been used to determine the chemical structure features of coals and coal chars.[7, 19] In addition to carbon aromaticity ($f_{a'}$), the distinction between aromatic carbons with and without attachments (such as hydrogen, carbon, or oxygen) is measured. The specification of the number of aromatic carbons per cluster (C_{cl})[7] provides the basis for the determination of many interesting chemical structure features. Probably one of the most useful quantities is the number of attachments per aromatic cluster, referred to as the coordination number (σ+1).

A high resolution ^{13}C NMR technique was recently developed and applied to model compounds, mixtures, and coal-derived liquid samples.[20] This technique uses spin-lattice relaxation to differentiate protonated from nonprotonated carbons, based on relaxation differences

arising from direct CH dipolar interactions. Average aromatic ring sizes and other lattice parameters are estimated using the procedures used for solid-state ^{13}C NMR.[7, 19]

Tar samples were dissolved in deuterated methylene chloride (CD_2Cl_2) and then filtered. A significant amount of residue was obtained for each tar. This tar residue was subsequently analyzed using the CP/MAS and dipolar dephasing solid-state ^{13}C NMR technique in the same fashion as that used for coal char.

Results and Discussion

Tars collected at 230 ms were analyzed using the ^{13}C NMR spin-lattice relaxation technique; data are presented in Tables 2 and 3. Data for char collected at 420 ms are also presented in Table 2. Analysis of the dissolved tar from the Illinois #6 coal is in progress. As seen in Table 3, 12 to 42% of the tar sample collected was deposited on the filter as residue. Also, lower amounts of tar were collected for the lower rank Illinois #6 and Blue #1 coals than for the hva bituminous Pitt #8 coal. The tar yields seem somewhat lower than reported in the literature, indicating that some tar may have deposited in the sampling apparatus. Other investigators have corrected their measured yields for estimated deposition in the sampling apparatus[17]; this correction will be performed for these data in the future.

Table 2
^{13}C NMR Analysis of Coals, Tars, and Chars[a]

Coal	Sample	f_a	f_a^C	$f_{a'}$	f_a^H	f_a^N	f_a^P	f_a^S	f_a^B	f_{al}	f_{al}^H	f_{al}^*	f_{al}^O
Pitt #8	coal	65	3	62	23	39	5	16	18	35	24	11	7
Pitt #8	dis. tar	69	2	67	38	29	5	15	9	31	2	11	na
Pitt #8	tar res.	83	3	80	34	46	8	18	2	17	1	7	2
Pitt #8	char	81	5	76	24	52	6	18	28	19	11	8	6
Blue #1	coal	6	5	55	19	36	8	13	15	4	29	11	7
Blue #1	dis. tar	63	7	56	27	29	8	16	5	37	27	1	na
Blue #1	tar res.	72	6	66	24	42	9	15	18	28	17	11	12
Blue #1	char	77	5	72	24	48	9	2	19	23	15	8	4
Illinois #6	coal	66	3	63	21	42	7	16	19	34	24	1	8
Illinois #6	tar res.	8	6	74	28	46	8	18	2	2	12	8	3
Illinois #6	char	78	6	72	25	47	8	19	2	22	13	9	4

[a]Percentage carbon (error): f_a = total sp^2-hybridized carbon (±3); $f_{a'}$ = aromatic carbon (±4); f_a^C = carbonyl, $\delta > 165$ ppm (±2); f_a^H = aromatic with proton attachment (±3); f_a^N = nonprotonated aromatic (±3); f_a^P = phenolic or phenolic ether, δ = 150-165 ppm (±2); f_a^S = alkylated aromatic δ = 135-150 ppm(±3); f_a^B = aromatic bridgehead (±4); f_{al} = aliphatic carbon (±2); f_{al}^H = CH or CH_2 (±2); f_{al}^* = CH_3 or nonprotonated (±2); f_{al}^O = bonded to oxygen, δ = 50-90 ppm (±2).

Table 3
Derived Properties of Coal, Tar, and Char[b]

Coal	Sample	X_b	C_{cl}	σ+1	P_o	B.L.	S.C.	V (daf)	Tar (daf)	tar resid.
Pitt #8	coal	0.29	14	4.8	0.48	2.3	2.5			
Pitt #8	tar	0.134	8	2.4	0.45	1	1.4	46	22	
Pitt #8	tar res.	0.25	12	3.9	0.73	2.8	1.1	46	22	0.25
Pitt #8	char	0.368	18	5.7	0.67	3.8	1.9	42	19	
Blue #1	coal	0.27	13	5	0.48	2.4	2.6			
Blue #1	tar	0.09	7	3	0.58	1.7	1.3	23	6	
Blue #1	tar res.	0.273	13	4.7	0.54	2.5	2.2	23	6	0.12
Blue #1	char	0.264	13	5.2	0.72	3.7	1.5	29	7	
Illinois #6	coal	0.3	15	5.5	0.52	2.9	2.6			
Illinois #6	tar res.	0.27	13	4.6	0.69	3.2	1.4	32	6	0.42
Illinois #6	char	0.278	13	4.9	0.67	3.3	1.6	35	11	

[b]X_b = fraction of bridgehead carbons, C_{cl} = aromatic carbons per cluster, σ+1 = total attachments per cluster, P_o = fraction of attachments that are bridges, B.L. = bridges and loops per cluster, S.L. = side chains per cluster, V = total volatiles yield, Tar = tar collected on filters (not corrected for tar deposited in the sampling apparatus), tar resid. = fraction of collected tar that did not dissolve in CD_2Cl_2.

It is interesting to compare the NMR data for the tar, tar residue, and char with that of the coal. The carbon aromaticity $f_{a'}$ of the dissolved tar is similar to that of the parent coal, while that of the tar residue is generally higher (and close to that of the char). Perhaps the most interesting result is that the average cluster size of the dissolved tar is 7 to 8 aromatic carbons, which is much lower than the values of 12-18 found in the coal, tar residue, or char. Previous data on coals and

chars[21] also found that the number of aromatic carbons per cluster in coals and chars (ranging from lignite to lv bituminous coals) ranged from 10 to 18. The fact that the aromatic carbons per cluster in the tar residue is higher in the dissolved tar suggests a wide distribution of species with varying molecular weights in the tar.

The number of aromatic carbons per cluster in the tar residue is very similar to that found in the coal and char. The number of attachments per cluster in the dissolved tar is also significantly smaller than in the coal, while $\sigma+1$ in the tar residue is only slightly less than in the coal. The small number of attachments per cluster in the tars is also reflected in the values of bridges and loops per cluster (B.L.) and side chains per cluster (S.C.).

The average values of chemical structure features for the composite tar can be determined from combining the values for the dissolved tar and tar residue, according to the respective weight fraction of tar residue. This would raise the number of aromatic carbons per cluster in the tar to 8 and 9 for the two coals, which is still more than 35% lower than in the parent coal. It has been shown with repeated data sets that the number of aromatic carbons per cluster in the char does not increase substantially during devolatilization.[8-10, 21] The fact that C_{cl} in the tar is lower than in the coal, coupled with the fact that C_{cl} in the char remains constant at the same value as the coal, *can only be explained by ring breakage and not bridge breaking.* It is known that bond energies in aromatic rings are large, but it is suggested that the heteroatoms (largely oxygen and sulfur) in the clusters weaken the stability of the clusters. This is an interesting development, and suggests that the current view of devolatilization, as explained by current devolatilization models, may be in error.

References

1. Anthony, D. B., J. B. Howard, H. C. Hottel and H. P. Meissner *15th Symposium (International) on Combustion*; The Combustion Institute, Pittsburgh, PA: **1974**; pp 1303-1317.
2. Kobayashi, H., J. B. Howard and A. F. Sarofim *16th Symposium (International) on Combustion*; The Combustion Institute, Pittsburgh, PA: **1976**; pp 411-425.
3. Ko, G. H., D. M. Sanchez, W. A. Peters and J. B. Howard *22nd Symposium (International) on Combustion*; The Combustion Institute, Pittsburgh, PA: **1988**; pp 115-124.
4. Solomon, P. R., D. G. Hamblen, R. M. Carangelo, M. A. Serio and G. V. Deshpande *Energy and Fuels* **1988**, *2*, 405-422.
5. Niksa, S. *Energy and Fuels* **1991**, *5*, 673-683.
6. Fletcher, T. H., A. R. Kerstein, R. J. Pugmire and D. M. Grant *Energy and Fuels* **1992**, *6*, 414.
7. Solum, M. S., R. J. Pugmire and D. M. Grant *Energy and Fuels* **1989**, *3*, 187.
8. Fletcher, T. H., M. S. Solum, D. M. Grant, S. Critchfield and R. J. Pugmire *23rd Symposium (International) on Combustion*; The Combustion Institute, Pittsburgh, PA: **1990**; pp 1231.
9. Pugmire, R. J., M. S. Solum, D. M. Grant, S. Critchfield and T. H. Fletcher *Fuel* **1991**, *70*, 414.
10. Fletcher, T. H., M. S. Solum, D. M. Grant and R. J. Pugmire *Energy and Fuels* **1992**, *6*, 643-650.
11. Fletcher, T. H., S. Bai, R. J. Pugmire, M. S. Solum, S. Wood and D. M. Grant *Energy and Fuels* **1993**, *7*, 734-742.
12. Solomon, P. R. and T. H. Fletcher The Combustion Institute, Pittsburgh, PA: **1990**; pp 463.
13. Smith, K. L., L. D. Smoot, T. H. Fletcher and R. J. Pugmire *The Structure and Reaction Processes of Coal*; Plenum: New York, **1994**.
14. Niksa, S. *Energy and Fuels* **1995**, *9*, 467-478.
15. Freihaut, J. D., W. M. Proscia and D. J. Seery *Energy and Fuels* **1989**, *3*, 692-703.
16. Freihaut, J. D., W. Proscia, N. Knight, A. Vranos, H. Kollick and K. Wicks "Combustion Properties of Micronized Coal for High Intensity Combustion Applications," Final Report for DOE/PETC Contract DE-AC22-85PC80263, **1989**.
17. Chen, J. C. "Effect of Secondary Reactions on Product Distribution and Nitrogen Evolution from Rapid Coal Pyrolysis," Stanford University, HTGL Report No. T-280, **1991**.
18. Monson, C. R. and G. K. Germane *Energy and Fuels* **1993**, *7*, 928-936.
19. Orendt, A. M., M. S. Solum, N. K. Sethi, R. J. Pugmire and D. M. Grant *Advances in Coal Spectroscopy*; H. L. C. Meuzelaar, Ed.; Plenum Press: New York, **1992**; pp 215-254.
20. Bai, S., R. J. Pugmire, C. L. Mayne and D. M. Grant *Analytical Chemistry* **1995**, *67*, 3433-3440.
21. Fletcher, T. H. and D. R. Hardesty "Milestone Report for DOE's Pittsburgh Energy Technology Center," contract FWP 0709, Sandia Report No. SAND92-8209, available NTIS, **1992**.